The Interplay Between SNAREs and Membranes: How Complexin's Binding Interactions Regulate Membrane Fusion

Akosua Pomaa Ofosuhene
Accra, Ghana

Bachelor of Arts, Colgate University, 2018

A Dissertation presented to the Graduate Faculty of the University of Virginia in Candidacy for the Degree of Doctor of Philosophy.

Department of Chemistry
University of Virginia
November 2024

© Copyright by Akosua Pomaa Ofosuhene

All Rights Reserved

November 2024

Abstract

Synaptic vesicle fusion with the neuronal plasma membrane is a highly regulated process that is essential for the release of neurotransmitters. Energetic barriers inhibit the spontaneous fusion of membranes and formation of the SNARE complex provides the energy needed to overcome these barriers. The SNARE complex, composed of Syntaxin, Synaptobrevin and SNAP25, can fuse membranes alone, but additional regulatory mechanisms are required to ensure rapid, calcium-triggered membrane fusion. One of these regulatory proteins involved is Complexin, which functions to both clamp spontaneous fusion and facilitate calcium-triggered release. Complexin interacts with both the SNARE complex and membrane bilayers and these interactions are critical for its functions. However, the precise mechanisms by which these interactions support its functions are not completely understood.

This dissertation explores Complexin's interactions with SNAREs and membrane bilayers using fluorescence anisotropy and continuous wave electron paramagnetic resonance. Our studies revealed that Complexin's membrane binding is sensitive to membrane properties. Increase acyl chain unsaturation or PIP2 concentration resulted in an increase membrane binding of complexin. Complexin can also inhibit its own membrane binding at low protein:lipid concentrations.

Although individual SNARE proteins in solution did not alter Complexin's membrane binding, membrane-anchored SNAP25 significantly enhanced this binding while membrane anchored Syntaxin and Synaptobrevin inhibited it. The ability of SNAP25 to increase Complexin's membrane binding was due to the action of its N-terminal SN1 domain. SNARE complexes formed with either SNAP25 and Syntaxin or SNAP25, Syntaxin and Synaptobrevin increases Cpx's membrane binding when anchored to lipid vesicles while the soluble complexes reduced Complexin membrane binding

We also found that Complexin can bind multiple SNARE complexes in solution, including Syntaxin alone, Syntaxin and SNAP25 complex or Syntaxin, SNAP25 and Synaptobrevin complex. However, when these same complexes were attached to membranes, Complexin only interacted with the ternary SNARE complex. These findings highlight the importance of membrane environment in altering the conformation of SNAREs.

Complexin's affinity for unsaturated lipids suggests that packing defects are important for its membrane binding. SNAP25 alone or complexed with other SNARE proteins may function to increase these packing defects that alter Cpx-membrane binding. By binding to these packing defects that promote fusion, Complexin can help stabilize these defects and therefore clamp fusion before the arrival of the calcium signal.

Table of Contents

List of Figures

Acknowledgements

I would first like to express my deepest gratitude to Prof. David S. Cafiso who has been an extraordinary mentor throughout my PhD journey. Your guidance, expertise and encouragement have been invaluable in writing my dissertation. From planning experiments, interpreting results, and overcoming roadblocks I encountered with my experiments, you have been instrumental in helping me grow as a scientist. I am incredible grateful for your patience, insight, and support.

I would also like to thank the members of my committee: Prof. Lukas Tamm, Prof. Michael Wiener, Prof. Jill Venton and Prof. Andreas Gahlmann for their valuable feedback and suggestions throughout my Candidacy Exams, 4th Year Seminar and my Thesis Defense.

Thank you to the professors who inspired me during my undergraduate studies, particularly Prof. Ephraim Woods III, in whose lab I worked over several summers. Your mentorship and passion for science nurtured my love for lab work and desire to pursue a PhD.

I am also grateful to past and present members of the Cafiso Lab whose knowledge, experience and friendship have made this experience enjoyable and productive. Dr. Qian Liang, thank you for showing me how to set up my experiments and for going out of your way to guide me, even when you were not physically present in lab. Your timely responses to my many questions when I was starting my Complexin assays were invaluable. I am grateful to Dr. Sarah Nyenhuis, who taught me the biochemistry techniques that were critical to my work. A special thank you to Monika Wieliniec, Dr. Virunga Wimalasiri, Dr. Abigail Graham and Dr. Vanessa Bijak for your advice and support throughout my time in lab.

To my friends and family, your encouragement and unwavering belief in me have been my greatest source of strength. To Fiona, Diana, Jide, Bella, and Mike thank you for always being there for me and cheering me on through every milestone. Our travels together have always been

something I looked forward to. Thank you for always opening up your homes to me, offering a sense of belonging and comfort during stressful times. Even when I could not always go back home, your hospitality made me feel as if I had a home away from home.

To my parents, Zenobia and Alfred Ofosuhene Appenteng, none of this would have been possible without your unwavering support and belief in me. Thank you for supporting my dreams and encouraging me every step of the way. To my siblings, Kwasi and Awo Ama, your love and encouragement have meant the world to me. Your messages of support and moments of shared laughter provided much-needed relief during my most difficult times. A special shoutout to my cousin, Isaac Owusu Afriyie for your continuous support and pride in my achievements.

Finally, I would like to thank Justin for his continuous and unwavering support during my PhD journey. Your belief in me, your encouragement through every challenge, and your love have been my anchor. You have been an amazing partner, and I am deeply grateful to have shared this journey with you. I love you.

Chapter 1 INTRODUCTION

1.1 Neuronal Transmission

Neuronal transmission is the process by which neurons communicate with each other and other cells in the body. This system is vital to all bodily functions, regulating both voluntary actions, like reading, running, and eating as well as involuntary actions such as heartbeat regulation, kidney functions, or temperature control. Neurons are the building blocks of the nervous system, with approximately 100 billion neurons in the brain alone, constantly exchanging information to maintain the body's activities.[1] The nervous system receives information from the body and the external environment, processes it, and initiates the proper responses. This communication between neurons underlies our very existence, enabling us to interact and adapt to the world around us.

1.1.1 The Nervous System and Neurons

The nervous system is composed of a complex network of neurons and supporting cells and is divided into two main components: the central nervous system (CNS) and the peripheral nervous system (PNS). These components work together, allowing the body to react to changes within its internal environment and the external world.[2] The CNS is composed of the brain and the spinal cord and serves as the major control center for the body. The brain is responsible for higher functions like thought, emotion, memory, and coordination of movement. The spinal cord acts as a channel between the brain and the rest of the body and also coordinates reflexes, which are involuntary, automatic responses to stimuli, without a conscious thought. The PNS consists of all other neurons that exist outside of the CNS, extending throughout the body to relay information between the CNS and other organs.

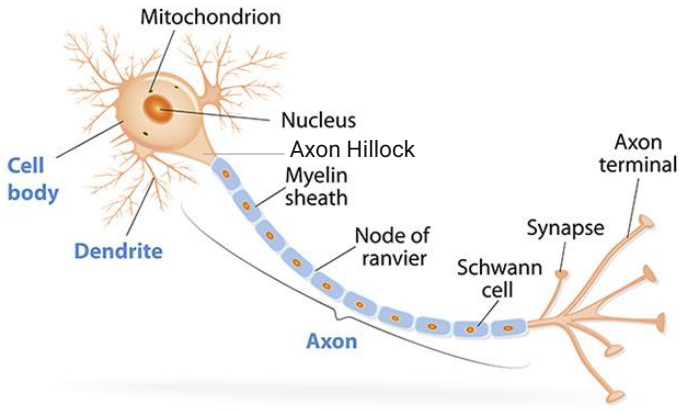

Figure 1-1 *Diagram depicting the major parts of a neuron. Figure modified from* [3]

Neurons are the fundamental building blocks of the nervous system and are responsible for detecting a signal, processing it, and sending that information to other neurons or target organs. Neurons possess different morphologies but have two main features: the cell body (or soma) and the processes that branch out from the soma (Figure 1-1). The soma contains the nucleus and surrounding cytoplasm, which houses essential organelles responsible for producing components necessary for the neuron's function and overall health. Since most neurons do not have the ability to divide or regenerate, the cell body plays a critical role in maintaining structural integrity.[4] From the soma extend several processes: the axon and dendrites. Dendrites are branch-like extensions that receive synaptic input from other neurons. The axon is a long projection from the cell body that relays electrical impulses from soma to other neurons, muscles, or glands. The myelin sheath is a protective insulating sheath that wraps around some axons. It is composed of lipids, proteins, and functions to increase the speed and efficiency of electrical signal transmission. It allows electrical

impulses to 'jump' between gaps in the sheath, known as nodes of Ranvier, allowing more rapid signal transmission.[5]

The transmission of signals through a neuron involves both electrical and chemical processes. Signals travel within the neuron via electrical signals and between neurons via chemical signals. Signal transmission begins when a neuron receives an external stimulus from another neuron, usually at the dendrites. This triggers an electrical impulse, also known as an action potential, which is generated by the movement of ions across the neuronal membrane.[2] Action potentials occur in an all-or none fashion, meaning that once a threshold stimulus is reached, the action potential will proceed. Neurons have a resting potential around -70 mV due to an unequal distribution of ions across the plasma membrane, that is maintained by ion pumps (Figure 1-2). When a stimulus reaches the neuron and surpasses the threshold (around -55 mV), voltage-gated Na^+ sodium channels open, allowing Na^+ ions to flow into the cell down a concentration gradient. This influx of positive ions causes the internal environment of the cell to become more positive. This rapid depolarization increases the voltage to around +30 mV (Figure 1-3). When the membrane potential reaches its peak, the sodium channels close and potassium channels open. Potassium ions flow out of the cell, restoring the membrane potential to its more negative value. This is known as repolarization. The membrane potential may become more negative than usual, a phase known as hyperpolarization, due to potassium channels being open for longer, allowing more K^+ ions to leave than is needed to return to resting membrane potential. Sodium-potassium pumps actively transport ions to restore original ion concentrations and bring the neuron back to its original resting potential to prepare for another round of signal transmission.

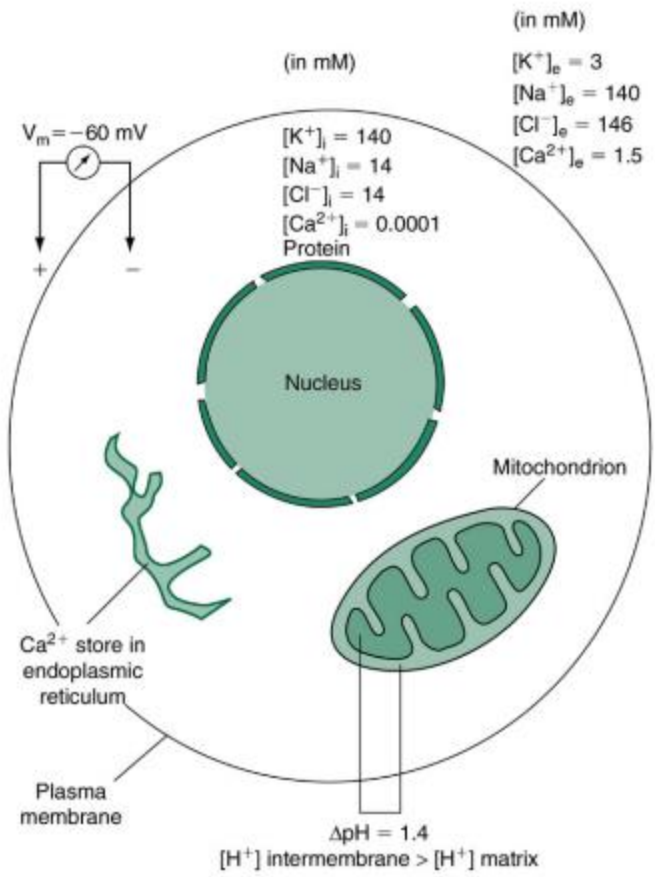

Figure 1-2 *Ionic concentrations of the intra- and extracellular environment of the neuron. The unequal distribution of ions generates the membrane potential, V_m. Figure adapted from* [2]

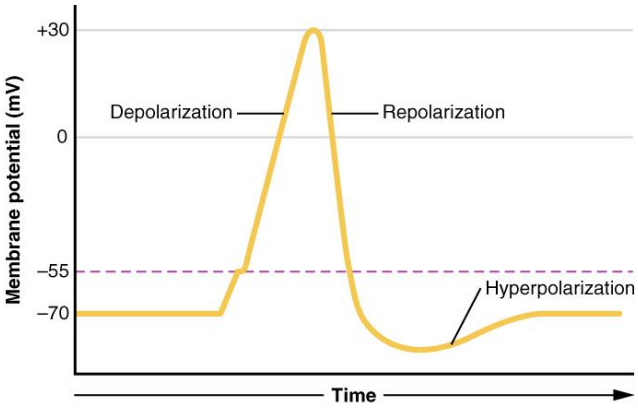

Figure 1-3 *Changes in membrane potential during an action potential. Figure adapted from* [5]

The action potentials are initiated at the axon hillock when incoming signals surpass the threshold. In myelinated neurons, transmission is accelerated by current that jumps between gaps in the myelin sheath known as the nodes of Ranvier.[5] The nodes contain a high concentration of ion channels that amplify the signals. The myelin sheath acts as an electric insulator resulting in signal 'jumping' from node to node. At each node, the signal is further amplified enabling the action potential to be propagated rapidly along the neuron.

At the axon terminus, the action potential triggers the release of neurotransmitters through a process that converts the electrical signal into a chemical one (Figure 1-4). When the action potential reaches the presynaptic membrane, it causes the opening of voltage-gated Ca^{2+} channels, allowing Ca^{2+} to flow into the neuron down its electrochemical gradient (Figure 1-5).[6] Synaptotagmin 1 acts as the Ca2+ sensor and together with the SNAREs (see below) facilitates the fusion of neurotransmitter-filled synaptic vesicles with the presynaptic plasma membrane.[7] Once fused, the vesicles release their neurotransmitters into the synaptic cleft. The neurotransmitters then bind to specific receptors on the post synaptic membrane, where they can initiate a new action potential. This process of signal transmission is repeated until the signal reaches its target organ.

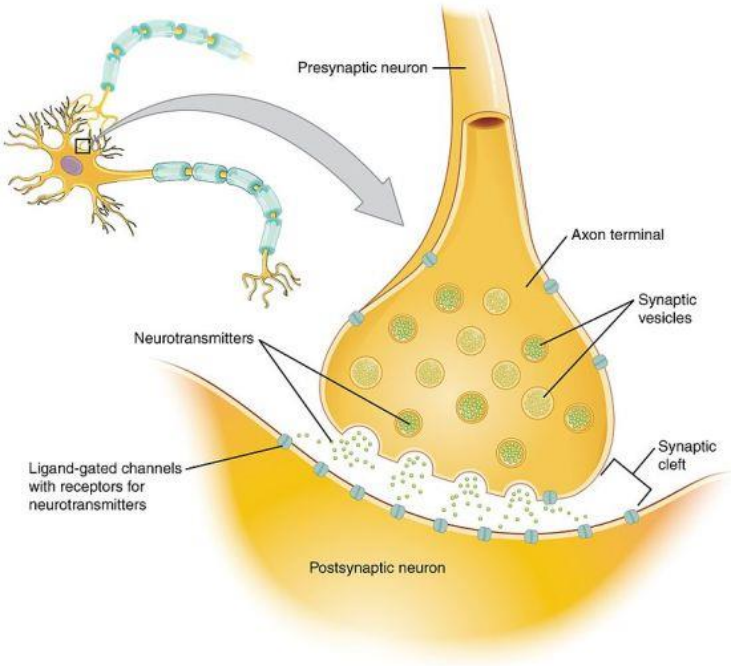

Figure 1-4 *Neuronal exocytosis at the synapse. At the presynaptic axon, vesicles containing neurotransmitters fuse with the plasma membrane and release their content into the synaptic cleft. The neurotransmitters bind to receptors on the postsynaptic neuron. Figure adapted from* [8]

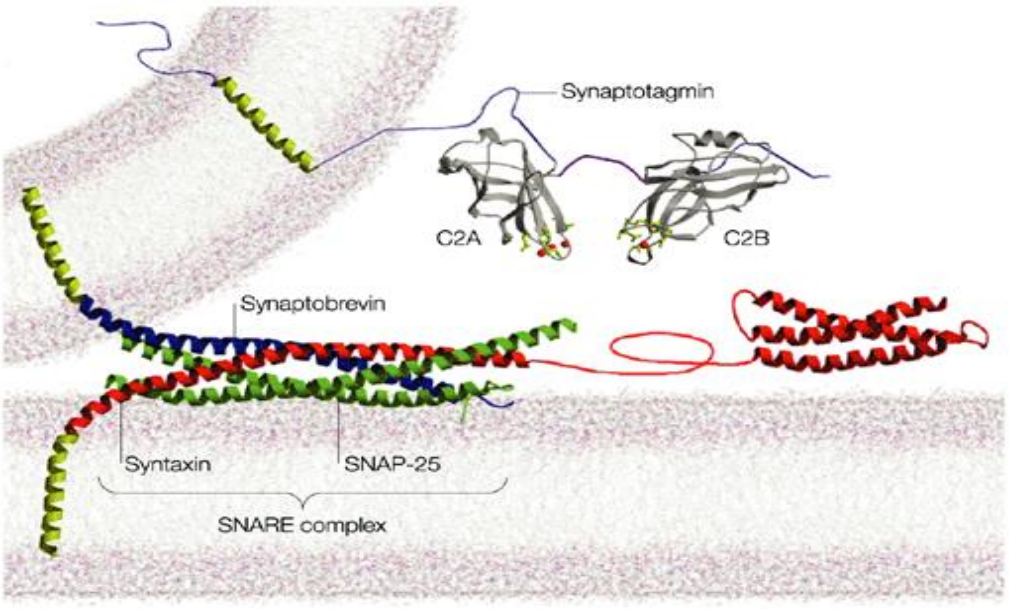

Figure 1-5 *Formation of the SNARE complex (composed of syntaxin, synaptobrevin and SNAP25) drives the synaptic vesicle to fuse with the plasma membrane. Synaptotagmin acts as the Ca^{2+}sensor for fusion. Figure adapted form* [9]

1.1.2 The Synapse

Neurons communicate through specialized connections known as synapses where electrical signals are converted to chemical signals for transmission to other neurons or target cells. These synapses play a crucial role in forming neural networks, which process and transmit information throughout the nervous system. Electrical signals, or action potentials, travel down the axon where upon reaching the presynaptic terminal, chemical secretion of neurotransmitters occurs. The neurotransmitters are released from synaptic vesicles into the synaptic cleft through a tightly regulated process known as neuronal exocytosis.

After neurotransmitter release, the SNARE complex, which is responsible for mediating fusion, is disassembled into its constituent proteins. This disassembly is facilitated by NSF (N-ethylmaleimide-sensitive factor) and SNAPs (soluble NSF attachment proteins) in an ATP-dependent process that is essential for "recharging" the SNAREs, allowing them to participate in future rounds of exocytosis.[10]

Following vesicle fusion, synaptic vesicles are recycled locally at the presynaptic terminal. The recycling process begins with the acidification of the synaptic vesicles creating an electrochemical gradient (Figure 1-6).[11,12] Acidification is necessary for the uptake of new neurotransmitters. Once filled with neurotransmitters, synaptic vesicles are trafficked to specialized areas on the presynaptic vesicles known as active zones. After docking, the vesicles undergo priming, which involves a series of molecular rearrangements that make the vesicles fusion competent.

Upon the arrival of an action potential, an increase in the intracellular concentration of Ca^{2+} triggers a cascade of molecular events that results in the fusion of the synaptic vesicle with the

presynaptic plasma membrane. Two types of fusion mechanisms can occur.[12] In the kiss-and-run mechanism, the vesicle fuses with the membrane and releases part of its contents (Figure 1-6). The vesicle then detaches from the membrane and is recaptured back into the presynaptic terminal. The vesicles can also completely collapse into the plasma membrane (known as kiss-and-stay) after releasing their content (Figure 1-6). This is followed by a clathrin-mediated exocytosis to recycle the vesicle. These processes ensure that synaptic transmission is sustained for further events.

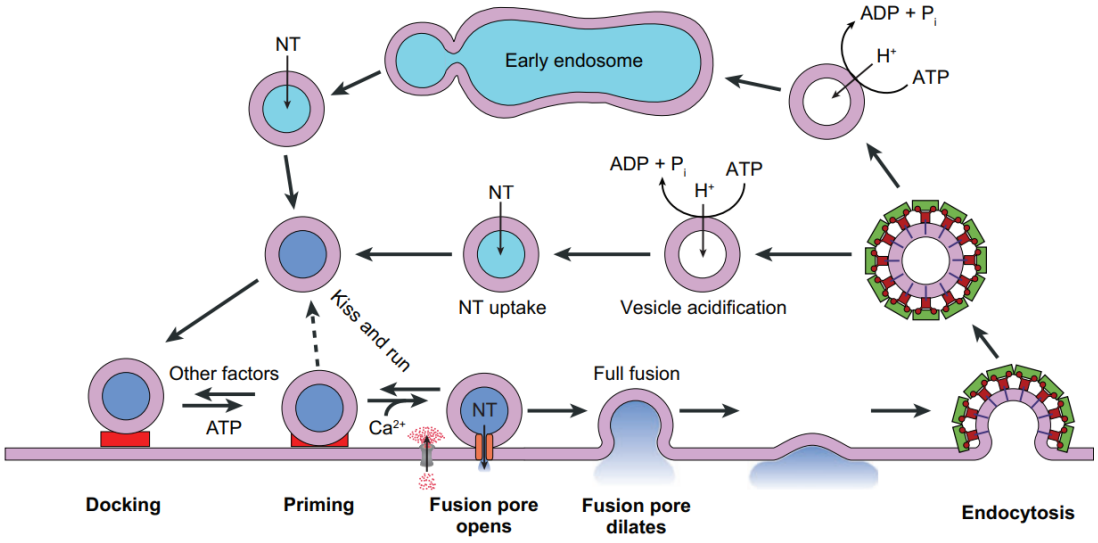

Figure 1-6 *Illustration of the life cycle of a synaptic vesicle. Figure adapted from*[12]

1.1.3 Membrane Fusion

Membrane fusion during synaptic vesicle exocytosis is a highly regulated process that allows neurotransmitter release within milliseconds of an action potential reaching the axon terminal. To ensure rapid fusion, synaptic vesicles are docked and primed awaiting fusion in response to calcium influx. The SNAREs (soluble N-ethylmaleimide sensitive factor attachment protein receptors) assemble into a complex and form the core machinery that drives fusion. In the neuron, the SNAREs

include synaptobrevin (Syb), syntaxin (Syx) and synaptosomal-associated protein of 25 kDa (SNAP25). These proteins contain a characteristic SNARE motif, a stretch of about sixty amino acids that allows them to interact and form a stable, four-helix bundle. Syntaxin, Syb and SN25 form the SNARE complex in a 1:1:1 ratio.[13] SNAP25 contributes two helices while Syx and Syb contribute a helix each to form this bundle. SNAP25 and Syx are localized on the plasma membrane while Syb is localized on the vesicle membrane and assembly of the SNARE complex provides the energy that is required to overcome the barrier to fusion.

Although the SNAREs are the minimal machinery required for fusion, when they are reconstituted alone, fusion is very slow, and off-pathway complexes of the SNAREs form that do not lead to fusion and are slow to disassemble. To ensure that SNAREs are assembled properly, and fusion occurs on a millisecond scale, there are several critical regulatory proteins required. Proteins like Munc13 and Munc18 act as chaperones to regulate the proper assembly of the SNARE complex while accessory proteins like synaptotagmin and complexin regulate speed and efficiency of fusion. Synaptotagmin functions as the calcium sensor for fusion and stimulates evoked fusion.

SNAREs assemble in an N- to C- terminal direction[14] and as the SNAREs assemble, they pull the membranes destined to fuse together. The energy released from assembly is used to overcome the energetic barriers to fusion, which include hydration energies, membrane deformation and electrostatic barriers. As the SNAREs begin to assemble, they form a trans-SNARE complex, in which Syx and SNAP25 are on the plasma membrane while Syb remains anchored on the vesicle membrane. This partially assembled state is primed for fusion but is held back by proteins like complexin, which clamp the SNARE complex and prevent full assembly. When an action potential arrives, the subsequent increase in calcium concentration triggers Syt to bind calcium, insert into the membrane and release the fusion clamp. This allows the SNARE complex to fully assemble and

drive membrane fusion. After fusion, the SNAREs now reside in the same membrane, forming a cis SNARE complex. The SNARE complex is then disassembled into its constituent proteins by NSF and SNAP to prepare for another round of exocytosis.

Fusion itself occurs in several stages. First, the vesicle and plasma membrane come into proximity and their outer lipid layers merge forming the hemifusion stalk. The distal monolayers then fuse, and this is followed by the opening of fusion pore. The fusion pore then expands to allow the neurotransmitters to be released into the synaptic cleft (Figure 1-7).

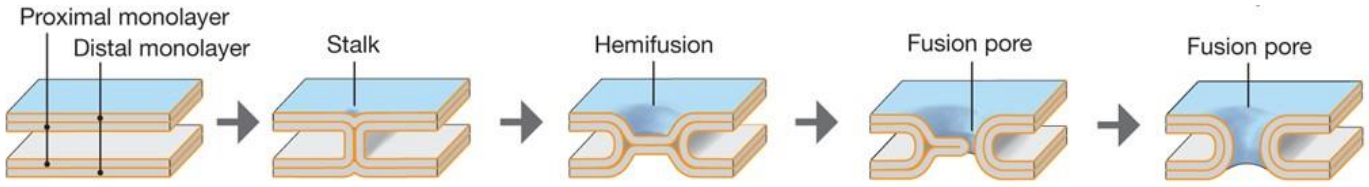

Figure 1-7 *Depiction of the membrane intermediates formed during fusion of the vesicle and plasma membranes. Figure adapted from*[10]

1.2 SNAREs and Regulatory Proteins

1.2.1 The SNARE complex

The SNARE complex is composed of Syx, SNAP25 and Syb, and this complex is the main driver of membrane fusion in neuronal exocytosis. When fully assembled, the SNARE complex is resistant to protease digestion while the individual SNAREs are not.[15] It is also SDS-resistant and heat-stable up to about 80 ^{0}C. Each SNARE protein contains a ~65 residue sequence known as the SNARE motif that has the ability to assemble into a coiled-coil structure that is essential for

function.[16] Syx and SNAP25 are localized on the plasma membrane while Syb is on the synaptic vesicle. Based on their localization, Syx and SNAP25 are often referred to as t-SNAREs (target membrane SNARE) while Syb is classified as a v-SNARE (vesicle SNARE).[10]

The SNARE complex is held together by layers of hydrophobic interactions that stabilize the complex. However, at the core of the complex, is a polar layer one arginine (R) residue from Syb and three glutamines (Q) from Syntaxin and SNAP25. Based on this, the SNARE motifs are also categorized as Q_a-SNARE (for Syntaxin**),** Q_b-SNARE (the N-terminal SN1 helix of SNAP25), Q_c-SNARE (the C-terminal SN2 helix of SNAP25), and R-SNARE (for Synaptobrevin).[17]

On the plasma membrane, SNAP25 lacks a transmembrane domain but is membrane anchored through palmitoylation of its native cysteines. It contributes two SNARE motifs to the SNARE complex; SN1 and SN2 that are connected by a long linker (Figure 1-8). Syntaxin is localized to the plasma membrane through a helix at its C-terminus followed by a SNARE forming motif that is connected by a short linker to a three-helix bundle at its N-terminus known as the H_{abc} domain (Figure 1-8).[18,19] The H_{abc} domain acts as a regulatory domain, and it has the ability to associate with the SNARE motif to form a closed conformation that prevents SNARE assembly.[20] This closed conformation is stabilized in the presence of Munc18 [20] and this syntaxin/Munc18 complex has been proposed as the starting point for SNARE complex assembly. On the vesicle membrane, the third SNARE protein, Syb, is anchored to the membrane by a C-terminal transmembrane helical region (Figure 1-8).

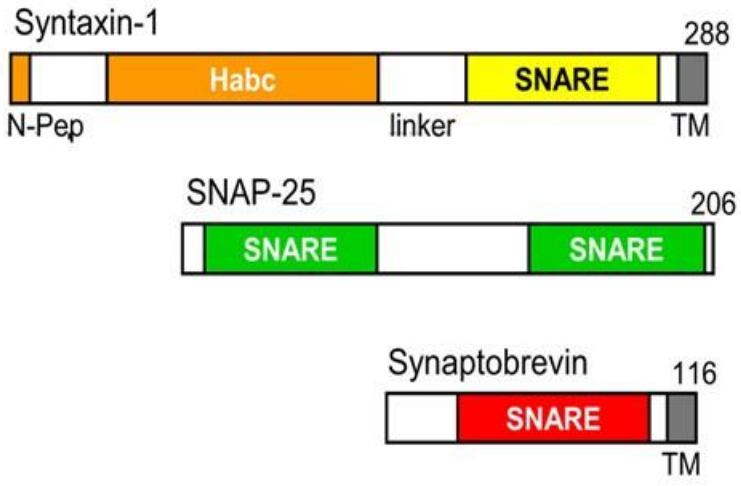

Figure 1-8 *Domain structure of the SNARE proteins Syntaxin, SNAP25 and Synaptobrevin. N-pep indicates N-peptide and TM is the transmembrane domain. Figure adapted from*[21]

1.2.2 Synaptotagmin

Synaptotagmin 1 (Syt1) is the calcium sensor responsible for triggering fast, synchronous neuronal exocytosis.[12,22] In humans, there are 17 isoforms of synaptotagmin but Syt1 is the main calcium sensor for fast, Ca^{2+}-triggered neuronal exocytosis.[22] Mutations that decrease Syt1's Ca^{2+} affinity lead to decrease in the probability of membrane fusion,[23–25] highlighting its crucial role in coupling increased calcium concentration to membrane fusion.

The cytoplasmic domain of Syt1 consists of two C2 domains, C2A and C2B, that are connected by a short linker (Figure 1-9).[26,27] The C2 domains are formed by eight-stranded β-sandwich that are connected by hydrophobic loops.[28,29] These loops form the calcium binding sites, and aspartic acid residues that coordinate the binding of Ca^{2+} in conjunction with acidic phospholipids allow insertion of loops into membranes containing negatively charged lipids. The C2A and C2B domains bind three and two Ca^{2+} respectively.[26] A long 60-residue flexible linker connects

C2A to the transmembrane domain that localizes Syt1 to the synaptic vesicle. The transmembrane domain ends in a short lumenal domain.

Syt1 interacts with both SNAREs and membranes and acts to synchronize Ca2+ mediated fusion. It functions to inhibit spontaneous fusion and promote evoked fusion. Studies have shown that in its apo state (not bound to calcium), Syt1 can interact with SNAREs and acts as a fusion clamp by blocking complete SNARE assembly.[30,31] The Ca^{2+}-bound conformation was shown to displace Cpx from the SNARE complex. This led to the fusion clamp model where Cpx binds to SNAREs inhibiting fusion and Ca^{2+}-bound Syt1 displaces complexin, releasing the clamp to allow fusion to proceed. This model has come under a lot of scrutiny. Cpx and Syt have been shown to interact simultaneously with the SNARE complex.[32,33] There is also evidence that Syt-SNARE interaction may not be physiological as the interaction is abolished at physiological concentration of ATP and Mg^{2+}, while its interactions to PIP2-containg membranes is maintained under the same conditions .[34]

Synaptotagmin also interacts with membranes. In addition to its calcium-dependent insertion into membranes, Syt1 also shows calcium-independent binding to PIP2 (phosphatidylinositol 4,5-bisphosphate)-containing membrane.[35] Specifically, the C2B domain contains a poly-lysine (K326, K327) motif that interacts with PIP2 in a Ca2+-independent manner and this is thought to drive Syt1 to the plasma membrane and to promote vesicle docking. Upon binding calcium, Syt1 is able to insert its Ca^{2+}-bound loops into membranes and triggers a series of molecular rearrangements that result in the release of the fusion clamp, allowing fusion to proceed. Although several models have been proposed to explain the mechanism by which Syt1 promotes membrane fusion,[36] there is not a consensus on how exactly this happens. One model suggests that Syt1 induces membrane curvature by inserting its C2 domains into the membranes, which deforms the membranes and facilitates their fusion.[37] Additionally, Syt1 may act as a molecular bridge,

bringing the synaptic vesicle and plasma membranes together by inserting its C2 domains into both opposing membranes. Another model proposes that synaptotagmin functions as an electrostatic switch, regulating the distance between the vesicle and plasma membrane and thus controlling membrane fusion.[38,39]

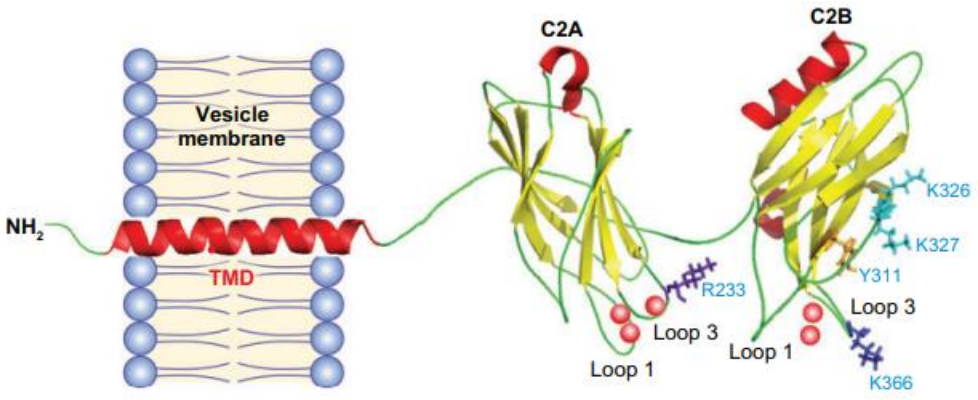

Figure 1-9 *Domain structure of synaptotagmin. The C2 domains are bound to Ca^{2+} (red spheres). The transmembrane domain (TMD) localizes synaptotagmin to the vesicle membrane. Figure adapted from[12]*

1.2.3 Complexin

Complexins (Cpx) are small (~15 kDa, 130-150 residue) cytosolic proteins that bind the SNARE complex and play a critical regulatory role in synaptic vesicle exocytosis. Complexin binds to the SNARE complex with high affinity, rapidly and at a 1:1 stoichiometry. [40–42] Cpx binds to SNARE complex in an antiparallel manner to the groove formed by the helices from Syb and Syx (Figure 1-10) .[42–44] In addition to its interaction with SNAREs, Cpx also binds membranes and has been shown to have a preference for small, highly curved vesicles.[45] Complexin performs a dual role in exocytosis, activating synchronous fusion while suppressing spontaneous fusion.[46] It also plays a role in priming synaptic vesicles.[47]

There are four known complexin isoforms in mammals: Cpx1, Cpx2, Cpx 3 and Cpx4. Cpx1 and Cpx2 share an 80% amino acid sequence identity and are the primary isoforms expressed in the central nervous system. Cpx3 and Cpx4 share a 60 % amino acid sequence identity and have a CAAX motif that undergoes prenylation, which anchors them to lipid bilayers.[48] These isoforms are predominantly found in the mammalian retina.[48]

Complexin is largely unstructured in solution but has four main functional domains (Figure 1-10).[42] The N-terminal region is unstructured and is necessary for triggering exocytosis. The accessory helix (AH) domain forms a stable alpha helix in solution and is involved in the inhibition of fusion. The central helix (CH) binds the assembled SNARE complex and is the most conserved across species.[49] This region is essential but not sufficient for all known Cpx's functions. The disordered C-terminal domain is proposed to be important for proper membrane localization of complexin. Complexin binds to small, highly curved liposomes via its C-terminal domain and it has been proposed to interact with the synaptic vesicle. [45,50] Although the C-terminal domain is largely unstructured in solution, it becomes partly helical when bound to membranes.[51] Complexin plays a dual role in fusion with studies showing that facilitative role is conserved across vertebrates and invertebrates while its inhibitory role is mainly present in invertebrates. The C-terminal domain is the least conserved across species and this variability is thought to account for the functional differences between vertebrate and invertebrates.[49,50]

There are several proposed mechanisms by which Cpx may inhibit fusion. One way is by interacting with and stabilizing the prefusion complex. The accessory helix of Cpx may interact with the C-terminal regions of Syb and SN25 complex and stabilize the prefusion complex.[52,53] This would prevent Syb's C-terminal complex from fully engaging with the SNARE complex. However, NMR and ITC analyses show that the accessory helix of complexin does not insert into SNARE complexes with

truncated Syb.[54] Complexin has also been proposed to bind to the prefusion SNAREs and form a zigzag pattern keeping the SNAREs in a clamped state.[55] Another proposed mechanism for Cpx to inhibit fusion is through electrostatic and steric repulsion generated between the synaptic vesicle and plasma membranes.[54] Mutations that increased the negative charges in the AH inhibited neurotransmitter release while mutations that increased positive charges favored release.[54] Despite some evidence for each, there is no agreed upon mechanism for complexin's inhibitory function.

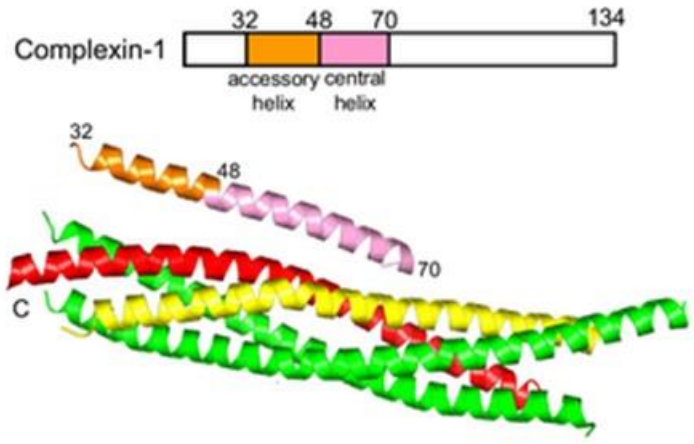

Figure 1-10 *Domain structure of complexin (top). Structure of complexin bound to the SNARE complex (bottom). The PDB ID of the structure is 1KIL. Figure adapted from [21]*

1.3 Biomembrane Environment

Biological membranes are important components of cells, defining their boundaries and enabling the maintenance of environments that are different from their surroundings. These membranes do not only surround the cell but also enclose intracellular organelles, allowing each organelle to maintain distinct conditions and contents for their specific functions. Membranes are needed for the transport of molecules into and out of cells, the passage of ions, and the acquisition of nutrients and removal of waste. They also serve as anchors for membrane proteins that mediate

signaling and transport processes. Lipids, together with proteins, form the primary structural framework of cell membranes, with lipids playing a central role in in maintaining the structural integrity of cellular environments, serving as energy stores, and acting as signaling molecules in intracellular and intercellular communication.[56]

The brain contains the highest concentration of lipids in the body[57] and brain membranes are rich in cholesterol and unsaturated lipids.[58,59] Myelin is a lipid-rich sheath that insulates the neuronal axon to promote fast signal propagation. Alterations in lipid composition in the brain can have profound effects on cellular function and are associated with various neurological disorders.[58,60–62] These changes can affect membrane fluidity, protein function, and overall neuronal health, demonstrating the critical role lipids play in both normal brain function and neurological diseases.

A defining feature of lipids that form biological membranes is their amphipathic nature. These lipids have a hydrophilic headgroup, while the tail, which forms the bulk of the lipid molecule, is hydrophobic. In aqueous environments, the hydrophobic tails cluster together to minimize their interactions with water, while the hydrophilic headgroups face outwards interacting with the surrounding water molecules (Figure 1-11). This arrangement favors the formation of bilayers, which serves as effective barriers to water and other water-soluble molecules. Hydrophobic interactions as well as van der Waals forces stabilize the bilayer structure, ensuring the membrane's integrity and providing a dynamic boundary.

The lipid bilayer is fluid and the distribution of lipids in its inner and outer layer are asymmetric, properties that are crucial for its function. The fluidity of membranes allows proteins and lipids to diffuse laterally within the plane of the bilayer. The degree of fluidity depends on several factors, including the lipid composition, the length and saturation of lipid chains, and the

surrounding temperature. In contrast, saturated lipids, with no double bonds, allow tighter packing, reducing fluidity. Additionally, lipid composition varies between different types of membranes, allowing each membrane to fulfill its specific functions. These different lipids act to affect membrane shape, curvature, fluidity and permeability.[56]

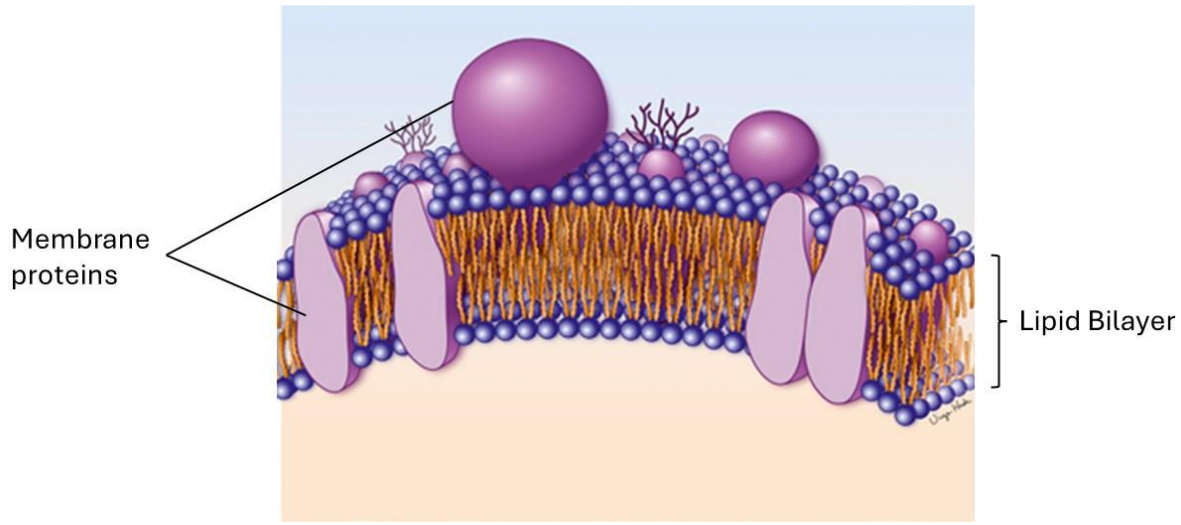

Figure 1-11 *Depiction of the lipid bilayers with embedded membrane proteins. Figure modified from* [63]

1.3.1 Lipid Diversity

In the central nervous system, there are more than 700 different types of lipids, including phospholipids, sterols and sphingolipids (Figure 1-12).[64,65] Each class of lipids has its unique structure that contributes to the overall function of membranes with phospholipids forming the most abundant lipids in biological membranes.[66] Phospholipids have a polar headgroup that contains a phosphate and two hydrocarbon tails. The fatty acid chains can differ in length (usually between 14

and 24 carbons) and degree of saturation. Saturated fatty acids contain no double bonds and tend to pack together tightly while unsaturated fatty acids have at least one double bond. The double bond introduces a "kink" in the chain and prevents tight packing which increases membrane disorder and fluidity. The length of the fatty acid also affects membrane properties like fluidity. Long, saturated chains tend to pack tightly into a rigid, gel-like state while short, unsaturated chains form more fluid membrane structures.

Phosphoglycerides are the main phospholipids present in animal cells and are built on a glycerol backbone. The glycerol is esterified with two fatty acid chains, while the third carbon in the glycerol is attached to a phosphate group. The phosphate group can in turn be attached to different polar headgroups, giving rise to different phosphoglycerides. These include phosphatidylcholine (PC), phosphatidylethanolamine (PE), phosphatidylserine (PS), phosphatidic acid (PA) and phosphatidylinositol (PI). At neutral pH , lipids like PC and PE are zwitterionic and carry net zero charge while PI and PS carry a negative charge. Phospholipids like PE, PS, PI favor the cytosolic leaflet.

Another important class of lipids is sterols with cholesterol (Chol) being the most abundant sterol in animal cells.[67] Cholesterol has a fused ring structure that is attached to a polar hydroxyl group and a short hydrocarbon chain. It plays a key role in maintaining the fluidity of membranes. Additionally, cholesterol can also order lipid membranes resulting in rigid and thicker bilayers. Cholesterol reduces permeability in phospholipid bilayers and plays an important role in controlling membrane curvature and asymmetry.[68] Cholesterol interacts with and mediates the activity of many integral membrane proteins. In mammals, cholesterol is a precursor of steroid hormones, which perform a variety of essential functions.[67]

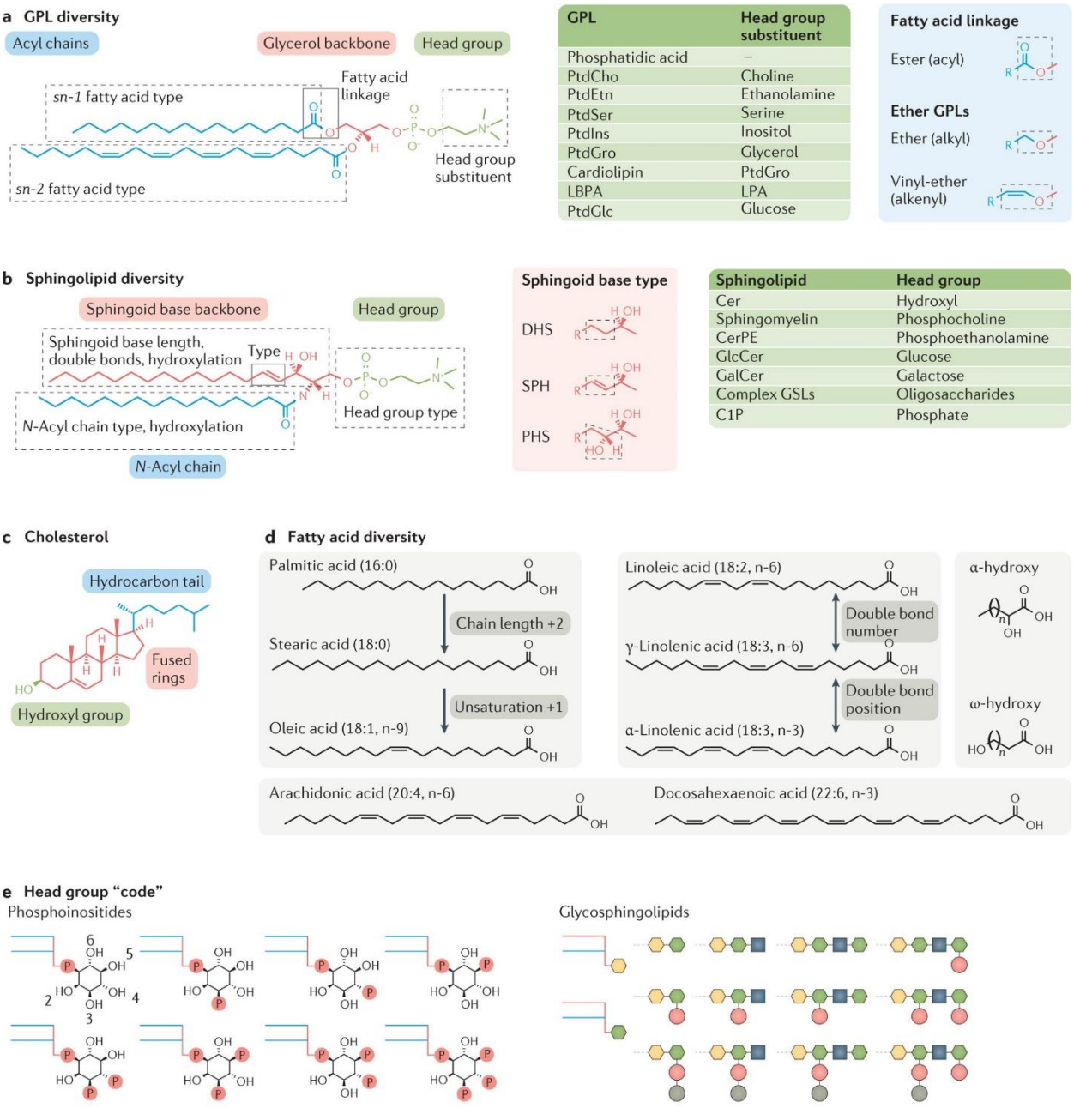

Figure 1-12 *Illustration of lipid diversity in mammalian membranes highlighting the variations inlipid composition and structure. Figure adapted from* [69]

1.3.2 Membrane Curvature

Fusion of the synaptic vesicle with the neuronal plasma membrane requires deformation of lipid layers into high-curvature intermediates. Membrane curvature can be altered by various factors including changes in lipid composition or by the action of integral or peripheral membrane proteins. Lipid molecules can contribute to membrane curvature depending on their structure (Figure 1-13). Lipids like phosphatidylcholine, which have a cylindrical shape, tend to form flat bilayers. On the other hand, lipids with smaller or larger headgroup have an inverted conical or conical shape respectively and this favors the formation of curved bilayers. This will induce a negative or positive curvature depending on the size of the headgroup relative to the volume the hydrocarbon chain occupies. Consistent with models for fusion, lipids with negative curvature are important for formation of the initial hemifusion state in fusion and lipids with positive curvature are important for the opening of the fusion pore.[70–72]

Proteins also play a vital role in generating and stabilizing membrane curvature (Figure 1-14). This can occur through different mechanisms, such as insertion of hydrophobic domains, membrane scaffolding and lipid clustering. For example, Syt induces membrane curvature when it inserts its C2 domains into membranes.[73] The C2 domains tubulate liposomes in a Ca^{2+}- dependent manner which promotes fusion.[73] Similarly, BAR domain proteins act as molecular scaffolds that bend bilayer into a curved shape.[74] As indicated above, complexin binding is sensitive to membrane curvature [51,75] and can remodel flat membranes into highly curved structures.[76] Coarse grain molecular dynamics shows that tSNARE clusters promote membrane curvature.[77] Curvature has the ability to bring two membranes closer together, and membrane deformation as a result of curvature stress may reduce the barrier to and promotes fusion.[78]

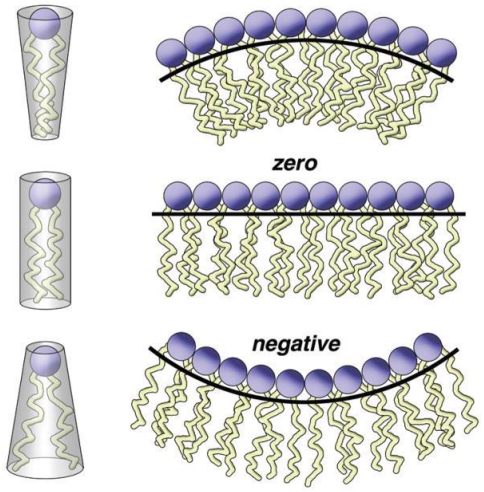

Figure 1-13 *The shape of the individual lipids (left) can influence the curvature of the lipid bilayer (right). Figure adapted from* [79]

Figure 1-14 *Proteins can remodel flat bilayers (A) into curved structures by inserting their hydrophobic domains into it (B), acting as molecular scaffolds (C) or clustering certain lipids (D). Figure adapted from*[66]

1.3.3 PIP2

Although phosphoinositides are a minor component (about 1%) of the cellular membranes, they are crucial components involved in a wide range of cellular processes. PIP2

(phosphatidylinositol 4,5-bisphosphate) is the most abundant phosphoinositides and is predominantly localized to the plasma membrane.[80] It plays critical roles in several cellular functions including exocytosis, endocytosis, membrane trafficking and enzyme activation.[81] Hydrolysis of PIP2 by phospholipase C generates DAG (diacylglycerol) and IP_3 (inositol-3,4,5P_3), both of which function as secondary messengers in cellular signalling.[82]

PIP2 headgroup is characterized by an inositol ring that is phosphorylated at the 4 and 5 positions (Figure 1-15). PIP2 has a net charge that can range from -3 to -5 depending on local pH and the presence of counterions.[81] It has a broad distribution of acyl chain composition with the most abundant being 1-stearoyl-2-arachidonyl (18:0/20:4) (Figure 1-15). Its unique structure allows PIP2 to recruit PIP2-binding proteins, including Syt, Munc13, CAPS, and Syx which are all important in the vesicle fusion process. It is also involved in priming the ready-releasable vesicles.[83]

PIP2 is abundant in the cytosolic leaflet of the plasma membrane and is localized at the site of exocytosis. It organizes into clusters and could form local concentrations of ≥ 6 mol% (with numbers as high as 80 mol% being reported) at their nanodomains.[81,84] These clusters play a significant role in vesicle fusion as they create microenvironments that facilitate protein recruitment and interaction. The levels of PIP2 is highly regulated and its dysregulation in brain leads to several neurological conditions.[80,85]

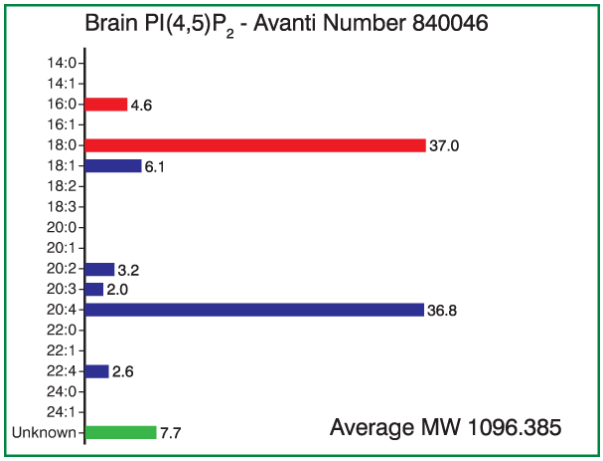

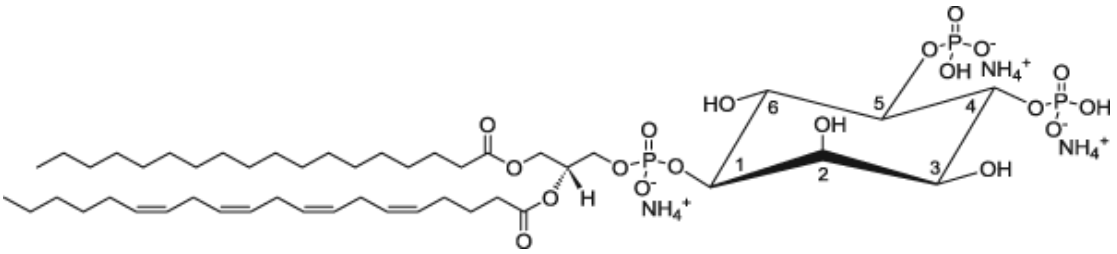

Figure 1-15 *Average fatty acid chain distribution of brain PIP2 (top). Molecular structure of the major brain PIP2 (bottom). Figure adapted from*[86]

1.4 Rationale and Objectives

Complexin plays an important role in synaptic vesicle exocytosis, serving as a regulatory protein for SNARE-mediated membrane fusion. Complexin interacts with both the assembled SNARE complex and membrane bilayers and these interactions are critical to its functions. Although previous studies have highlighted Cpx's function both in promoting and inhibiting vesicle fusion, the exact molecular mechanism by which it accomplishes this are still not fully understood. The goal of this dissertation is to examine how Cpx's interactions with membranes and SNAREs contribute to its function. This was undertaken using fluorescence anisotropy and Electron Paramagnetic Resonance. With anisotropy, protein-free or SNARE anchored vesicles were titrated into a solution of fluorophore-labelled Cpx, and the anisotropy was measured. From the measured anisotropies, the affinity of Cpx to the vesicles was calculated. By varying membrane properties or the SNARE proteins used, we could measure how these changes affected Cpx-membrane interactions. Fluorescence anisotropy enabled us to work with low concentrations of Cpx, since high concentrations of Cpx led to reduced membrane binding affinities. To carry out the EPR measurements, Cpx was spin-labelled along its length and the EPR spectra of Cpx in the presence of lipid vesicles and SNAREs were collected. This allowed us to probe the localized interactions made at sites on Cpx.

The first objective of this research was to investigate how membrane lipid composition affects Cpx's interaction with lipid vesicles. Although the exact lipid composition at the site of fusion is not known, membrane properties such as increased lipid disorder and PIP2 concentration are known to promote fusion.[87,88] These properties may enable Cpx to regulate the fusion process by modulating Cpx's interactions with membrane lipids at fusion sites. We hypothesized that Cpx preferentially binds to membranes with properties that facilitate fusion and these membrane properties may play

a role in recruiting Cpx to the site of fusion. By varying lipid unsaturation and PIP2 concentrations, we were able to determine how different lipids and membrane properties modulated the membrane binding of Cpx. Our data also indicated that Cpx binding rapidly saturates and that Cpx interferes with its own membrane binding at very low protein:lipid ratios.

The second objective was focused on understanding how the SNAREs influence the membrane affinity of Cpx. The individual SNAREs, Syx and SNAP25, were added to solution either as soluble proteins or incorporated into the vesicle membrane, and their effects on Cpx's membrane affinity were measured. This study found that the individual SNARE proteins when present in solution did not alter the membrane affinity of Cpx. However, SNAP25 and Syx had opposite effects on the membrane affinity of Cpx when membrane associated. When SNAP25 was membrane associated, it significantly increased the Cpx-membrane affinity. In contrast, membrane-bound Syx diminished the membrane affinity of Cpx. The SN1 and SN2 domains of SNAP25 have been found to function differently, so we tested their contributions to SNAP25's ability to increase Cpx-membrane affinity. It was also found that the ability of SN25 to enhance Cpx's membrane binding was primarily driven by its N-terminal SN1 domain. Additionally, the effect of assembled SNARE complexes on Cpx-membrane interactions was explored. Both an acceptor tSNARE complex and the ternary SNARE complex were added as soluble proteins in solution along with lipid vesicles or added as membrane-bound complexes. In both cases, the membrane bound forms increased the measured affinity of Cpx and the soluble SNARE complexes reduced membrane affinity, presumably due to Cpx's preference for binding to assembled SNARE complexes over lipid vesicles. Importantly, the increase in membrane affinity was primarily driven by the C-terminal region of Cpx. These findings underscore the importance of membrane-bound SNAREs in modulating Cpx's interactions with membranes.

Another question we wanted to address was when Cpx begins interacting with the SNARE complex. Although the state of the prefusion SNARE complex is not known, it has been suggested that Cpx binds to an acceptor complex composed of Syx and SNAP25 and blocks the insertion of Syb. We looked at Cpx's interactions with different configuration of SNAREs in solution and anchored onto membranes. Although the binding of Cpx to the SNAREs is well characterized, most studies have utilized truncated forms of the SNAREs and focused on the interactions of Cpx with SNAREs in solution. Since the membrane environment plays a crucial role in the fusion process and can modulate SNARE conformation, this study examined the interaction of Cpx with individual SNARE proteins (Syx, SNAP25), the acceptor tSNARE complex (Syx and SNAP25) and the fully assembled ternary SNARE complex (Syx, SNAP25 and Syb) in solution and the membrane. It was observed that while complexin interacts with Syx, a tSNARE complex, and the ternary complex in solution, it only binds to the membrane-bound ternary SNARE complex. This suggests that interactions that occur in solution are not be important on the membrane, and it demonstrates that when SNAREs are membrane bound, Cpx only interacts with a complex where all three SNARE proteins are present and assembled. These results challenge they hypothesis that Cpx blocks fusion by preventing the insertion of Syb into the SNARE complex. Instead, they indicate that Cpx's interactions with the assembled SNARE complex may function to regulate fusion at a later stage.

Finally, the interactions between Cpx, SNARE proteins, and Munc18 were investigated. By incubating membrane-bound SNARE complexes with Munc18, this study explored how Munc18 modulates Cpx's interactions with both lipid membranes and SNARE proteins, providing further insights into the regulatory mechanisms governing synaptic vesicle fusion.

Chapter 2 Materials and Methods

Table 1 Materials used in Lab experiments

Materials	Source
Pfu reaction buffer	Agilent
Pfu polymerase	
dNTPs (deoxynucleotide triphosphates)	Bio Basic
DpnI	New England Biolabs
Kanamycin	Chem-Impex
SOC media (Super Optimal broth with Catabolite repression)	Quality Biological
IPTG (Isopropyl β-D-1-thiogalactopyranoside)	GoldBio
HEPES (4-(2-Hydroxyethyl)piperazine-1-ethane-sulfonic acid)	Bio Basic
Sodium chloride	Sigma
Imidazole	GFS Chemicals
Potassium Chloride	IBI scientific
Triton X-100	EMD Millipore
Sodium Cholate	MP Biomedicals
Urea	Sigma / Research Products International

Glycerol	Research Products International
DPC	Anatrace
Aprotinin	Research Products International
AEBSF (4-(2-aminoethyl)benzenesulfonyl fluoride hydrochloride)	Cayman Chemical Company
Leupeptin	Research Products International
Benzonase Nuclease	Santa Cruz Biotechnology
Ni-NTA resin	Bio-Rad
Thrombin	Sigma
DTT (Dithiothreitol)	G Biosciences
dDMTS (Dodecyl Methanethiosulfonate)	Toronto Research Chemicals
Acetonitrile	Fisher Scientific
Alexa Fluor 546	Thermo Scientific
BODIPY® FL N-(2-aminoethyl)maleimide	
MTSL (2,2,5,5-tetramethyl-l-oxyl-3-methyl methanethiosulfonate)	Santa Cruz Biotechnology
Ethanol	Decon Laboratories
Chloroform	Sigma
Sucrose	Sigma
KH_2PO_4	Fisher Scientific
Perchloric Acid	Sigma

Ammonium Molybdate	Mallinckrodt Chemical Works
Ascorbic Acid	sigma
Methanol	LabChem
1-palmitoyl-2-oleoyl-glycero-3-phosphocholine (POPC)	Avanti Polar Lipids
1-palmitoyl-2-oleoyl-sn-glycero-3-phosphoethanolamine (POPE),	
1-palmitoyl-2-oleoyl-sn-glycero-3-phospho-L-serine (POPS)	
Cholesterol (Chol)	
brain L-α-phosphatidylinositol-4,5-bisphosphate (PIP2)	
1,2-dipalmitoyl-sn-glycero-3-phosphocholine (DPPC)	
1,2-dipalmitoyl-sn-glycero-3-phosphoethanolamine (DPPE)	
1,2-dipalmitoyl-sn-glycero-3-phospho-L-serine (DPPS)	
1,2-dioleoyl-sn-glycero-3-phosphocholine (DOPC)	
1,2-dioleoyl-sn-glycero-3-phosphoethanolamine (DOPE)	

1,2-dioleoyl-sn-glycero-3-phospho-L-serine (DOPS)	
1-stearoyl-2-arachidonoyl-sn-glycero-3-phosphocholine (SAPC)	

2.1 Site Directed Mutagenesis

Site directed Mutagenesis is a polymerase chain reaction (PCR) based technique used to introduce specific nucleotides within a plasmid DNA. This allows for the introduction of specific mutations into a protein sequence. In this study, single cysteine mutations (Q7C, K18C, D27C, A40C, K54C, D68C, S115C and T119C) were introduced into cysteine-free Cpx. To make mutant Cpx, primers containing the desired mutations were designed and ordered from Integrated DNA Technologies (IDT). The PCR reaction mixture was set up as shown in Table 2.

***Table 2**: Volumes of reagents for PCR reaction*

Reagent	Volume (µL)
10 X Pfu Turbo reaction buffer	5
DNA template (3 ng/µL)	1
dNTPs (10 mM)	1
Forward primer (10 µM)	1
Reverse primer (10 µM)	1
Pfu polymerase (2.5 U/µL)	1
Double deionized water	40

The PCR was performed using the T100 thermal cycler (Bio-Rad) with the following parameters:

Phase 1: Initial denaturation at 90 ^{0}C for 2 minutes

Phase 2: Amplification (30 cycles)

- Denaturation: 95 ^{0}C for 30 seconds
- Annealing: usually around 55^{0}C to 65 ^{0}C for 60 seconds
- Extension: 72 ^{0}C for 10 minutes

Phase 3: Final extension: 72 ^{0}C for 10 minutes

The annealing temperature used was based on the melting temperature (Tm) of the primers. A range of annealing temperatures (Tm – 5 °C, Tm °C, and Tm + 5 °C) were typically used to optimize primer binding. Following PCR, 1 uL of DpnI restriction enzyme was added to the PCR product and incubated at 37 ^{0}C for an hour. DpnI digests methylated DNA, therefore removing the template DNA while leaving the newly synthesized DNA. To confirm the success of the mutagenesis, the PCR products were analyzed using agarose gel electrophoresis.

2.2 Transformation into Competent Cells

After PCR, the plasmid containing the desired mutation was transformed into chemically competent *Escherichia coli* Top10 cells using standard heat-shock transformation protocol. The transformed cells were then plated onto LB-agar plates with kanamycin as an antibiotic. The plates were incubated overnight at 37 °C. The following day, a single colony was picked and inoculated into a 6 mL autoclaved LB media containing 40 mg/L kanamycin. The cell culture was incubated overnight with shaking at 200 rpm to allow bacterial growth and plasmid replication. After incubation, the plasmids were purified with GeneJet Plasmid Miniprep kit

(Thermo Fisher Scientific), following the manufacturer's protocol. The concentration and purity of the purified plasmid were determined using a Nanodrop spectrometer. The purified plasmid DNA was sent to Genewiz/Azenta Life Sciences for sequencing to verify the presence of the desired mutation. The sequencing results were analyzed by comparing the modified sequence with the wild-type sequence to confirm successful introduction of the mutation.

2.3 Protein Expression

Recombinant proteins were expressed in the *Escherichia coli* strain BL21 (DE3) using heat shock transformation protocol. 0.5 – 2 uL of plasmid DNA (concentration: 3 ng/uL) was added to 15 – 25 uL of competent BL21 (DE3) cells. Following a standard heat shock procedure, the cells were placed in a 42 ^{0}C water bath for 45 seconds. 150 uL of SOC media was added to the cells, and they were incubated at 37 ^{0}C for 2 hours with shaking. The transformed cells were added to LB-agar plates containing kanamycin and incubated at 37 ^{0}C overnight.

The next day, a single colony was picked and inoculated into 50 mL of autoclaved LB media with 40 mg/L kanamycin. The preculture was incubated at 37 ^{0}C with shaking at 200 rpm overnight to allow cell growth. The preculture was then added to 950 mL of LB media with the same antibiotic concentration. The main culture was incubated at 37 °C with shaking at 200 rpm until the optical density (OD600) reached 0.6-1. Isopropyl β-D-1-thiogalactopyranoside (IPTG) was added to the to the culture to a final concentration of 0.5 mM to induce protein expression. The temperature was lowered to 18 °C and the culture was allowed to shake overnight. The cells were harvested by centrifugation at 5000 rpm for 15 min. The cell pellet, which contains the expressed protein, was used immediately or stored at -20 ^{0}C for use later.

2.4 Protein Purification

Table 3: *Purification buffers for Cpx, SNAP25, Syb$_{1-96}$ and Munc18*

Name	Components	Concentration
Extraction Buffer	HEPES	20 mM
	NaCl	500 mM
	Imidazole	8 mM
Wash Buffer	HEPES	20 mM
	NaCl	500 mM
	Imidazole	20 mM
Elution Buffer	HEPES	20 mM
	NaCl	500 mM
	Imidazole	400 mM

Table 4: *Purification Buffers for Syx$_{1-262}$*

Name	Components	Concentration
	HEPES	20 mM

Extraction Buffer	NaCl	500 mM
	Imidazole	8 mM
Wash Buffer I	HEPES	20 mM
	NaCl	500 mM
	Imidazole	20 mM
Wash Buffer II	HEPES	20 mM
	NaCl	500 mM
	Imidazole	20 mM
	Triton X-100	1 %
Wash Buffer III	HEPES	20 mM
	NaCl	500 mM
	Imidazole	20 mM
	Sodium Cholate	1 %
Elution Buffer	HEPES	20 mM
	NaCl	500 mM
	Imidazole	400 mM

Table 5: *Purification Buffers for $Syx_{183-288}$ and full length Syx.*

Name	**Components**	**Concentration**

Extraction Buffer	HEPES	20 mM
	NaCl	500 mM
	Imidazole	8 mM
	Triton X-100	2 %
Wash Buffer I	HEPES	20 mM
	NaCl	500 mM
	Imidazole	20 mM
	Urea	6 M
	Glycerol	10 %
	Triton X-100	1 %
Wash Buffer II	HEPES	20 mM
	NaCl	500 mM
	Imidazole	20 mM
	Glycerol	20 %
	Triton X-100	1 %
Wash Buffer III	HEPES	20 mM
	NaCl	500 mM
	Imidazole	20 mM
	Triton X-100	1 %

Wash Buffer IV	HEPES	20 mM
	NaCl	500 mM
	Imidazole	20 mM
	n-Dodecyl-phosphocholine (DPC)	0.1 %
Elution Buffer	HEPES	20 mM
	NaCl	500 mM
	Imidazole	400 mM
	n-Dodecyl-phosphocholine (DPC)	0.1 %

Table 6: *Purification buffers for* $Syb_{1\text{-}116}$

Name	**Components**	**Concentration**
Extraction Buffer	HEPES	20 mM
	NaCl	500 mM
	Imidazole	20 mM

	Sodium Cholate	25 %
Binding Buffer	HEPES	20 mM
	NaCl	500 mM
	Imidazole	20 mM
Wash Buffer I	HEPES	20 mM
	NaCl	750 mM
	Imidazole	50 mM
	Urea	6 M
	Glycerol	10 %
	Sodium Cholate	1 %
Wash Buffer II	HEPES	20 mM
	NaCl	750 mM
	Imidazole	50 mM
	Glycerol	20 %
	Sodium Cholate	1 %
Wash Buffer III	HEPES	20 mM
	NaCl	750 mM
	Imidazole	50 mM

	n-Dodecyl-phosphocholine (DPC)	0.1 %
Elution Buffer	HEPES	20 mM
	NaCl	500 mM
	Imidazole	400 mM
	n-Dodecyl-phosphocholine (DPC)	0.1 %

2.4.1 Ni-NTA Affinity Chromatography

All the proteins were purified using affinity chromatography, followed by ion exchange or size exclusion chromatography as required. The proteins were initially purified using Ni-NTA affinity chromatography with the buffers listed in **Table 3** to **Table 6**. All buffers were prepared at pH 7.4. The cell pellets were resuspended in 25 mL of extraction buffer. Protease inhibitors aprotinin, AEBSF and leupeptin were added to prevent protein degradation. Benzonase nuclease was also added to degrade DNA and RNA to facilitate their removal during the purification process. The cells were lysed using a French press to release intracellular contents, including the protein of interest. The protein was kept on ice during the French press to preserve the integrity of the protein. For the SNARE proteins, 2M of urea was added to SNAP25 and 6M of urea was added to Syx and Syb and incubated for 30 to 60 minutes on ice to prevent the formation of inclusion bodies.

The cell lysate was centrifuged at 32,000 rpm for 45 minutes to remove cell debris. A volume of 2 to 10 mL of Ni-NTA resin was added to a glass column (Bio-Rad) and washed with extraction

buffer. The supernatant from centrifugation was added to the resin and incubated for at least 2 hours at 4 °C to allow the His-tagged proteins to bind to the resin. The resin was washed thoroughly with the appropriate wash buffers to remove contaminants. The protein was then eluted with an elution buffer in 2 mL fractions. Fractions that contained protein were identified using Bradford reagent which turns from a reddish-brown color to blue when protein is present. Fractions with protein were collected and incubated with 1 mg of thrombin for 2 hours at room temperature or overnight in the cold room to remove the His-tag.

2.4.2 Ion Exchange

Complexin, SNAP25, Syx_{1-262}, Syb_{1-96} were taken through a further ion exchange chromatography purification step. The proteins were first dialyzed against a 20 mM HEPES buffer (pH 7.4) using dialysis tubing (Spectrum Laboratories) with the appropriate molecular weight cutoff. Ion exchange was performed using a HiTrap Q HP column on an AKTA purifier system. Syb_{1-96} required and SP column for cation exchange. A salt gradient was generated using 20 mM HEPES and 20 mM HEPES with 1 M NaCl buffers. The proteins were eluted at specific salt concentrations, as tracked by the chromatogram.

Fractions containing protein were further analyzed with SDS-PAGE to confirm the presence and purity of proteins. Samples before and after thrombin incubation were also run on the SDS-PAGE to confirm successful cleavage of the His-tag. The purified proteins were dialyzed against a reconstitution buffer (RB150, 20 mM HEPES, 150 mM KCl, pH 7.4). The proteins were then concentrated by centrifugation with Amicon Ultra centrifugal filters. The proteins were quantified using a nanodrop and then used for later experiments or stored in a -80 ^{0}C freezer.

2.4.3 Size exclusion

FL Syntaxin, Syntaxin$_{183-288}$ and Syb$_{1-116}$ were purified using size exclusion chromatography. After elution from Ni-NTA column, the proteins were concentrated to 0.5 mL and loaded onto a Superdex 200 Increase 10/300 GL column using a Bio-Rad system. The running buffer used contained 20 mM HEPES, 150 mM KCl and 0.1 % DPC at pH 7.4. The proteins were eluted based on their size and their presence and purity verified with SDS-PAGE. Fractions containing purified proteins pooled, concentrated, and quantified using a nanodrop. The proteins were then stored at -80 ^{0}C. All buffers used for purification were filtered and thoroughly degassed by sonication or under vacuum.

2.5 Alkylation of SNAP25, dSN1 and dSN2

SNAP25 does not have a transmembrane domain and relies on palmitoylation of its native cysteines for membrane contact. To generate SNAP25 that can adhere to membranes, an alkyl chain was engineered onto it. After purification with ion exchange chromatography, SNAP25 with all its native cysteines present, was buffer exchanged into a spin label buffer (20 mM HEPES, 500 mM NaCl, 0.1% DPC, pH 7.4). The buffer was thoroughly degassed prior to use. SNAP25 was then concentrated down to 0.5 ml with a concentration greater than 1 mM. To reduce any disulfide bonds, DTT was added to the SNAP25 solution at 20-fold molar excess per cysteine. SNAP25 contains four native cysteines and the total DTT concentration was calculated accordingly. The reaction was allowed to proceed for 2 hours at room temperature on a rocker. A PD10 desalting column (Cytiva) was used to separate SNAP25 from DTT.

Dodecyl methanethiosulfonate was dissolved in acetonitrile and added in 10-fold molar excess and allowed to react at room temperature for 2 hours. A PD10 desalting column was used to separate the dodecylated SNAP25 (dSNAP25) from any unreacted dodecyl methanethiosulfonate. dSN25 was concentrated and further purified with size exclusion chromatography to obtain its monomeric form. A native page gel electrophoresis was run and fractions containing monomeric dSN25 were collected, concentrated, and quantified. The purified protein was stored at -80 °C for further experiments. The alkylated forms of SN1 and SN2 were generated using a similar protocol.

2.6 SNARE complex assembly

To assemble the tSNARE acceptor complex, Syx was added to SNAP25 in a 1:1 molar ratio dropwise with stirring. For the ternary SNARE complex, SNAP25 and Syb were first mixed together, followed by a dropwise addition of Syx final molar ratio of 1:1:1. The mixtures were stirred gently while adding Syx and incubated overnight on a rocker in a cold room to allow formation of the complex.

2.7 Labelling Proteins

Complexin was labelled with Alexa Fluor 546 C5 maleimide for fluorescence anisotropy experiments or with MTSL (2,2,5,5-tetramethyl-l-oxyl-3-methyl methanethiosulfonate) for cwEPR (continuous wave Electron Paramagnetic Resonance) experiments. MTSL is sold as a powder and was dissolved in ethanol before use. To label complexin, its native cysteine at position 105 was mutated into a serine. Single cysteine mutations (Q7C, K18C, D27C, A40C, K54C, D68C, S115C and T119C) were introduced into cysteine free complexin using site directed mutagenesis. Spin labels were introduced at all mutated sites while only position 119 was fluorophore labelled.

After the complexin mutants were purified, they were buffer exchanged into a degassed labelling buffer (20 mM HEPES, 500 mM NaCl, pH 7.4). Complexin was then concentrated to a concentration greater than 1mM and volume of 0.5 mL to ensure efficient labelling. To reduce any disulfide bond formation, 20-fold molar excess DTT was added to the protein solution and allowed to react for 2 hours at room temperature on a rocker. A PD10 desalting column was used to remove DTT to ensure there were no residual reducing agents prior to labeling. DTT- free Cpx was then reacted with 10-fold molar excess fluorophore or spin label for 2 hours at room temperature on a rocker. Tubes with the protein being labelled were wrapped in aluminum foil and the entire setup was kept in the dark. Another PD10 column was used to separate the labelled protein from unreacted label. The protein was dialyzed into a reconstitution buffer (20 mM HEPES, 150 mM KCL, pH 7.4).

2.8 Vesicle Preparation and Quantification

Different vesicle preparation methods were employed depending on the specific experimental requirements. When dried lipids were solubilized in aqueous buffers, they formed large multilamellar vesicles. To prepare small unilamellar vesicles that were uniform in size, the vesicles had to undergo further preparation methods. The methods used to prepare these vesicles are discussed below. All lipids used were obtained either in a powdered form or dissolved in chloroform. The powdered lipids were dissolved in chloroform prior to use.

2.8.1 Drying Lipids

For all vesicle preparations, the appropriate amount of lipids was measured into a glass tube. When preparing lipid mixtures containing PIP2, a drop or two of methanol was added to improve its solubility. The chloroform was evaporated under a gentle stream of nitrogen, to prevent oxidation of

lipids, leaving behind a thin, uniform lipid film on the glass surface. The lipids were placed in a vacuum chamber for at least two hours to remove any residual chloroform. The dried lipids were used to form lipid vesicles.

2.8.2 Extrusion of Sucrose Loaded Vesicles

After drying, the lipids were resuspended in a sucrose buffer (20 mM HEPES, 256 mM sucrose, pH 7.4) which was freshly made on the day of use. After thoroughly vortexing, the hydrated lipid film formed large multilamellar vesicles. The lipid suspension underwent at least five freeze-thaw cycles. This involved alternating between freezing the samples in liquid nitrogen and thawing them in room temperature water, which aids in disrupting the multilamellar structure and facilitates the extrusion process. The extruder was set up with filter supports (Cytiva) and two 100 nm polycarbonate membrane (Whatman). The syringes and extruder were pre-equilibrated with sucrose buffer. The lipid suspension was then passed through the extruder at least 10 times to obtain 100 nm sucrose-loaded vesicles.

To remove the extravesicular sucrose, the suspension was diluted with RB150 and centrifuged at 100,000 x g for an hour at 20 °C. The lysate was discarded, and the vesicle pellet was resuspended in RB150. The sucrose loaded vesicles were ready for use.

2.8.3 Sonication

To prepare vesicles via sonication, the dried lipids were first resuspended in RB150 and thoroughly vortexed. The hydrated lipids were sonicated using a probe sonicator under a stream of argon gas. The argon gas was used to reduce lipid oxidation. The sonication process generates heat, so samples were kept on ice to prevent overheating. Sonication results in the formation of small unilamellar vesicles.

2.8.4 Detergent Dialysis

To incorporate membrane proteins into lipid vesicles, the vesicles were prepared with detergent dialysis. The dried lipids were solubilized in RB150 containing 25 mM sodium cholate. For vesicles containing SNAREs, the proteins were added, and the mixture was allowed to equilibrate at room temperature for an hour. The lipid-detergent mixture was diluted with RB150 to lower the final sodium cholate concentration to 16 mM, just above the critical micelle concentration. The suspension was dialyzed against RB150 overnight to remove the detergent. The vesicles were subjected to two additional dialysis, each lasting for four hours, to ensure complete removal of the detergent. This method yielded vesicles that had SNARE proteins incorporated into their bilayers.

2.9 Phosphate Assay for the Quantification of Lipids

Lipid vesicle preparations result in a final concentration that is lower than the initial amount due to losses during the preparation process. To ensure accurate lipid concentrations for subsequent experiments, the concentration of the lipid vesicles needs to be quantified. This study used a modified version of the phosphate assay based on methods developed by Pokorny and Barlett.[89,90] A standard solution of 1mM KH_2PO_4 was prepared to generate a standard curve. To prepare the standards, volumes of 0, 20, 40, 80, 100, 150 and 200 µL of the KH_2PO_4 solution were added to glass tubes. The volume in each tube was adjusted to 300 µL with ddH_2O. For the lipid samples, 5 to 15 µL of the lipid vesicles were added to a glass tube and ddH_2O was added to a volume of 300 µL. All samples and standards were prepared in triplicate.

To hydrolyze the phosphate group, 700 µL of perchloric acid was added to all standard and sample tubes. The glass tubes were covered with glass marbles and placed in a heating block at 200 °C for an hour in a fume hood. The samples were cooled down completely to room temperature. 2

mL of 1 % ammonium molybdate solution was added to each tube and vortexed to ensure thorough mixing. 2 mL of 4 % ascorbic acid solution was then added to each tube, followed by vortexing. The samples are placed in a water bath at 37 °C for 30 minutes to develop a blue color indicative of the presence of phosphate. The intensity of the blue color is proportional to the phosphate concentration (**Figure 2-1**). The absorbance of each sample and standard was measured at 800 nm using a spectrophotometer. Absorbance readings of KH_2PO_4 standards were used to generate a standard curve. The concentration of lipids was determined from the standard curve.

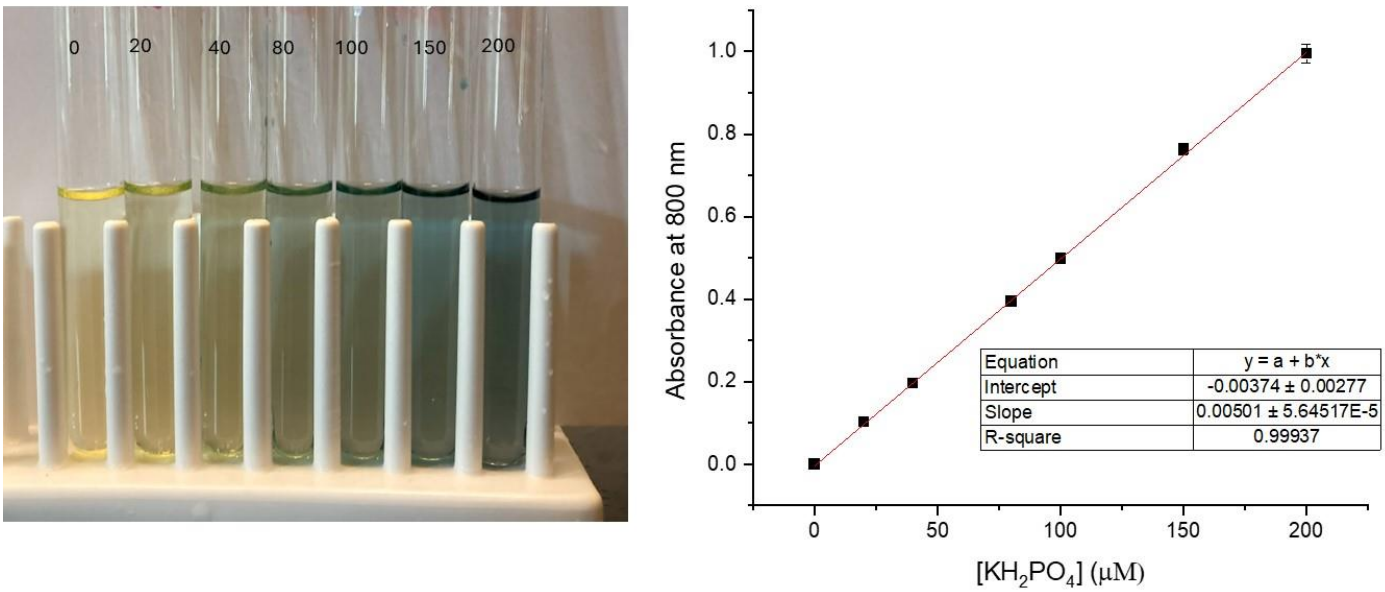

Figure 2-1 *Standards for Phosphate Assay: The left panel shows glass tubes containing varying concentrations of KH_2PO_4 after the addition of ammonium molybdate and ascorbic acid. The color intensity increases with increasing phosphate concentration. The right panel represents the corresponding standard curve with absorbance measured at 800 nm.*

2.10 Ultracentrifugation Sedimentation Assay

Sedimentation assay was used to determine binding between Alexa labelled Munc18 or BODIPY labeled C2AB, and sucrose loaded vesicles. This technique allowed the separation of vesicle-

bound protein from unbound protein using ultracentrifugation (Figure 2-2). A constant concentration of 100 nM of the labelled Munc18 or 200 nM of C2AB was added to all the ultracentrifugation tubes. Increasing concentrations of sucrose loaded vesicles (preparation described in Section 2.8.2) were added to the tubes. They were then diluted with RB150 to 1 mL and incubated for 10 minutes. Centrifugation at 100,000 x g, 20 ^{0}C for an hour was performed to pellet the vesicles. Protein that was bound to vesicles were pelleted together with the vesicles while the unbound protein remained in the supernatant. The fluorescence emission was used to determine protein binding to sucrose loaded vesicles and the partition coefficient was determined similarly to fluorescence anisotropy.

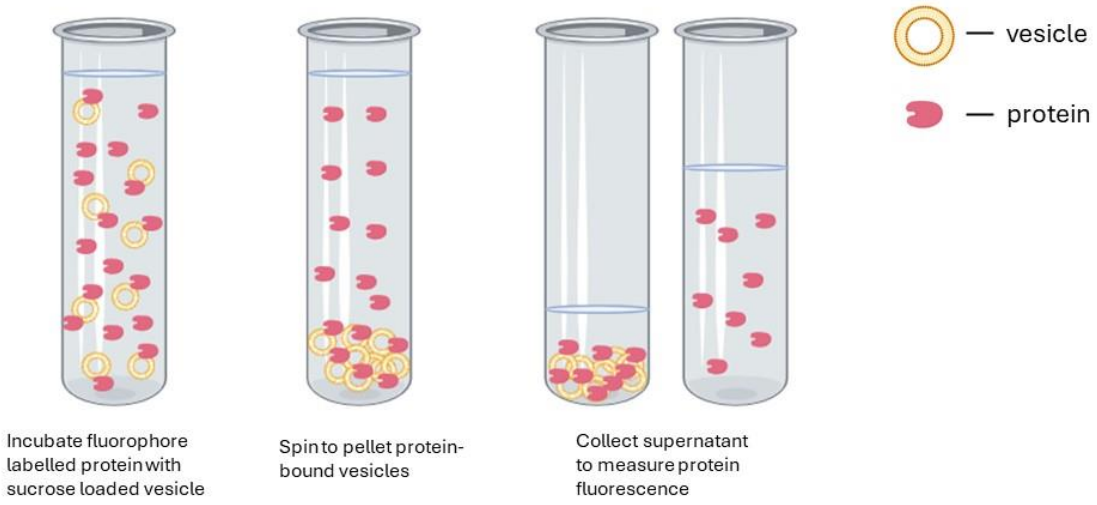

Figure 2-2 *Ultracentrifugation sedimentation assay workflow. Image created with BioRender.com.*

2.11 Fluorescence Anisotropy

Fluorescence anisotropy is a powerful technique that can be used to study biomolecular interactions in solution. One major advantage of anisotropy is its ability to work with low concentrations of labeled proteins. This is especially important for measuring Cpx-membrane interactions, which is sensitive to the concentration of Cpx present. Another advantage is that measurements can be taken at room temperature, and it is tolerant to photobleaching due to ratio

measurements. Also, the fraction of protein bound can be measured directly without the need for separating it from unbound protein.[91]

When unpolarized light passes through a polarizer, it isolates light travelling in a specific direction. This polarized light is absorbed by a fluorophore, exciting it (**Figure 2-3**). The excited fluorophore emits fluorescence, and the emitted light is passed through another polarizer which separates the light into two components: one that is parallel to the excitation light and another that is perpendicular. Fluorescence anisotropy measures the degree to which emitted light remains polarized relative to the excitation light and is given by Equation 2.1.

$$r = \frac{I_{\parallel} - I_{\perp}}{I_{\parallel} + 2I_{\perp}} \qquad Equation\ 2.1$$

where r is the anisotropy, $I_{\parallel}$ and $I_{\perp}$ are the fluorescence intensities of the parallel ($I_{\parallel}$) and perpendicular ($I_{\perp}$) components of the emitted light.

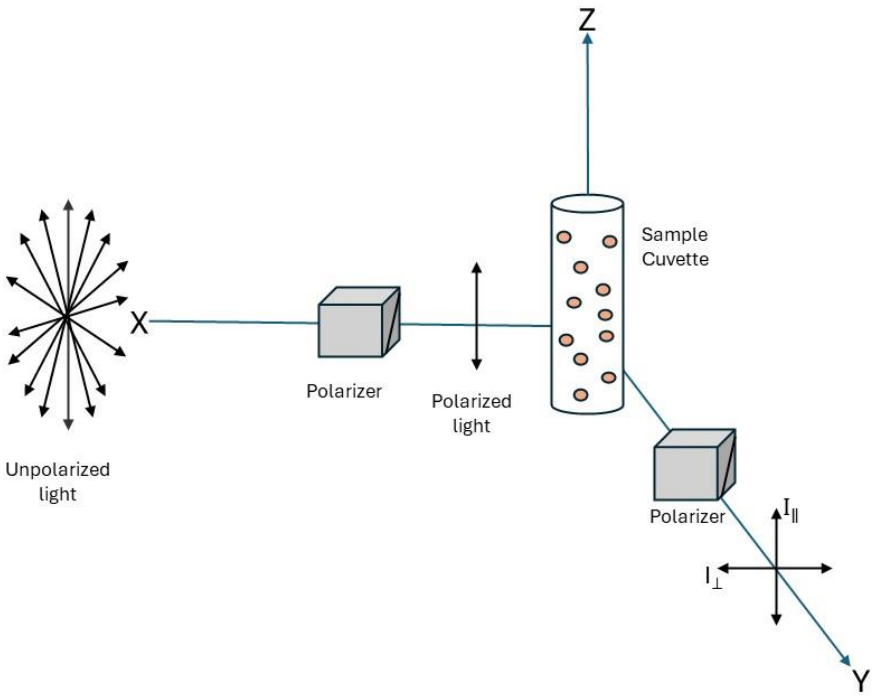

Figure 2-3 *Principle of fluorescence anisotropy. Unpolarized light passes through a polarizer and the polarized light excites the fluorophore in the cuvette. The parallel and perpendicular intensities of the fluorescence emission are used to determine the anisotropy.*

Perrin's equation describes the relationship between fluorescence anisotropy, rotational diffusion, and molecular size:

$$\frac{r_0}{r} = 1 + \frac{\tau}{\theta} = 1 + 6D\tau \qquad Equation\ 2.2$$

where r_0 is the fundamental anisotropy, τ is the fluorescence lifetime, D is the rotational diffusion coefficient and θ is the rotational correlation time and is defined as:

$$\theta = \frac{\eta V}{RT} = \frac{\eta M}{RT}(v + h) \qquad Equation\ 2.3$$

where η is the viscosity, V is the volume, R is the gas constant, T is the temperature, M is the molecular weight, v is the specific volume and h is the hydration.

Anisotropy is sensitive to factors that change rotational diffusion of the fluorophore.[92] These include viscosity, temperature of the solution as well as apparent molecular size. The fluorophore labelled protein rotates rapidly in solution, leading to depolarization of the emitted light. This results in lower anisotropy. When the fluorophore labelled protein binds to a vesicle, its molecular size increases and it tumbles more slowly in solution. As a result, the emitted light retains the polarization of the excitation source, leading to higher anisotropy (**Figure 2-4**).

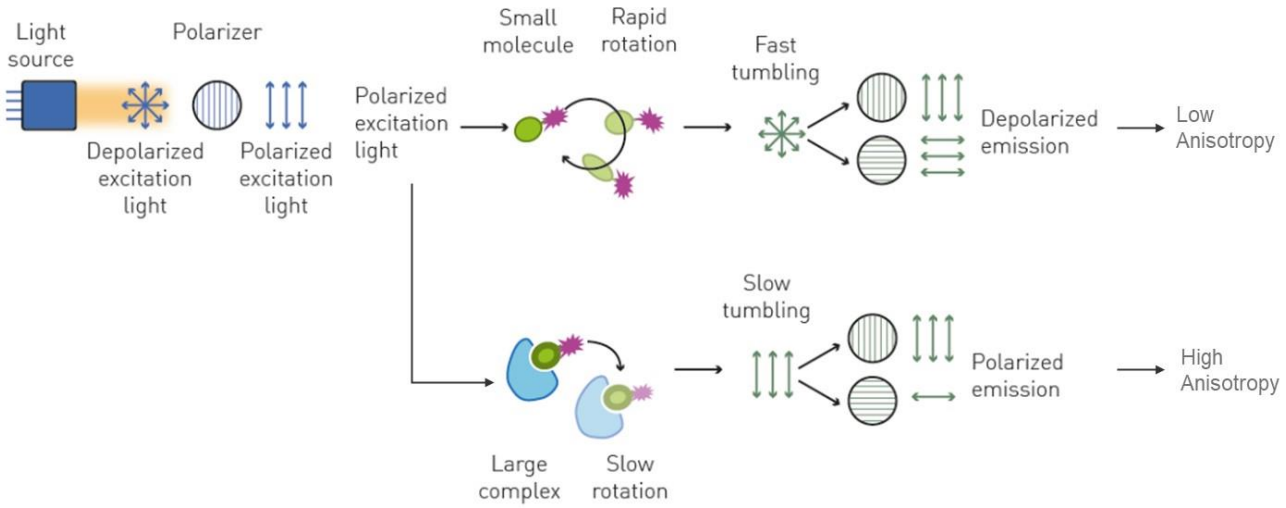

Figure 2-4 *Measurement of anisotropy. The anisotropy depends on the size of the complex to which the fluorophore is attached. The larger the complex, the less depolarized the emission, resulting in a high anisotropy. Figure modified from* [93]

For our experiments, Cpx labelled at position 119 with Alexa546 was added to a cuvette at a concentration of 50 nM in a total volume of 1.2 mL. The excitation and emission wavelengths were set at 546 nm and 573 respectively. Anisotropy measurements were performed with a Horiba fluorometer with the temperature set at 20 ^{0}C. Increasing concentrations of lipids, prepared either by sonication or dialysis, were added to the cuvette, and the anisotropy recorded after each addition.

The interaction between Cpx and lipid vesicles can be quantified using the partition coefficient K_p, which represents the ratio of the concentration of Cpx bound to lipid vesicles ([Cpx_{bound}]) to concentration complexin free([Cpx_{free}]) in solution and is described by Equation 2.4.

$$K_p = \frac{[Cpx_{bound}]}{[L][Cpx_{free}]} \qquad Equation\ 2.4$$

where [L] is the accessible lipid concentration and is the lipid on the outer leaflet of the lipid vesicles that are available for interaction with Cpx. The fraction of complexin bound to membranes (f_b) is given by:

$$f_b = \frac{[Cpx_{bound}]}{[Cpx_{bound}] + [Cpx_{free}]} = \frac{K_p[L]}{K_p[L] + 1} \qquad Equation\ 2.5$$

The fraction bound can also be expressed in terms of anisotropy:

$$f_b = \frac{r_{free} - r}{r_{free} - r_{bound}} \qquad Equation\ 2.6$$

where r_{free} is the anisotropy of Cpx in solution without any binding partners and r_{bound} is anisotropy when complexin is completely membrane bound. The data is plotted in OriginPro 7.5 using Equation 2.7 and r_{free} is kept constant while varying r_{bound} and K_p.

$$r = \frac{r_{free}}{1 + K_p[L]} + \frac{K_p[L]r_{bound}}{1 + K_p[L]} \qquad Equation\ 2.7$$

2.12 Electron Paramagnetic Resonance

Electron paramagnetic resonance (EPR) is a highly sensitive and specific spectroscopic technique used to study systems containing unpaired electrons. It works by detecting the absorption of electromagnetic radiation by paramagnetic centers that are placed in a magnetic field. In continuous wave EPR (cwEPR) a sample is continuously irradiated by a low intensity microwave radiation. One of the key advantages of EPR is its specificity: since biological samples typically lack unpaired electrons, EPR only detects the paramagnetic species that is introduced, such as a spin label. This eliminates any potential background signal from non-paramagnetic components. Also, EPR is a non-denaturing technique, allowing samples to be recovered after experiments for further studies. EPR allows the study of proteins in physiological buffers and at room temperatures, allowing proteins to remain in their native conformations. Importantly, EPR enables the quantification of molecular interactions between bound and unbound species without the need for physically separating them, making it an ideal tool for studying protein-protein and protein-lipid interactions.

Since most biological samples do not contain an unpaired electron, site directed spin labeling (SDSL) is employed to introduce paramagnetic probes into specific sites on a protein.[94,95] This helps provide information on the local environment of the probe. SDSL-EPR can be used to probe local structural changes due to conformational change or interactions with other substrates, depth of spin label in membrane bilayers or the distance between labelled sites.[96]

SDSL involves the attachment of a spin label containing an unpaired electron to a specific site on a protein. One of the most well studied and commonly used spin labels is 2,2,5,5-tetramethyl-l-oxyl-3-methyl methanethiosulfonate (MTSL).[97] It contains an unpaired electron that resides primarily on the ^{14}N atom. This label reacts with a cysteine residue to form the R1 side chain (Figure 2-5). To ensure site-specific labeling, native cysteines in the protein are substituted with other amino

acids using site-directed mutagenesis or shown to be unreactive to the spin label. In our experiments, the single cysteine in Cpx at position 105 was mutated to a serine before the introduction of new cysteines at our sites of interest. Previous studies have shown that introduction of the MTSL label does not substantially alter the structure or function of labelled proteins.[98–101]

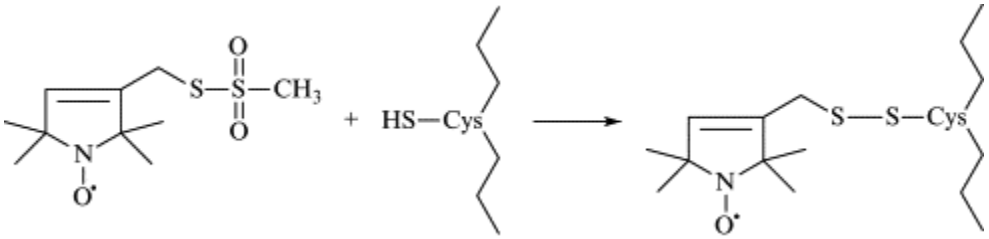

Figure 2-5 *MTSL reacts with a cysteine residue of a protein forming the R1 side chain. Figure adapted from*[96]

2.12.1 Theory of EPR

Electrons have an intrinsic angular momentum known as spin. The electron spin can exist in two states that differ in orientation but have the same magnitude of angular momentum. These spin states have the same energy and are described as degenerate. The magnetic moment of an electron is related to the spin by:

$$\mu_e = m_s g_e \beta \qquad Equation\ 2.8$$

where μ_e is the magnetic moment, m_s is the electron spin quantum number, g_e is the g-factor of a free electron and g_e=2.0023, $\beta$is the Bohr magneton. In the presence of a magnetic field, the energy (E) of the magnetic moment is given by:

$$E = m_s g_e \beta B_0 \qquad Equation\ 2.9$$

where B_0 is the magnetic field intensity. The magnetic field produces two different energy levels; a lower energy level where the electron's moment is aligned with the magnetic field and a higher energy level where the moment is against the magnetic field. Since the electron can be in two states with m_s = +1/2 for the antiparallel state or -1/2 for the parallel state, the electron spin energy is given by:

$$E_{\pm} = \pm\frac{1}{2g_e\beta B_0} \qquad Equation\ 2.10$$

and

$$\Delta E = h\nu = g_e\beta B_0 \qquad Equation\ 2.10$$

The splitting of the spin energy level in the presence of an applied magnetic field is known as the Zeeman effect (Figure 2-6). Equation 2.10 is the fundamental equation of EPR. An unpaired electron in the lower energy level can absorb radiation energy and move to the higher level by absorbing energy equal to ΔE.

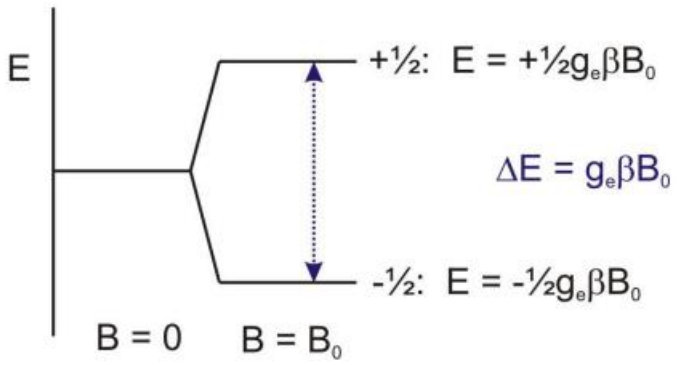

Figure 2-6 Illustration of the electron Zeeman effect. Figure adapted from [102]

From Equation 2.10, EPR experiments can be carried out in two ways. First, the magnetic field can be kept constant while frequency is varied or the frequency kept constant while magnetic field is varied. Depending on what is being varied, when the frequency of the microwave radiation matches

the magnetic field intensity, resonance conditions are met, and microwaves are absorbed.[103] In practice, the radiation frequency is kept constant while the magnetic field is varied. As the magnetic field increases, the separation between energy levels increases. At resonance conditions, when the energy difference matches the microwave radiation, the electron absorbs energy and can transition between the energy levels and this absorption is converted to a spectrum.

Electrons in an atom experience an extra magnetic field from their interaction with the nucleus and this is referred to as the hyperfine interaction (**Figure 2-7**). This gives rise to further splitting of the EPR line. For a nucleus with an angular momentum I, the EPR will be split into 2I + 1 components. For our nitroxide spin label with an I =1, the EPR is divided into three lines. The resonance condition is then:

$$\Delta E = h\nu = g_e \beta B_0 + A m_I \qquad Equation\ 2.11$$

where A is the hyperfine coupling constant and m_l is the magnetic quantum number of the nucleus. The allowed EPR transitions occur between energy levels that obey the selection rule (Δm_s = ±1 and Δm_I = 0). In order to improve the signal to noise ratio, a small 100 kHz modulation is applied to the magnetic field and any signal that does not have this 100 kHz encoding is filtered out by the detector. This results in an EPR spectrum that is the first derivative of the absorption spectrum.

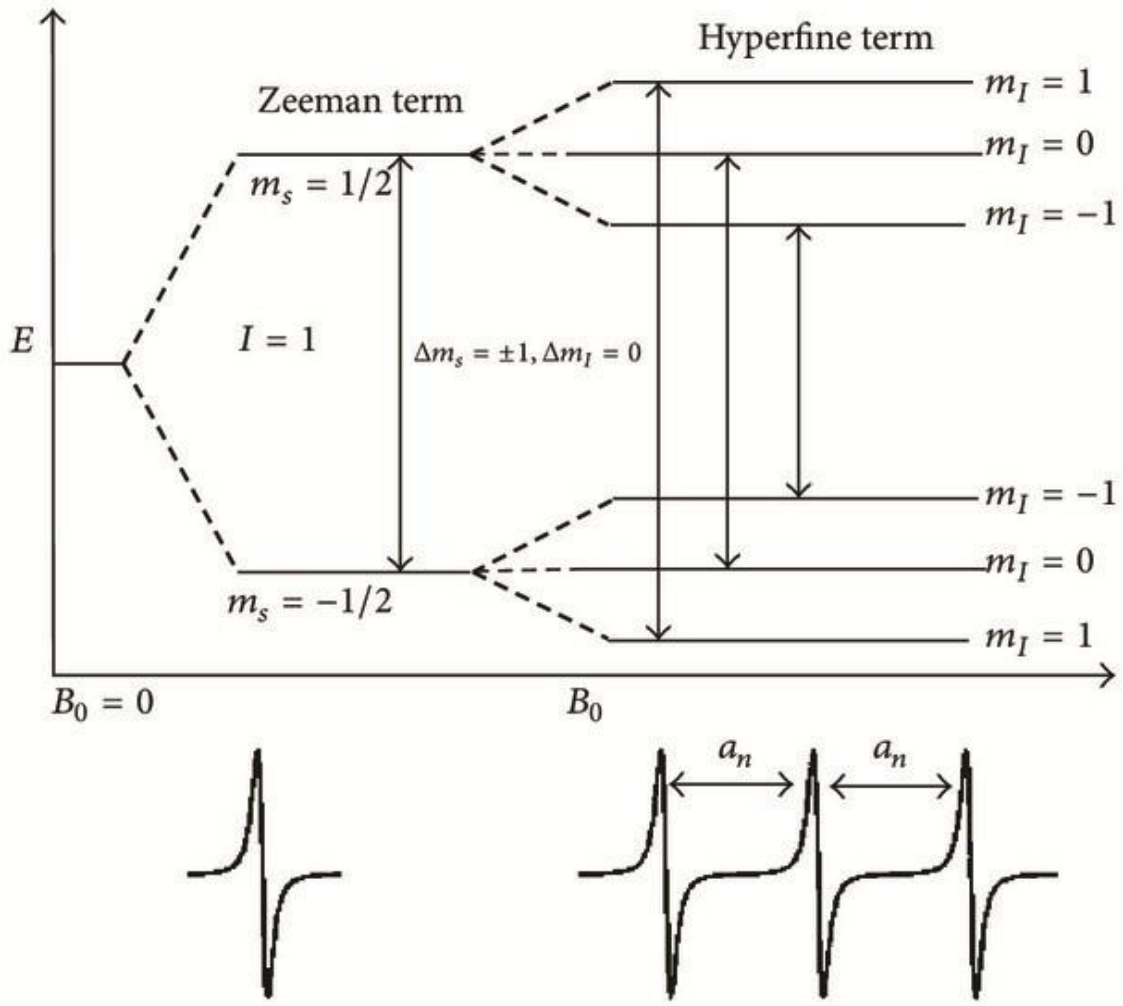

Figure 2-7 *Illustration of the hyperfine interaction of the nitroxide spin label. Figure adapted from* [104]

The g and A values are anisotropic and depend on the orientation of the molecule relative to the applied magnetic field.[104] When the motion of the spin label is not restricted, it tumbles rapidly in solution, averaging the anisotropic hyperfine and Zeeman interactions. This produces a spectrum with narrow, sharper lines. When the motion of the nitroxide spin label is hindered, by for example interaction with another protein or a vesicle, this leads to broadening of the EPR spectrum due to incomplete averaging of the g and A values. Since the EPR spectrum is sensitive to rotational motion, it can be used to probe Cpx's interaction with SNAREs or vesicle membranes.[105] When the spin

labelled Cpx is in solution without any binding partners, the EPR spectrum yields narrow, sharp lines. When bound, motion of the spin label is restricted yielding a broadened spectrum with decreased amplitude. The intensity of each line is proportional to the product of its amplitude and square of its width, and the amplitudes decrease as the lines broaden.[96] We measured Cpx's interactions with intensity ratio (Equation 2.12) with lower values indicating stronger interactions.

$$Intensity\ ratio = A_{pp}/A_{pp(free)} \qquad Equation\ 2.12$$

where A_{pp} is the peak-to-peak amplitude of CpxR1 with interacting partners and $A_{pp(free)}$ is peak-to-peak amplitude of Cpx R1 free in solution (Figure 2-8).

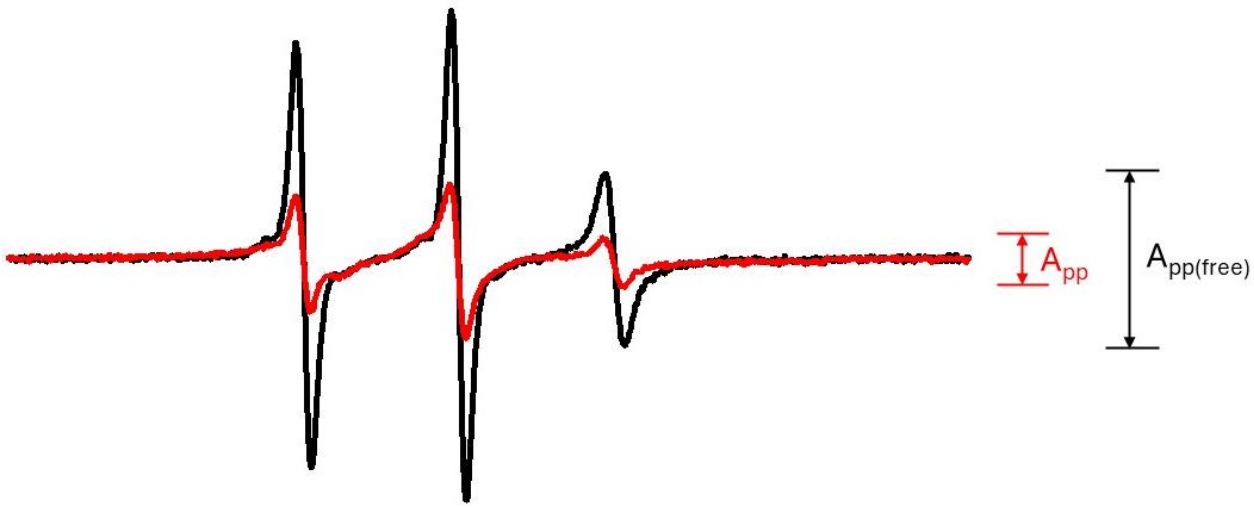

Figure 2-8 *Measurement of the peak-to-peak (A_{pp}) of the high field resonance line*

To run the cwEPR experiment, a 6 uL sample was loaded into a 0.6 X 0.8 (ID x OD) 100 mm long borosilicate glass capillary (VitroCom) with a Hamilton syringe. Measurements were performed on a Bruker EMX X-band spectrometer using a 5 mm dielectric resonator, an incident microwave

power of 2 mW, a modulation amplitude of 1 G, and a modulation frequency of 100 kHz. The magnetic field was swept over 100 G and up to 30 scans were averaged to increase the signal-to-noise ratio. The spectra were processed and normalized using in-house programs and plotted using Origin 2024.

Chapter 3 RESULTS

3.1 Complexin interacts with membranes and is sensitive to membrane properties.

3.1.1 Complexin prefers to bind to unsaturated lipid vesicles

Complexin (Cpx) is well known to interact with membranes and it has a preference for highly curved membranes.[51,105] This preference may be the result of an increase in packing defects that occur in curved membranes.[106] Membrane packing defects are regions at the membrane-aqueous interface where the hydrophobic acyl chains are exposed, and a number of factors in addition to curvature may promote these defects. For example, lipids whose shape departs from the canonical cylindrical shape may introduce imperfections in lipid packing and thereby promote defects.[74] Additionally, acyl chains with double bonds introduce a "kink" in the chain. This increases the lipid chain disorder and allows the chain to occupy a larger volume, which may also promote defects. The membrane binding of Cpx is mediated by its C-terminus, and it is proposed that the C-terminal domain of Cpx preferentially inserts its hydrophobic residues into these packing defects.[51,106]

Lipid chain disorder also appears to play a role in the function of other proteins that mediate membrane fusion. In their study, Kiessling et al. discovered a correlation between the tilt angle of SNAREs in membranes and their fusogenic activity.[88] They observed that Synaptotagmin when it binds membranes, disorders the lipid acyl chains, leading to conformational changes in the juxta-membrane region of SNAREs. This alteration facilitates a transition of the SNAREs from a trans to cis conformation, thereby enhancing their fusogenic potential.

To directly measure the effect of acyl chain disorder on the Cpx-membrane affinity, fluorescence anisotropy is employed. Fluorescence anisotropy (see Methods) is sensitive to the

rotational diffusion of the fluorophore, and when a fluorophore-labelled protein binds to a membrane, its rotational diffusion decreases dramatically. As a result of this slower diffusion, there is an increase in anisotropy that can be measured with a fluorometer.

In the work described here, Cpx was labelled at position T119 with an Alexa 546 fluorophore and used for the anisotropy measurements. Lipid vesicles were prepared via sonication and quantified with a phosphate assay. The lipid vesicles were titrated into a solution containing 50 nM of the labeled Cpx. As the concentration of lipids is increased, more Cpx binds to the vesicle membrane, leading to an increase in anisotropy. The change in anisotropy as a function of accessible lipid concentration was fit to a simple binding isotherm (see Eq. 2.7 in Materials and Methods). From this, the fraction of bound protein could be calculated and reciprocal molar partition coefficient determined. The partition coefficient is a measure of the membrane binding affinity, and a larger value indicates a stronger Cpx-membrane interaction.

The lipid bilayers used here had fixed headgroup composition which we refer to as PM1. The PM1 lipid composition is PC:PE:PS:Chol:PIP2 = 34:30:15:20:1. To test the effect of acyl chain order, the chain composition was varied and included dioleoyl (DO), palmitoyl oleoyl (PO), or dipalmitoyl (DP) acyl chains. The designation POPM1 would indicate a lipid with a PM1 headgroup composition and palmitoyl oleoyl (PO) acyl chains. The results of varying the acyl chain composition indicate the partition coefficient of Cpx increases as the lipid acyl chain unsaturation in the lipid bilayer increases. The partition coefficient is shown in Figure 3-1 A, B, and indicates that there is a 20-fold increase in partition coefficient when going from DPPM1 to POPM1 and a 30-fold increase in affinity when going from DPPM1 to DOPM1. With the most saturated lipid chains (DPPM1), there is the least interaction between Cpx and the sonicated vesicles. With the introduction of unsaturation in one chain while keeping the other chain saturated in POPM1, there is a significant increase in Cpx-membrane interaction which is further increased in doubly unsaturated DOPM1. It is known that as

acyl chain unsaturation increases, the lipids are not able to pack together as tightly, the area per lipid increases, and there is an increased exposure of the acyl chains at the membrane interface.[74] Our hypothesis is that Cpx binding affinity increases with unsaturation because there are more packing defects to accommodate the insertion of Cpx C-terminus.

In previous work, cholesterol was found to increase Cpx-membrane interactions by increasing the area of packing defects.[106] The increase in the area of packing defects was accompanied by a decrease in the number of packing defects.[106] Cholesterol was able to do this by connecting smaller defects to form larger packing defects. The increased defect area resulted in an increased Cpx membrane interaction.[106] To test the effect of cholesterol on the membrane binding of Cpx, we produced sonicated POPM1 or POPM1 vesicles without cholesterol (PC:PS:PE:PIP2) for anisotropy measurements. From the calculated partition coefficient, it can be observed that cholesterol does increase Cpx's interaction with lipid vesicles (Figure 3.1-1, C).

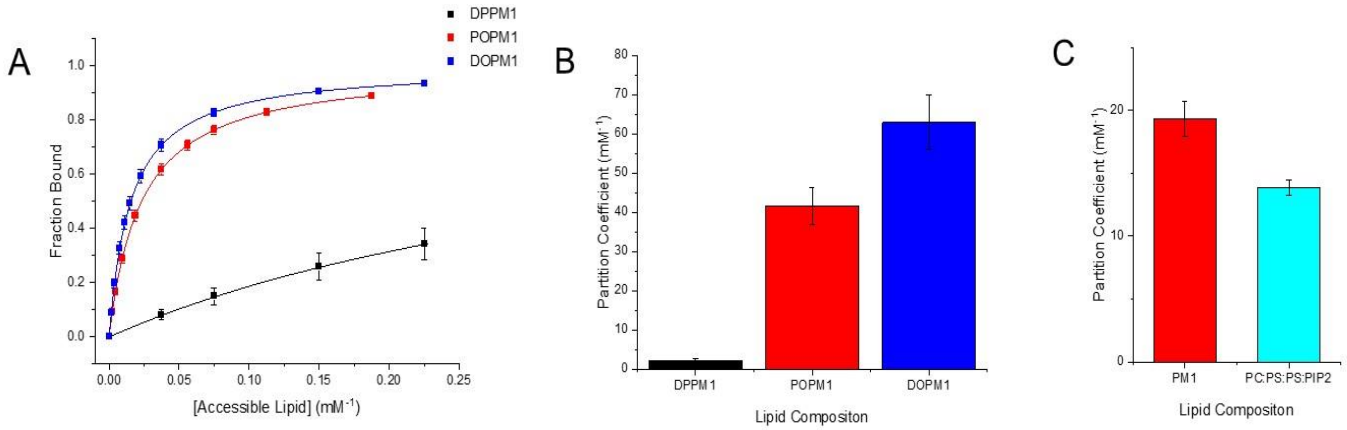

Figure 3-1 *Unsaturation in lipid vesicles increases Cpx-membrane affinity. (A) Fraction of Cpx bound as a function of accessible lipid concentration. 50 nM of CpxT119Alexa546 was used in anisotropy measurements with DPPM1(black), POPM1 (red), or DOPM1 (blue). The lipid composition used was PC:PE:PS:Chol:PIP2 = 34:30:15:20:1. (B) Partition Coefficients derived from (A). (C) Partition Coefficient of POPM1 with (red) or without (cyan) cholesterol.*

3.1.2 Complexin prefers to bind to lipid vesicles containing PIP2

Phosphatidylinositol-4,5-bisphosphate (PIP2) is a unique lipid characterized by a large phosphatidylinositol headgroup, multiple negative charges, and a polyunsaturated lipid chain. Despite forming a minor fraction of available lipids, it is a vital component of the plasma membrane. PIP2 is involved in various cellular processes such as membrane trafficking, endocytosis and exocytosis.[81] It binds proteins like Syntaxin, CAPS, Munc13 and Synaptotagmin, which function at various steps of the exocytotic process.[34,35,87,107–110] For Cpx, while lipids like POPE and POPS showed some increase in Cpx-membrane affinity, PIP2 showed the most significant enhancement when incorporated into lipid vesicles.[111]

To directly assess the effects of PIP2 on Cpx-membrane interaction, sonicated vesicles were prepared with the following lipid composition: POPC:POPE:POPS:Chol:PIP2 = 35-x:30:15:20:x where x represents 0% (POPM0), 1 % (POPM1) or 5 % (POPM5) of PIP2. As the concentration of PIP2 in vesicles increases, membrane partition coefficient increased as well (Figure 3-2 A, B, result published in [111]). This effect can be observed with small sonicated vesicles and larger 100 nm extruded vesicles or planar supported bilayers.[112]

To determine whether this increase in affinity is due to unsaturated chains or the headgroup, 5% of PIP2 in POPM5 was replaced with 5 % 1-stearoyl-2-arachidonoyl-sn-glycero-3-phosphocholine (SAPC). SAPC replaces PIP2's phosphatidylinositol headgroup with phosphocholine. With this modified lipid composition (POPM/SAPC), there was a decrease in calculated partition coefficient (Figure 3-2 A, B), and Cpx's membrane affinity approached a value seen with POPM0. This shows that Cpx's affinity is not the result of PIP2's polyunsaturated chain. Given that the PO lipids already contain unsaturated chains, the addition of 5% of PIP2 is unlikely to

increase the overall unsaturation present in the lipid vesicles. Therefore, the polyunsaturated chain of PIP2 does not substantially contribute to an increased membrane affinity.

Because PIP2 is highly negatively charged, it is possible that the increase in the membrane affinity of Cpx with PIP2 is due to electrostatic interactions with the membrane interface. To test this, we repeated the anisotropy measurements and increased the ionic strength. This should screen electrostatic interactions. The salt concentration of the buffer was increased from 150 mM to 300 mM, and this resulted in a decreased partition coefficient. This suggests that at least some of the affinity of Cpx to PIP2 containing membranes is due to electrostatics. However, POPS, another negatively charged lipid, did not have a significant effect on Cpx's affinity even when present at 15% molar ratio, suggesting that charge is not important.[111] In addition to charge, the large headgroup of PIP2 could contribute to its effect on Cpx's membrane binding by inducing local curvature strain. This might increase membrane defects and account for the increased membrane affinity observed with PIP2.

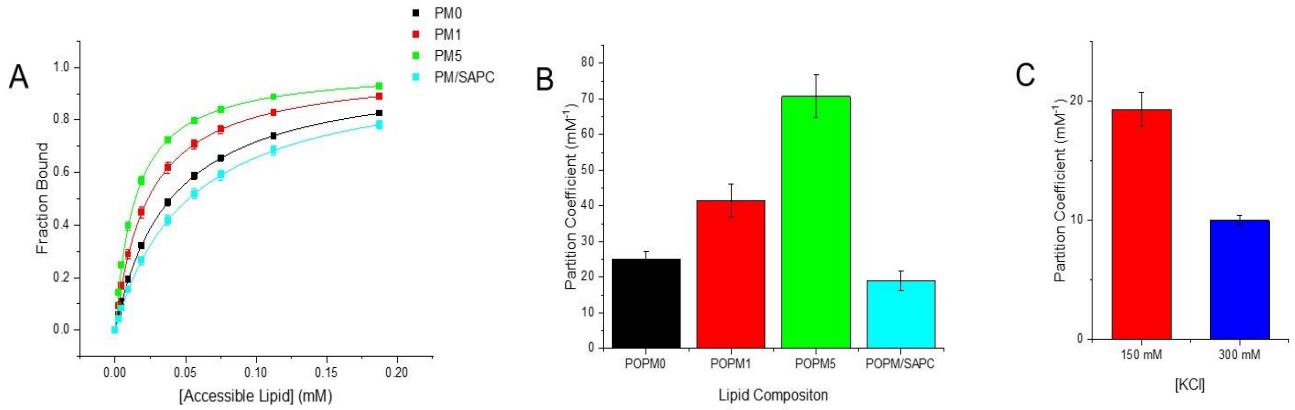

Figure 3-2 *Complexin prefers to bind to lipids containing PIP2. Fraction of Cpx bound as a function of accessible lipid concentration. 50 nm of CpxT119Alexa546 was used in anisotropy measurements with POPMx vesicles where x represents 0% (POPM0, black), 1% (POPM1, red) or 5% (POPM5, green) of PIP2. 5% of PIP2 in POPM5 was replaced with 5% 1-stearoyl-2-arachidonoyl-sn-glycero-3-phosphocholine (SAPC)shown in cyan. (B) Partition coefficients derived from binding isotherms in (A). (C) Partition coefficients of Cpx binding to POPM1 vesicles in 150 mM KCl (red) or 300 mM KCl (blue).*

3.1.3 Complexin Interferes with its own membrane binding

An observation made in the Cpx membrane studies was that the measured membrane partition coefficient was dependent on concentration of Cpx used in the measurement.[111] Increasing the concentration of Cpx form 2 uM to 80 uM resulted in a 44-fold increase in partition coefficient.[111] This suggested that Cpx was inhibiting its own binding at low protein concentrations. To investigate this, we performed anisotropy experiments with the Alexa labelled Cpx and sonicated POPM1 vesicles. At the highest concentration of lipids, where most of the labelled Cpx was membrane associated, unlabeled wild-type Cpx was titrated into the solution. As the concentration of unlabeled Cpx increased, there was a sharp drop in anisotropy (Figure 3-3A). This indicates that the previously membrane bound, fluorophore labeled Cpx was now rotating freely in solution. Therefore, the unlabeled Cpx was displacing the labelled Cpx from the membrane surface. Cpx inhibited its membrane binding at low Cpx concentrations, and this effect was independent of the presence of PIP2 (Figure 3-3B). This suggests that there are a limited number of binding sites on the membranes, and they get saturated at low Cpx:lipid ratios.

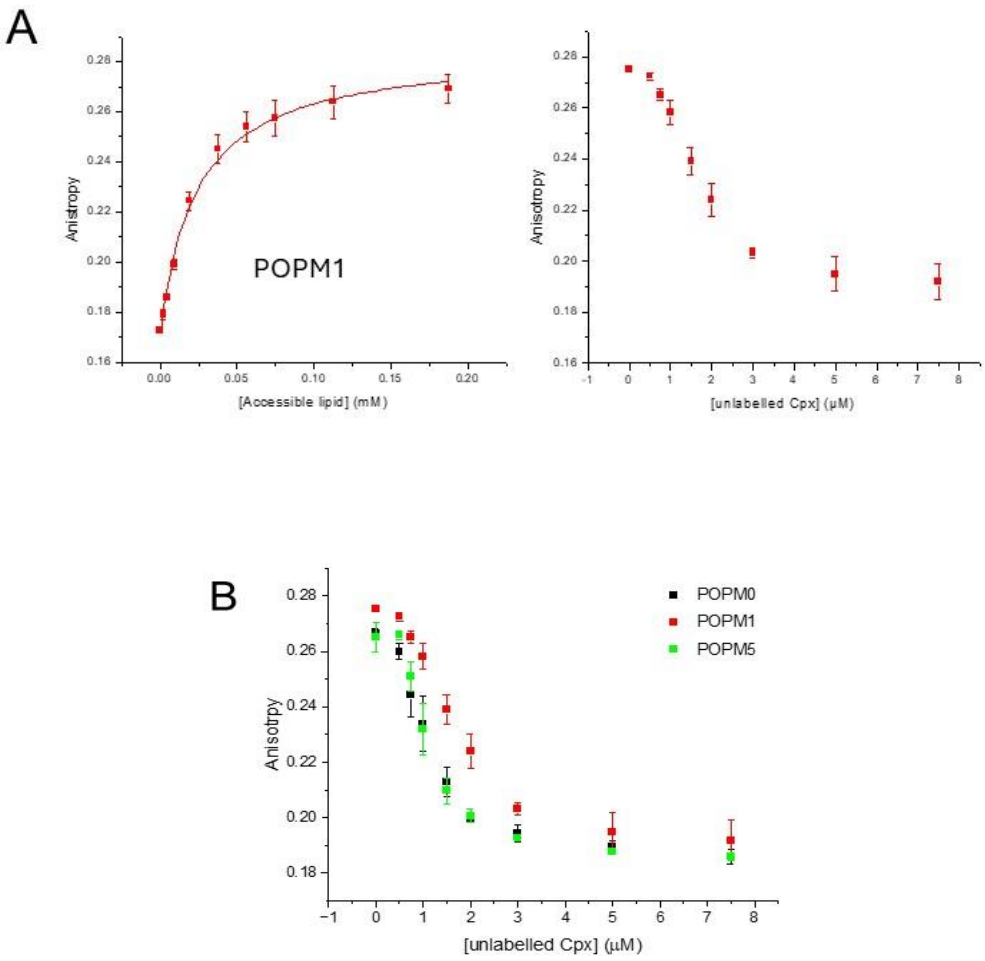

Figure 3-3 *Complexin competes with itself for membrane binding. (A) Anisotropy of CpxT119Alexa546 as a function of accessible POPM1 lipid concentration (left). At the highest POPM1 concentration, unlabeled Cpx was titrated into the solution and the anisotropy recorded (right). (B) Anisotropy of CpxT119Alexa546 with POPM vesicles as a function of unlabeled Cpx concentration. The lipid composition used POPM0 (black), POPM1(red) or POPM5(green).*

3.2 When SNAREs are tethered to the membrane, SNAP25 is needed to allow Cpx membrane interaction.

Complexin (Cpx) is known to interact with both SNAREs and membranes, and these interactions are crucial for its function. Given that Cpx is sensitive to the properties of the membrane, we wanted to determine whether individual SNAREs and SNARE complexes contributed to Cpx-membrane interactions. To explore how SNAREs affect Cpx's ability to interact with membranes, we prepared proteoliposomes consisting of POPM1 vesicles and SNARE proteins using dialysis. These interactions were investigated with continuous-wave electron paramagnetic resonance (cwEPR) and fluorescence anisotropy.

3.2.1 dSNAP25 increases Cpx's membrane affinity

SNAP25 is a unique SNARE in the neuronal system that contributes two helices to the SNARE complex. SNAP25 lacks a transmembrane domain and palmitoylation of its native cysteine residues localizes it to the plasma membrane. SNAP25 has been shown to enhance the membrane affinity of Cpx in POPC:POPS lipids.[105] Since PIP2 has been shown to be a vital component of Cpx-membrane interaction, we wanted to replicate this experiment using a more complex and more native POPM1 lipid mixture. To obtain a bacterially expressed version of SNAP25 that would be membrane associated, expressed, and purified SNAP25 was alkylated with a dodecyl group (see Methods), allowing it to be membrane associated despite not having a transmembrane domain.

To form lipid vesicles with membrane associated SNAP25, the dodecylated SNAP25 (dSN25) was added to POPM1 lipids along with sodium cholate. After extensive dialysis, the detergent was removed leading to the formation of lipid vesicles . For soluble SNAP25 (sol SN25), lipid vesicles were formed via dialysis and SNAP25 was then added post dialysis, resulting in a solution with

POPM1 vesicles and untethered SNAP25. The protein:lipid ratio used in both cases was 1:100. The lipid vesicles with either acylated dSN25 or soluble SN25 were titrated into a 50 nM solution of fluorophore-labelled Cpx, the anisotropy at each lipid addition was measured, and membrane affinity was calculated as in previous experiments. When SNAP25 is membrane bound, there was a 3-fold increase in partition coefficient compared to the protein-free vesicles (Figure 3-4). However, this increase absent when SNAP25 is in solution and not membrane bound.

3.2.2 Increased membrane affinity of Cpx is primarily due to dSN1

SNAP25 contains two α-helical SNARE motifs: an N-terminal SN1 and C-terminal SN2. These two motifs are connected by a long, flexible linker. Recent experiments have shown that these two helices behave differently.[113] They have been shown to have different structures and interact differently with other SNARE proteins and Munc18.[113] Since they behaved so differently, it may be appropriate to regard them as two independently acting entities rather than a single protein. Therefore, we wanted to see how these two proteins contributed to the effect of SNAP25's on the membrane binding of Cpx. SN1 and SN2 were dodecylated and independently attached to membranes to mimic the state of dodecylated SNAP25. As was the case for full-length dSN25, there was a 3-fold increase in membrane partition coefficient with dSN1-POPM1 compared to POPM1 alone (Figure 3-5). With dSN2-POPM1, the membrane partition coefficient was similar to that observed for the protein free sample (Figure 3-5B). This indicates that dSNAP25's effect on Cpx membrane binding is primarily due to the presence of dSN1 and not from dSN2. The result seen for dSN2 also indicates that the effect of SNAP25 is not a result of the acylation on the protein (the dodecyl chains) but rather to SNAP25 itself.

From anisotropy measurements, SN1 seems to be more important than SN2 in influencing Cpx-membrane interactions. The sites on dSN25 that are dodecylated are located immediately

following the SN1 motif, with a long linker connecting SN1 to SN2. Therefore, SN1 will be positioned close to the membrane, and this may play a role in its effect on Cpx membrane binding. On the other hand, SN2 may be further from the membrane and may not even be close enough to interact with the membrane interface.

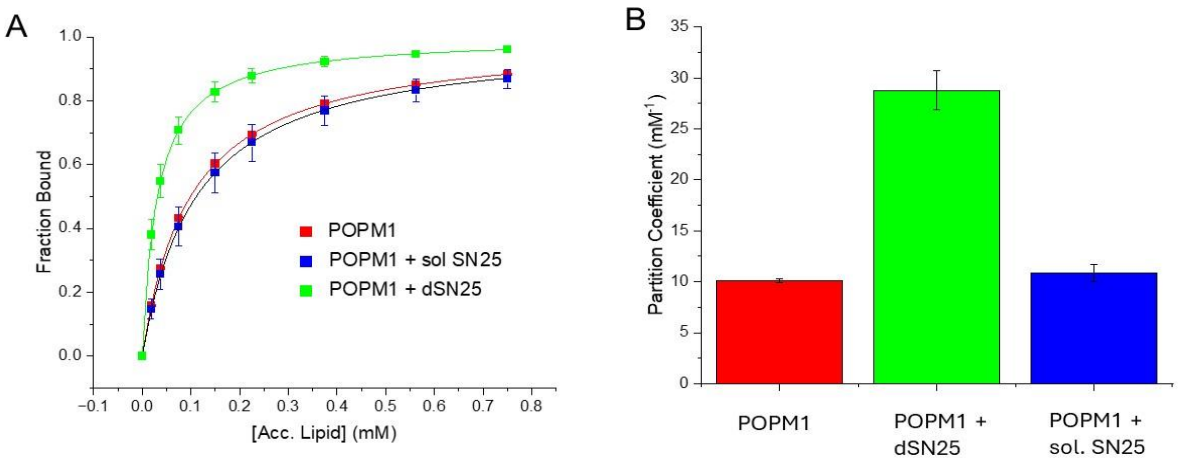

Figure 3-4 *Membrane-bound SNAP25 increases Cpx-membrane affinity. (A) Fraction of Cpx bound to POPM1 (red), POPM1 and soluble SNAP25, or POPM1 with membrane-bound dSN25. (B) Partition coefficients derived from (A)*

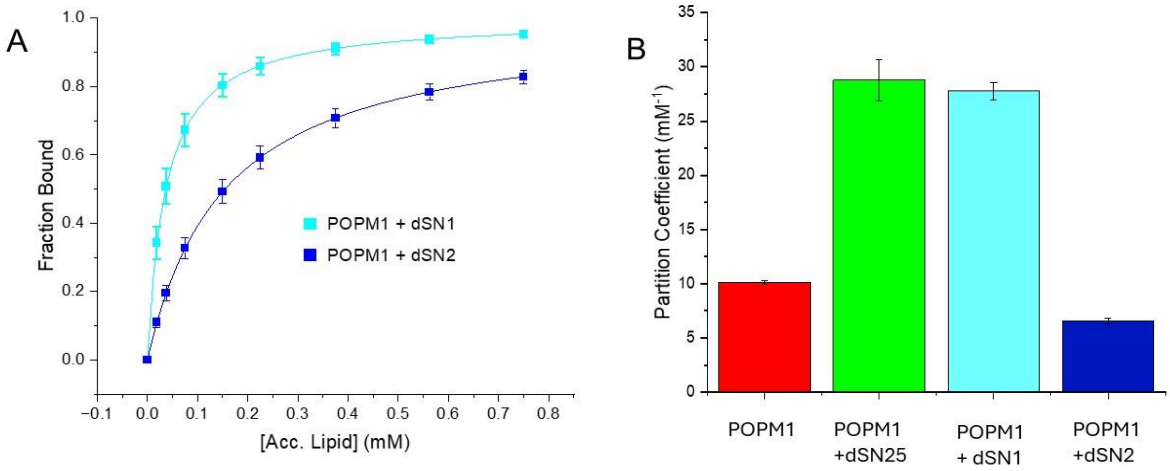

Figure 3-5 *Increased affinity is due to the action of dSN1. (A) Fraction of Cpx bound to POPM1 with membrane bound SNAP25 fragments. (B) Partition coefficient comparing Cpx binding to protein free (red), dSN25- (green), dSN1- (light blue) or dSN2- (blue) POPM1 vesicles.*

3.2.3 SNAP25 does not interact with Cpx or Lipid Vesicles

To understand the increase in partition coefficient due to the presence of dSN25, we measured SNAP25's affinity to Cpx and to POPM1 lipid vesicles. SNAP25 might interact with membranes or directly, and thereby modify Cpx membrane binding, or SNAP25 might interact with Cpx, and this protein-protein interaction might account for the increased anisotropy. To investigate this hypothesis, SNAP25's affinity to Cpx and vesicles was measured using fluorescence anisotropy and cwEPR. Adding SNAP25 to labeled Cpx saw minimal change in the anisotropy (Figure 3-6A). Using cwEPR, we also found that Cpx does not interact with SNAP25 as evidenced by the absence of a change in line shape when SNAP25 is added to Cpx (Figure 3-6B). This was not unexpected as previous reports have indicated that SNAP25 does not directly interact with Cpx.[114–116] To measure SNAP25's affinity to vesicles, SNAP25 was labelled with a fluorophore and anisotropy measurements were conducted as described previously. Again, there was minor change in anisotropy when POPM1

vesicles were added (Figure 3-6C). This observation was repeated with cwEPR measurements with a 30 mM POPM1 concentration (Figure 3-6D). In all measurements, SNAP25 did not show any significant interactions with either Cpx or lipid vesicles.

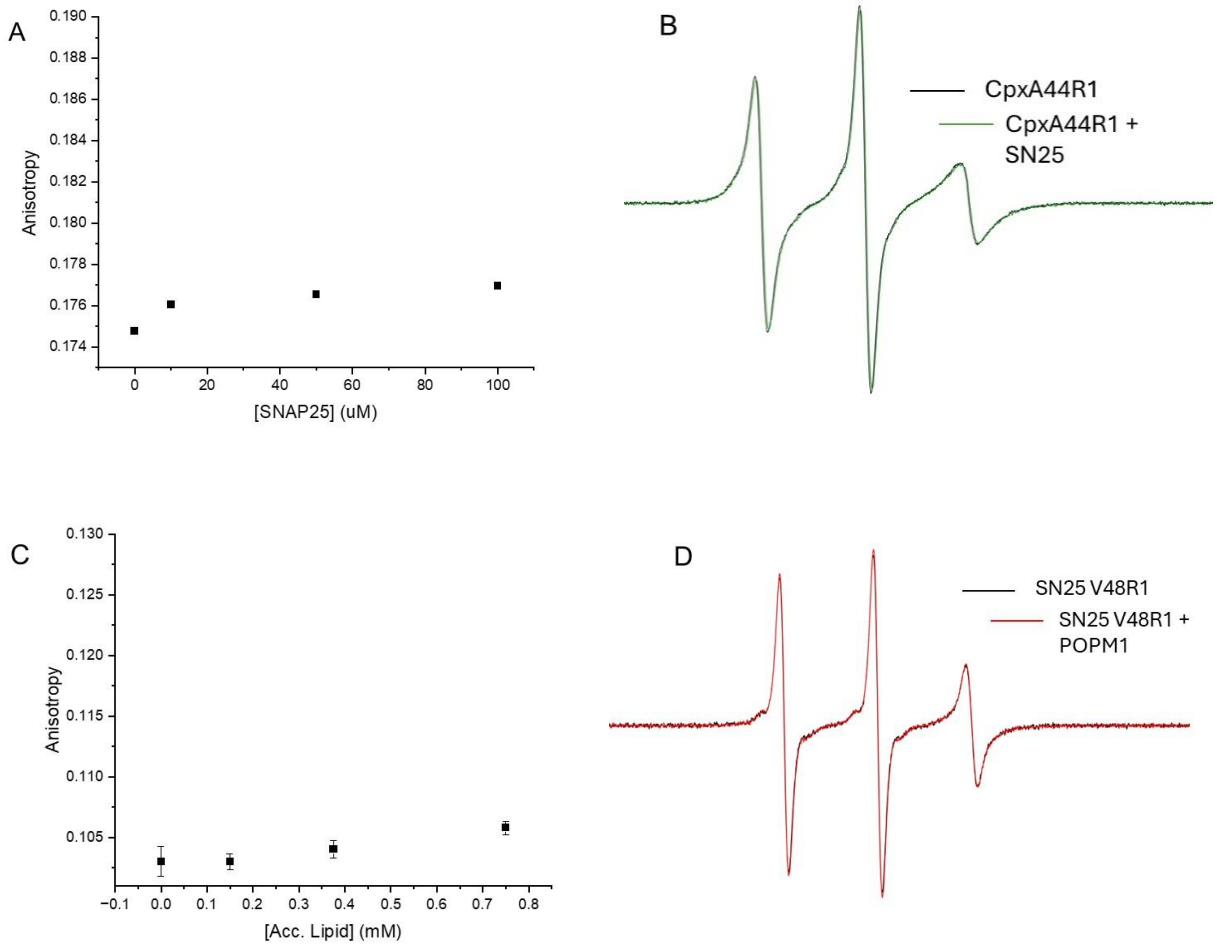

Figure 3-6 *SNAP25 does not interact with Cpx or POPM1 vesicles. (A) Anisotropy of fluorophore-labelled Cpx as a function of SNAP25 concentration. (B) Normalized EPR spectra of Cpx in the absence (black) and presence (red) of SNAP25. (C) Anisotropy of fluorophore-labelled SNAP25 as a function of accessible lipid concentration. (B) Normalized EPR spectra of SNAP25 in the absence (black) and presence (red) of 30 mM POPM1 sonicated vesicles.*

3.2.4 dSN25 increases Cpx's membrane affinity independent of PIP2 or other negatively charged lipids

In previous experiments, PIP2 has been shown to have the greatest effect on Cpx's membrane affinity compared to any of the other lipids used here.[111] For that reason, dSNAP25 experiments were repeated with lipid vesicles without PIP2 (POPM0). If SNAP25 is able to change the distribution of PIP2 in the membrane bilayer, this could affect Cpx's affinity. However, the presence of PIP2 does not explain the observed dSN25 effect (Figure 3-7A, C). Although POPM0 showed an overall decreased partition coefficient, the presence of dSNAP25 increased the membrane binding of Cpx with dSN25-POPM0. Even when all the negatively charged lipids (PIP2 and POPS) are removed, the dSNAP25 effect did not disappear (Figure 3-7 B, C). This shows that SNAP25 increases affinity in a way that is not dependent on PIP2 or negatively charged lipids.

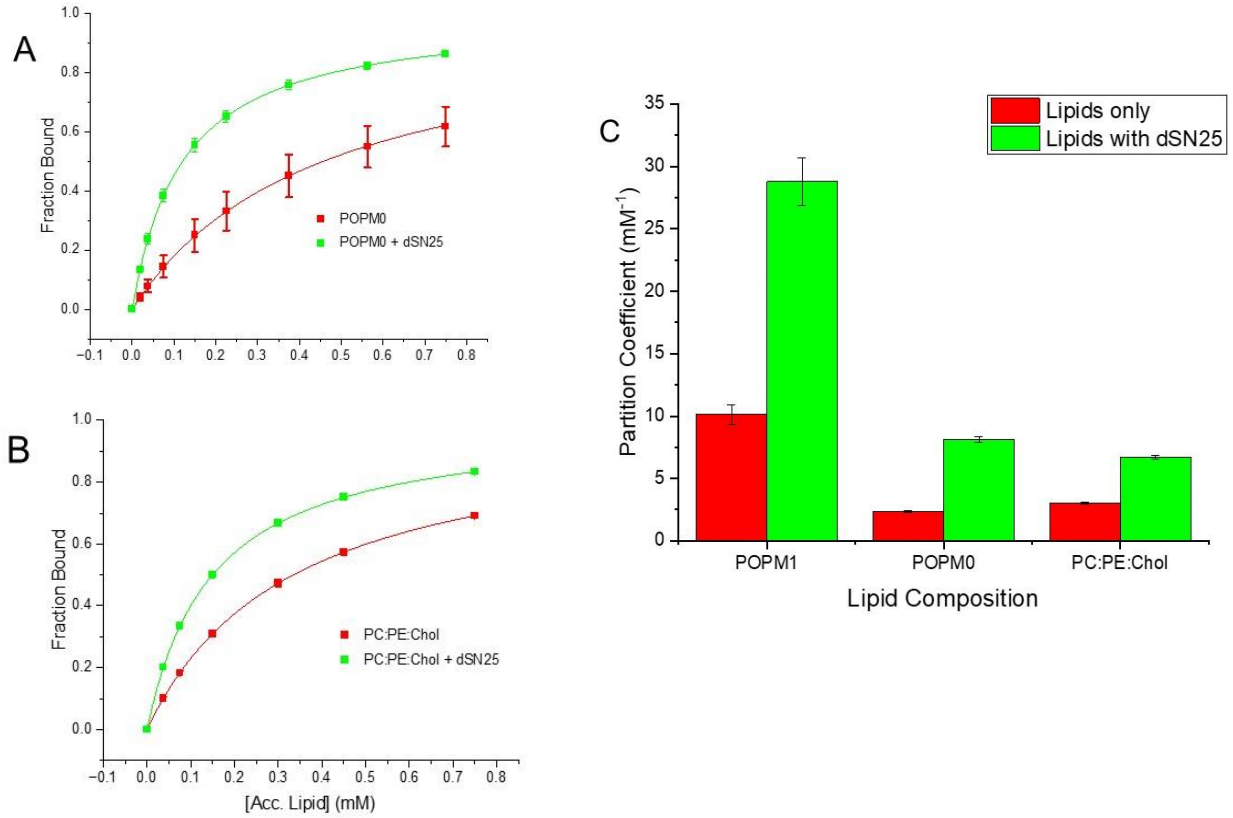

Figure 3-7 *dSNAP25 increases Cpx-membrane affinity independent of PIP2 or negatively charged lipids. (A) Fraction of Cpx bound as a function of accessible POPM0 (red) or dSN25-POPM0 (green) lipid concentration. (B) Fraction of Cpx to lipid vesicles composed of PC:PE:Chol with and without membrane-embedded SNAP25. (C) Partition coefficient measuring Cpx's affinity to lipid vesicles with or without dNS25*

3.2.5 SNAP25 increases Cpx-membrane interaction at Cpx's C-terminal domain

As indicated above, measurements with soluble SNAP25 indicate that it does not bind with significant affinity to either membranes or Cpx. However, when dSNAP25 is anchored on the membrane, the effective lipid concentration is increased dramatically. On the membrane interface, dSN25 might experience lipid concentrations as high as 0.50 to 1M. Therefore, SN25 might still bind when anchored to the membrane interface, even though binding is not detected in assays with soluble components where the lipid concentrations that can be used are limited. Being membrane anchored might explain why SNAP25, despite its inability to bind lipid vesicles (or Cpx) is able to enhance Cpx's membrane affinity.

As a check on the findings made using anisotropy, EPR spectroscopy was used to independently measure Cpx's interaction with membranes and SNAREs, allowing for the use of membrane-bound dSN25 under a different set of conditions. The nitroxide spin label used in these EPR measurements is sensitive to the local dynamics and conformational changes in proteins, and interactions with lipids or SNAREs result in a change in the lineshape of the EPR spectrum.

Cpx was labelled along its length at N-terminal (Q7, K18), accessory helix (D27, A40), central helix- (K54, D68), and C-terminal (S115, T119) domains. Cpx is known to interact with membranes via its N- and C-terminal sequence and with SNAREs via its accessory and central helices. With

cwEPR, we can distinguish between membrane and SNARE interactions.[105] Membrane interactions are facilitated by the N- and C-terminal domains and labels in these regions show distinct changes in motion upon membrane interaction, but no changes upon SNARE interaction. Labels in the accessory and central helices interact with SNAREs and show distinct changes in lineshape when binding to the SNAREs but show little change upon membrane binding. Protein free or dSN25 bound POPM1 vesicles were added to 30 μM of spin-labelled Cpx. At the lipid concentration of 2 mM used here, there is only a weak interaction between Cpx and POPM1 vesicles (Figure 3-8A). However, in the presence of dSN25 proteoliposomes, there was a decrease in the normalized amplitude at position T119 (Figure 3-8B, C). All other positions showed no changes in the lineshape indicating that Cpx does not bind to SNAP25 even when SNAP25 is membrane anchored. Although SNAP25 does not interact directly with Cpx, it can alter membrane properties, thereby increasing Cpx's membrane affinity. This increased membrane association is mediated primarily through the C-terminal region of Cpx.

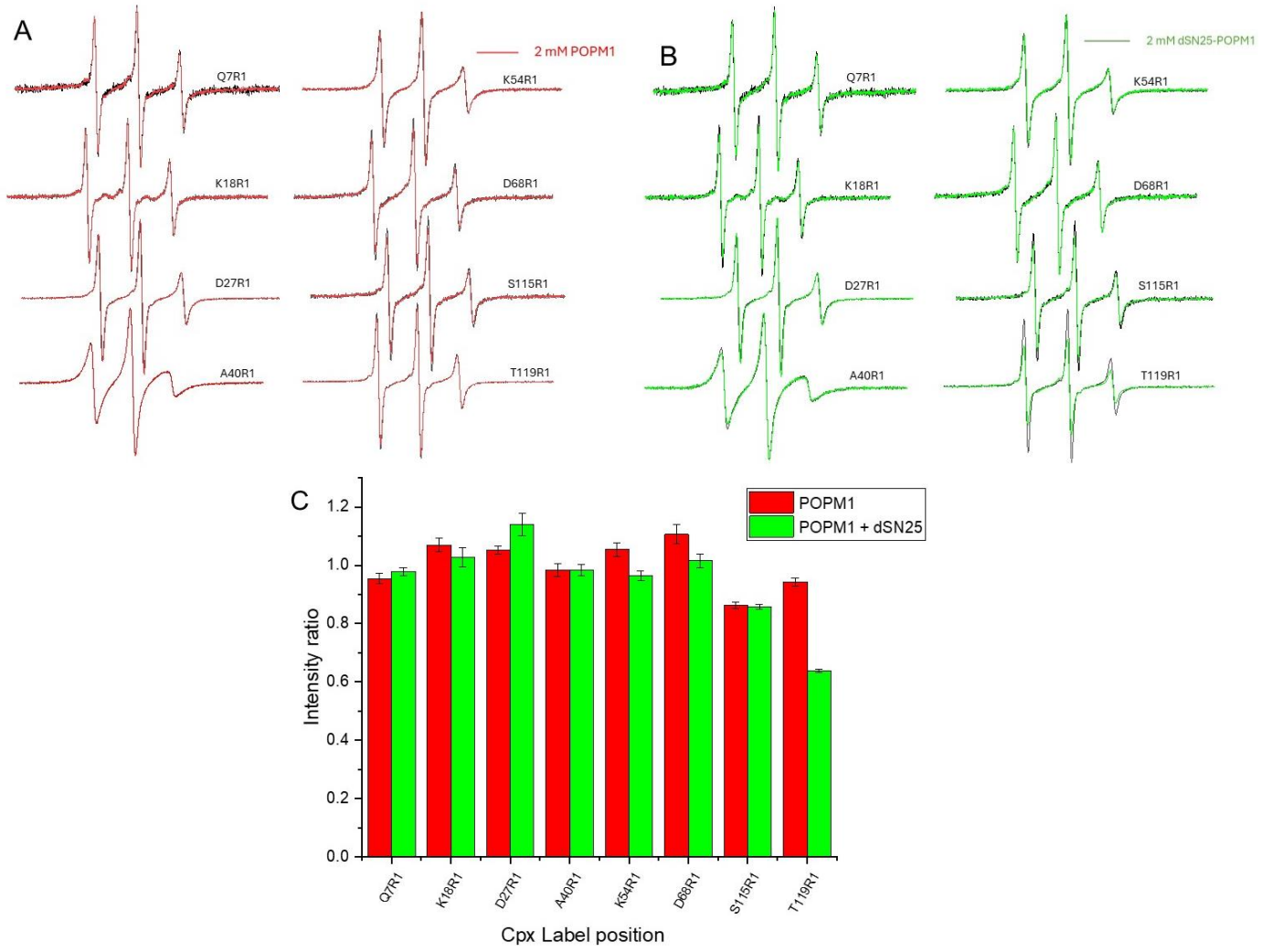

Figure 3-8 *Increased Cpx's membrane interaction is driven by its C-terminal domain. (A,B)Normalized EPR spectra of Cpx mutants in the absence (black) or presence of POPM1 (red) or dSN25-POPM1. (C) Intensity ratio of the high field resonance line of EPR spectra in (A) and (B)*

3.2.6 Syntaxin blocks the membrane binding of Cpx independent of PIP2

Next, we sought to measure the effect of Syntaxin (Syx) on the membrane binding of Cpx. To make membrane bound Syx, $Syx_{183-288}$ was reconstituted to POPM1 membrane vesicles via dialysis. For soluble Syntaxin (sol Syx), POPM1 vesicles were prepared using dialysis and Syx_{1-262} was added post vesicle formation. When Syx was in solution with vesicles, it had no significant effect on the membrane partition coefficient (K) of Cpx. However, when membrane attached, Syx significantly

reduced the measured partition coefficient (Figure 3-9). This effect can be seen with both full length syntaxin (FL Syx) and $Syx_{183-288}$. Thus, Syx's inhibitory effect is only seen when it is membrane bound.

Like dSNAP25, Syx's inhibitory effect was again studied with cwEPR. Complexin was labelled with a spin probe at its C- and N-terminal domains. These are regions known to drive Cpx-membrane interactions. Complexin did not show any membrane interaction when Syx was membrane bound. This is evidenced by the lack of change in the line shape (Figure 3-10A).

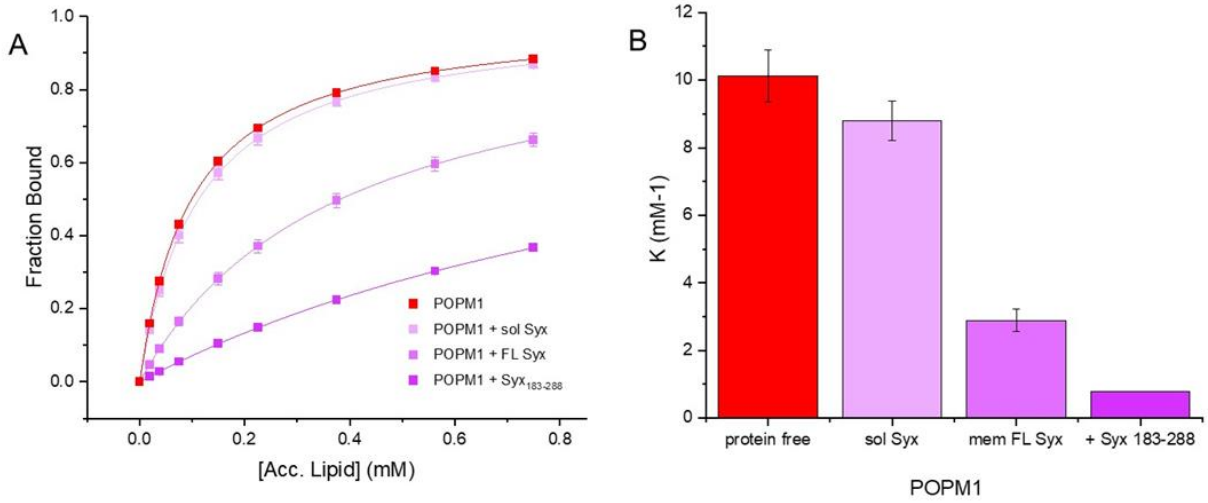

Figure 3-9 *(A) Fraction of Cpx T119Alexa546 bound as a function of accessible lipid concentration. Binding isotherms of Cpx's interaction with POPM1 vesicles that are protein free or with soluble of membrane bound Syx mutants. (B) Partition coefficients of Cpx-lipid binding derived from (A).*

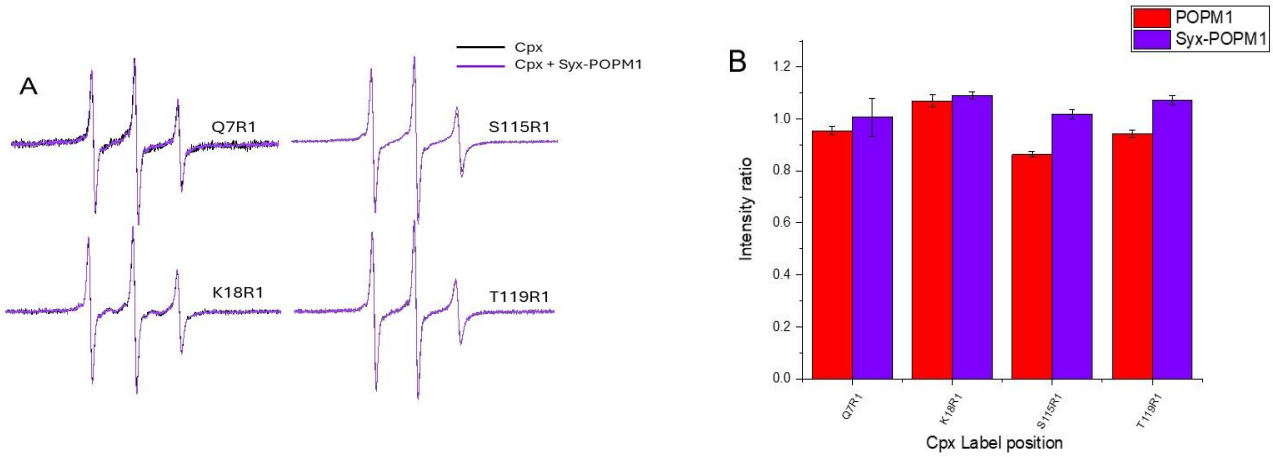

Figure 3-10 *(A) Normalized EPR spectra of Cpx mutants alone (black) or with 2 mM Syx$_{183-288}$-POPM1 proteoliposomes (violet). (B) Intensity ratio of high field resonance line of Cpx with POPM1 (red) or Syx$_{183-288}$-POPM1 (violet).*

To investigate whether the decreased affinity was from Syx preventing Cpx from accessing the lipid bilayer, spin labelled Cpx was added to 10 mM POPM1 or Syx$_{183-288}$-POPM1. At 10 mM lipid concentration, Cpx is membrane bound (Figure 3-11). When Cpx is added to 10 mM membrane bound Syx, we obtain a line shape similar to Cpx in solution alone. This shows that Cpx is no longer interacting with lipid vesicles and is free in solution with no binding partners. This shows that Syx is directly blocking Cpx from accessing membranes.

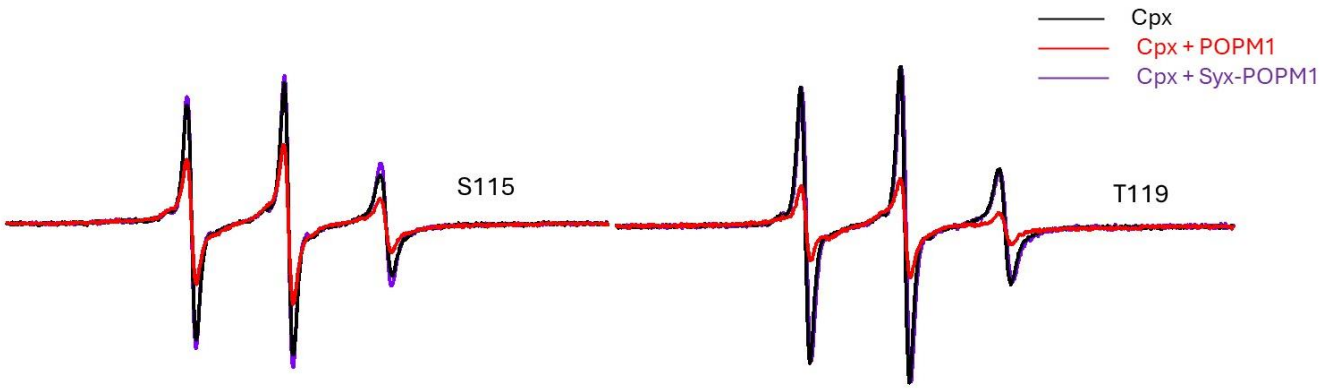

Figure 3-11 *Normalized EPR spectra of Cpx mutants alone (black), with 10 mM POPM1(red) or with 10 mM Syx$_{183-288}$-POPM1 proteoliposomes (violet).*

Syntaxin is known to bind to PIP2 containing membranes.[117] Therefore, if it directly interacts with PIP2, Syx could sequester PIP2 and this could explain Cpx's reduced affinity. To explore this further, experiments with Syx$_{183-288}$-POPM1 and Cpx were replicated using POPM0. Anisotropy measurements showed a decrease in partition coefficient when Syx is membrane bound to POPM0 vesicles (Figure 3-12A, B). Experiments with cwEPR were conducted with 15 mM POPM0 or Syx$_{183-288}$-POPM0 and spin labelled Cpx. At 15 mM POPM0, Cpx can interact with POPM0 vesicles; however, this interaction is abolished when Syx is membrane bound, indicating that membrane-bound Syx blocks Cpx's interaction with lipid vesicles in a PIP2 independent manner.

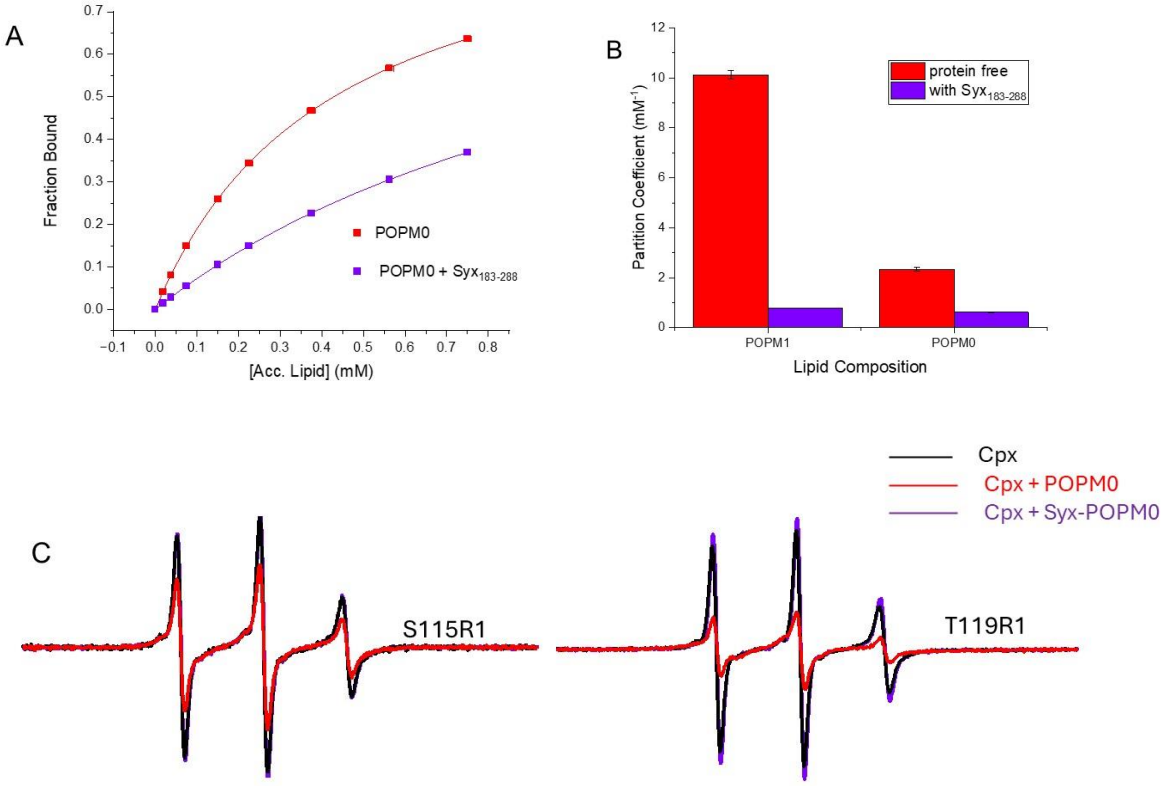

Figure 3-12 *Syntaxin blocks Cpx's membrane access independent of PIP2. (A) Fraction of CpxT119 bound as a function of accessible lipid concentration. The POPMO lipid vesicles were protein free (red) or bound to* $Syx_{183\text{-}288}$ *(violet). (B) Comparison of the partition coefficient of protein free or Syx membrane-bound vesicles. (C) Normalized EPR spectra of Cpx mutants in the absence (black) or presence of POPM0 (red) or Syx-POPM0 vesicles (violet). The lipid concentration was 15 mM.*

3.2.7 Membrane bound tSNAREs increase the membrane affinity of Cpx

Anisotropy and EPR measurements have shown that the membrane-bound tSNARE complex increases the affinity of Cpx to POPC:POPS vesicles.[105] We wanted to repeat this experiment in membranes formed from the POPM1 lipid mixture, because it is more native and supports membrane fusion. To make the tSNARE binary complex, $Syx_{183\text{-}288}$ was added to dSNAP25 in a 1:1 molar ratio and then allowed to incubate overnight. The preassembled binary complex was added to lipids and dialyzed to form membrane bound tSNARE complex. The tSNARE complex showed an increased

affinity, as measured by the partition coefficient, compared to protein free membranes (Figure 3-13A). The partition coefficient was similar to that obtained in dSN25-POPM1 proteoliposome (Figure 3-14A). This contrasts with what was previously reported.[105] In POPC:POPS vesicles, partition coefficient with membrane bound tSNARE was about four times greater than that with membrane bound dSNAP25.[105] This discrepancy could be explained by the different lipid mixtures used. EPR measurements revealed a small decrease in intensity ratio of t-SNARE POPM1 compared to dSN25-POPM1(Figure 3-14B). This indicates that tSNARE may moderately enhance Cpx-membrane association compared to dSN25, but not by as much as found previously using the POPC:POPS lipid mixture.

It should be noted that this result indicates that SNAP25 can reverse Syx's inhibitory effect on Cpx-membrane binding (Figure 3-13B). With dSN25:$Syx_{183\text{-}288}$, there was a significant increase in the partition coefficient for Cpx compared to $Syx_{183\text{-}288}$ in POPM1 vesicles(Figure 3-13B). When dSN25: FL Syx was used to form the binary complex, there was still a significant enhancement in Cpx binding relative to just FL Syx (Figure 3-13B). However, this was not to the level seen with dSNAP25:$Syx_{183\text{-}288}$. This could be because $Syx_{183\text{-}288}$ lacks the Habc domain and as a result interacts more strongly with dSN25 compared to FL Syx. FL Syx includes the Habc domain, which may assume a closed conformation, making the H3 (SNARE forming) domain less available for interactions with other SNAREs. EPR measurements show that the increased partition coefficient comes from the interaction of the C-terminal domain of Cpx with POPM1 vesicles (Figure 3-15). The N-terminal domain of Cpx showed no evidence for a membrane interaction at the concentrations of POPM1 used here. These results indicate that when dSN25 forms a complex with Syx, it can undo Syx's inhibitory activity on Cpx membrane interactions.

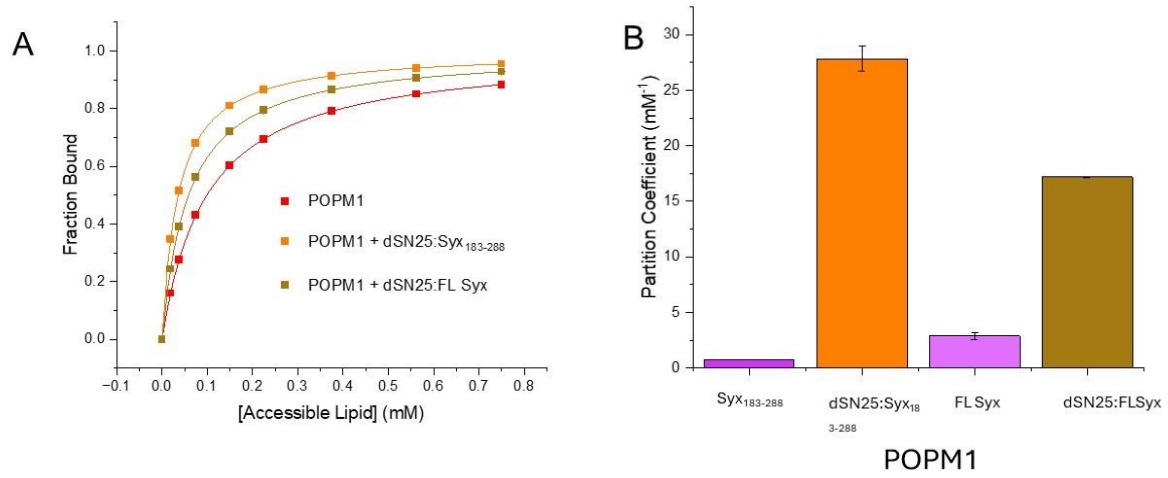

Figure 3-13 *(A) Fraction of CpxT119Alexa546 as a function of accessible tSNARE-POPM1 lipids. The tSNAREs were prepared with dSN25 and either full length Syntaxin (FL Syx) or Syx183-288. (B) Partition coefficients of Syntaxin mutants or tSNAREs composed of dSNAP25 and Syx.*

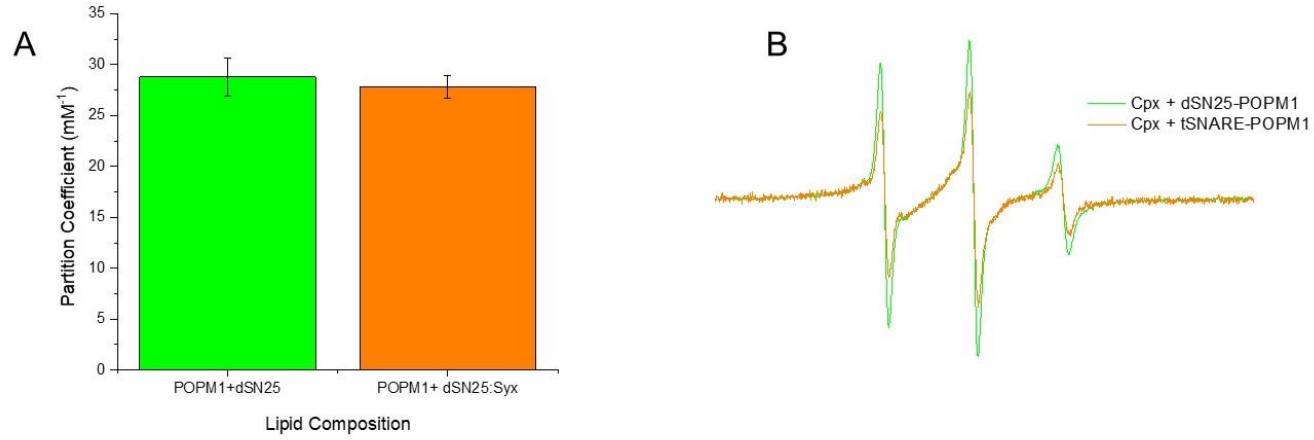

Figure 3-14 Partition Coefficient of membrane bound dSN25 (green) or dSN25:Syx183-288 (orange) POPM1 vesicles. (B) Normalized EPR spectra of CpxT119 with membrane bound dSN25 (green) or dSN25:Syx183-288 (orange) POPM1 vesicles.

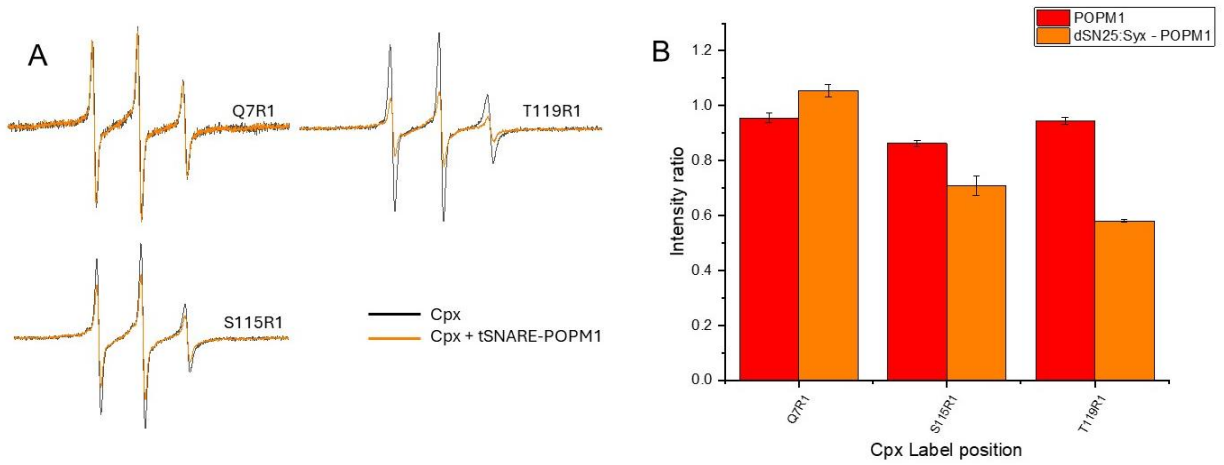

Figure 3-15 *(A) Normalized EPR spectra of Cpx mutants alone (black) or with 2 mM dSN25:Syx$_{183-288}$-POPM1 proteoliposomes (orange). (B) Intensity ratio of high field resonance line of Cpx with POPM1 (red) or dSN25:Syx$_{183-288}$-POPM1 (orange).*

In previous experiments (see section 3.2.2), it was observed that dSNAP25's impact on altering membrane binding of Cpx was primarily due to dSN1. To investigate this further, we replicated the experiments with membrane bound binary complex and substituted dSN25 with dSN1. Syx$_{183-288}$ was combined with dSN1 in a 1:1 ratio and allowed to assemble overnight. The preassembled complex was then reconstituted into POPM1 vesicles as previously described. Anisotropy measurements were carried out with the membrane bound dSN1:Syx complex. As shown in Figure 3-16, dSN1:Syx increases the partition coefficient similar to that seen for dSNAP25:Syx. This shows that dSN1 is able to successfully counter Syx's inhibitory effect on Cpx's membrane binding. The ability of dSNAP25 to undo Syx's inhibitory effect on Cpx-membrane interaction is driven by dSN1.

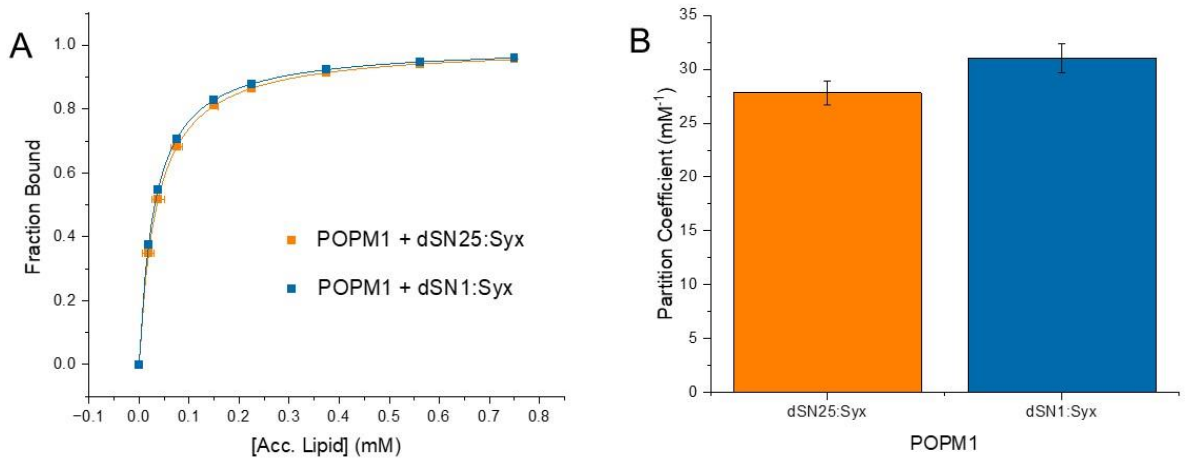

Figure 3-16 *dSN1 behaves similarly to dSN25. (A) Binding Isotherm comparing fraction of CpxT119Alexa546 bound as a function of accessible lipid composed of membrane bound SN25:Syx (orange) or dSN1:Syx (blue). (B) Partition coefficients derived from (A)*

3.2.8 Membrane bound ternary SNARE complex increases the membrane association of Cpx

Next, we moved to the fully assembled SNARE complex and examined its effect upon Cpx membrane interactions. To make the POPM1 membrane bound ternary complex (mem TC-POPM1), dSN25, $Syx_{183-266}$ and Syb_{1-116} were mixed in a 1:1:1 ratio, allowed to incubate overnight to form an assembled complex, which was then incorporated into vesicles. Anisotropy experiments on labeled Cpx indicated that there was a 5-fold increase in the membrane partition coefficient of Cpx when membrane bound ternary SNARE was present compared to protein free vesicles (Figure 3-17). Additionally, there was a 2-fold increase in partition coefficient with mem TC-POPM1 compared with dSN25-POPM1 or tSNARE-POPM1 (Figure 3-17). EPR measurements indicated that this increase was due to enhanced Cpx-membrane interaction (Figure 3-18). Most of this interaction was mediated through the C-terminal complex of Cpx, although, there was also some membrane interaction from the N-terminal domain, as indicated by the decrease in intensity ratio at position K18 (Figure 3-18).

Replacing dSN25 with dSN1 in the ternary complex also resulted in an increased partition coefficient for Cpx, although not to the same level as observed with the original SNARE complex (Figure 3-19).

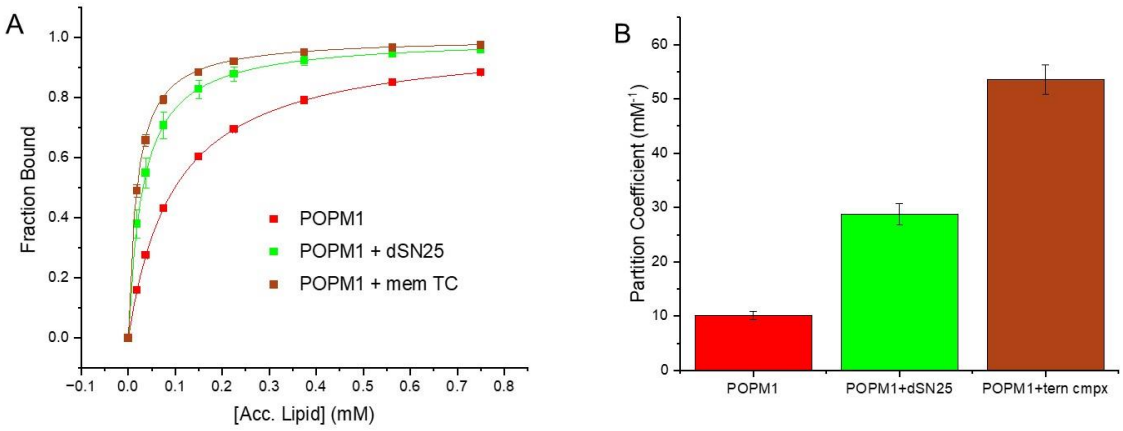

Figure 3-17 *(A) Fraction of CpxT119Alexa546 bound as a function of accessible lipids. 50 nM of Cpx was used in anisotropy measurements. (B) Partition Coefficient comparing affinity of Cpx to protein free (red), membrane bound dSN25 (green) or membrane bound ternary SNARE complex (Brown) POPM1 lipid vesicles.*

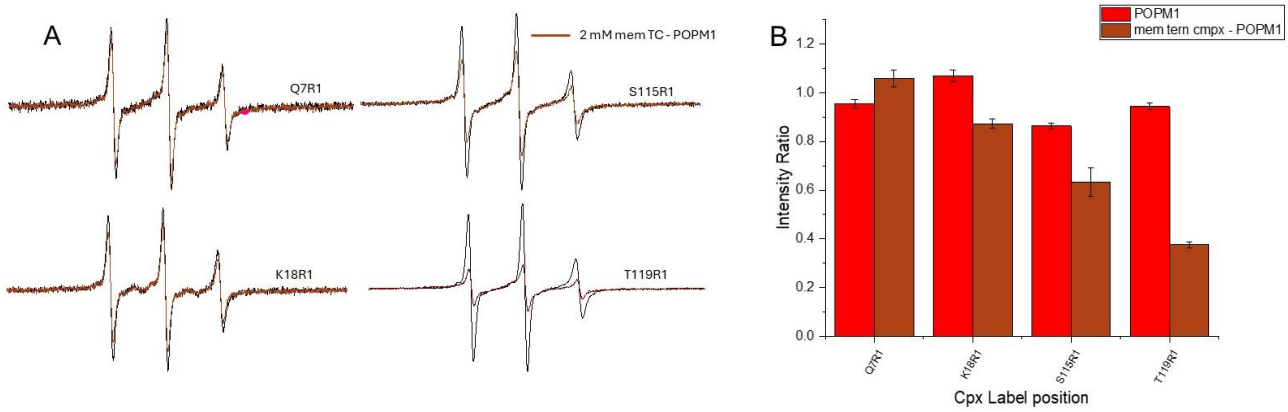

Figure 3-18 *(A) Normalized EPR spectra of Cpx mutants alone (black) or with dSN25:Syx$_{183-288}$:Syb$_{1-116}$-POPM1 proteoliposomes (brown). (B) Intensity ratio of high field resonance line of Cpx with POPM1 (red) or dSN25:Syx$_{183-288}$:Syb$_{1-116}$-POPM1 (brown).*

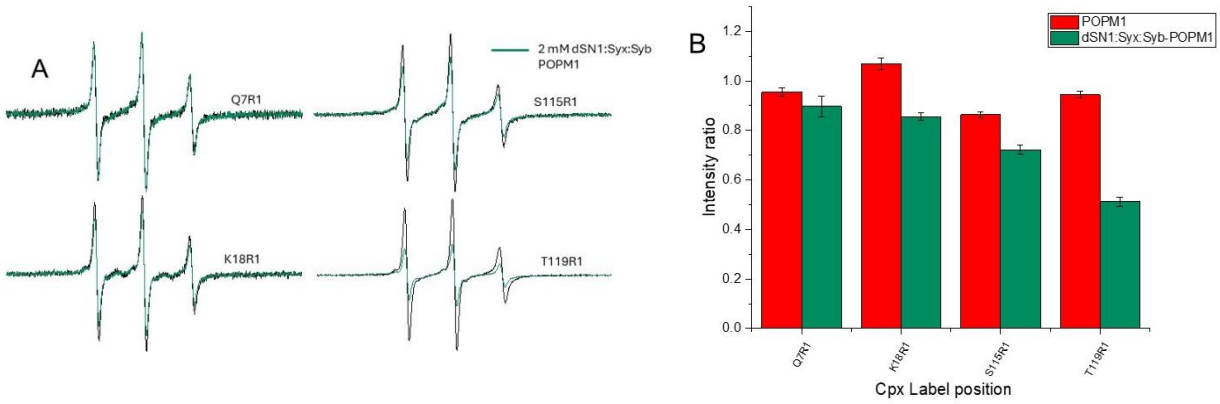

Figure 3-19 *(A) Normalized EPR spectra of Cpx mutants alone(black) or with dSN1:Syx$_{183-288}$:Syb$_{1-96}$-POPM1 (cyan). (B) Intensity ratio of high field resonance line of Cpx with POPM1 (red) or dSN1:Syx$_{183-288}$:Syb$_{1-116}$-POPM1.*

3.2.9 When SNAREs are tethered to the membrane, SNAP25 is needed to allow Cpx membrane interaction

In the presence of protein-free membrane vesicles, Cpx interacts with and is sensitive to the properties of the membrane. Anisotropy measurements demonstrate that when Syx or Synaptobrevin (Syb) is membrane-bound, Cpx fails to interact with membranes (Figure 3-20A,B). Syntaxin effectively blocked Cpx from accessing the lipid bilayer in a PIP2-independent manner. However, this phenomenon changed in the presence of dSNAP25. Membrane bound dSN25 increased the Cpx-membrane association relative to that in protein-free lipids. Additionally, the presence of dSNAP25 along with Syx or Syx and Syb resulted in an increased membrane binding of Cpx. The highest increase in partition coefficient was observed with membrane bound ternary complex. While Cpx could interact with protein free membranes, the presence of membrane bound SNAREs required SNAP25 for Cpx to interact with vesicles.

Anisotropy allows us to measure the binding affinity of Cpx to membranes with reconstituted SNAREs but does not allow us to distinguish whether Cpx is interacting primarily with the SNAREs or with the lipid bilayer. EPR enables us to address this question and determine the interactions

contributing to the membrane association. For the spin label at position 119 (T119R1), the intensity ratio of the EPR spectrum with and without membranes is sensitive to lipid association at the Cpx C-terminus (Figure 3-20B).[105] Membrane bound dSN25 showed a substantial decrease in intensity ratio indicating that the Cpx C-terminus is interacting with lipids. With dSN25:Syx or dSN1:Syx:Syb, possible intermediates in the SNARE complex formation process, there were further decreases in intensity ratio. The fully assembled SNARE complex led to another major drop in intensity ratio, showing the strongest membrane interaction under all studied conditions.

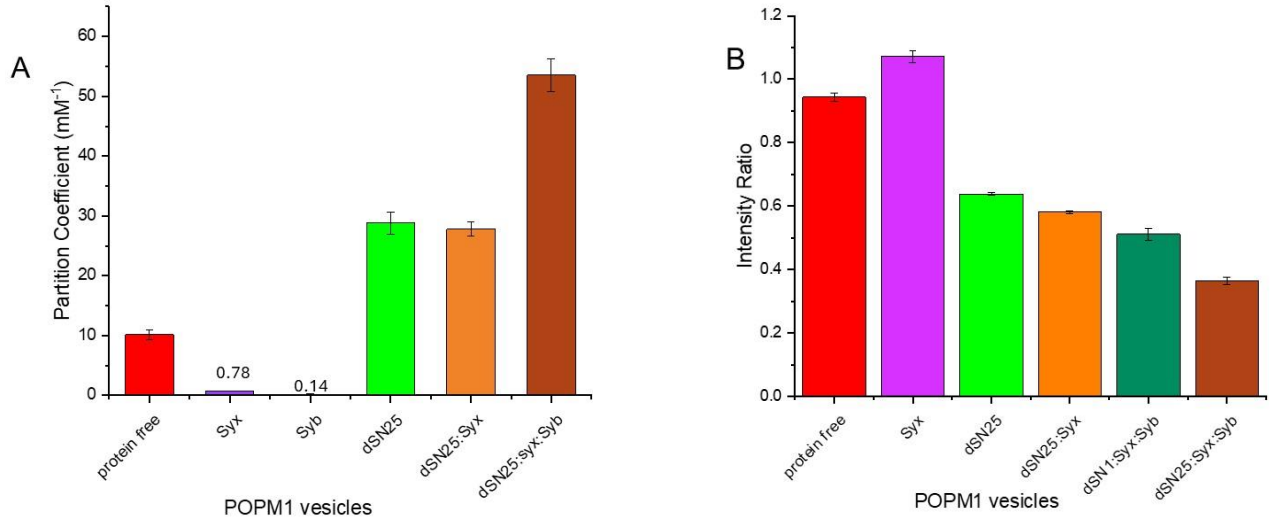

Figure 3-20 *(A) Partition coefficient of Cpx binding to protein free or membrane bound SNAREs. (B) Intensity ratio of EPR spectra of CpxT119 with protein free or membrane bound SNAREs.*

3.3 When SNAREs are in solution, Cpx can interact with different SNARE configurations but only binds to the ternary complex when SNAREs are membrane bound

Complexin is known to bind to the assembled post fusion complex in solution, but information on its interaction with membrane bound SNAREs is limited as previous studies on Cpx-SNARE interactions have focused mainly on cytosolic SNAREs. The assembled SNARE complex is known to be very stable.[15,118] However, circular dichroism has revealed that SNARE complexes that include their linker and transmembrane regions are more resistant to thermal and chemical denaturation compared to their cytosolic counterparts.[119] Further structural insights revealed that Syb and Syx formed continuous helices through their SNARE motifs, linker and transmembrane regions.[119] The SNARE motifs of Synaptobrevin (Syb) and Syntaxin (Syx)are connected to their transmembrane regions which contributes to the stability of the of the ternary SNARE complex .[15]

We used fluorescence anisotropy and cwEPR to investigate Cpx-SNARE interactions when SNAREs are either in solution or membrane-bound. This study explored the interactions of Cpx with individual SNARE proteins, potential SNARE intermediates and the fully assembled ternary SNARE complex. In these measurements we aim to determine how the lipid environment influences Cpx-SNARE interactions and to determine the minimal SNARE configuration necessary to promote a Cpx interaction. Understanding these interactions will potentially reveal the initial point at which Cpx interacts with SNAREs during the SNARE assembly process.

3.3.1 Complexin interacts with Syntaxin but not SNAP25 in solution.

To begin understanding Cpx's interactions with SNARE, we started with the individual t-SNARE proteins. The affinity of Cpx to the SNAREs was measured using fluorescence anisotropy and

continuous wave electron paramagnetic resonance (cwEPR). For these experiments, Cpx was labelled at position T119 with Alexa Fluor 546. The SNARE proteins were titrated into 50 nM solution of fluorophore-labelled Cpx, and the change is anisotropy was recorded and used as a measure of the Cpx-SNARE interaction.

With SNAP25, there was very little change in anisotropy, indicating a very low affinity for Cpx in solution (Figure 3-21A). EPR experiments corroborated this, showing no measurable interaction between SNAP25 and Cpx (Figure 3-21B). This result was expected, as several studies had previously reported a lack of interaction between SNAP25 and Cpx.[105,115,116]

However, in the presence of Syntaxin (Syx_{1-262}), there was a noticeable Cpx-Syx interaction. At low Syx concentrations (10 μM), there is minimal change in the anisotropy (Figure 3-21A). As the concentration of Syx increased, Cpx began to interact more strongly with it (Figure 3-21A). Previous studies investigating the Cpx-Syx interaction have yielded inconsistent results which could be due to the different concentrations of Syx used.[105,115,116]. Our results suggest that Cpx exhibits a weak affinity for Syx so that at low concentrations of Syx there is little interaction that becomes more apparent as the Syx concentration is increased. Syx oligomerizes and forms clusters especially at high concentrations,[120,121] and Cpx may be interacting with these clusters.

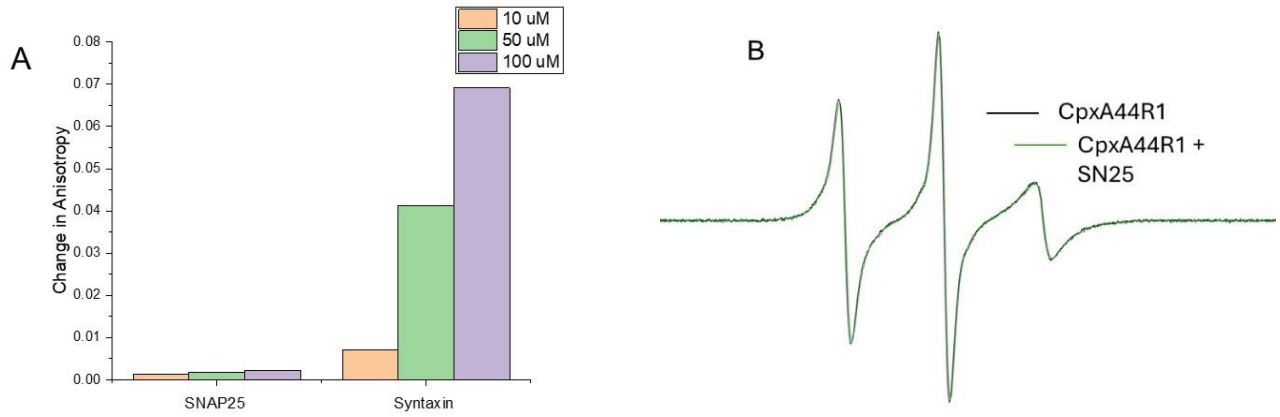

Figure 3-21 *Complexin interacts with Syntaxin but not SNAP25 in solution. (A) Change in the anisotropy of CpxT119Alexa546 in the presence of increasing concentrations of SNAP25 or Syntaxin. (B) EPR spectra of Cpx the absence or presence of SNAP25.*

3.3.2 Complexin interacts with an assembled tSNARE or ternary SNARE complex in solution

The binary t-SNARE complex was prepared by mixing SNAP25 and Syntaxin (Syx_{1-262})in a 1:1 molar ratio and incubating the mixture overnight. Similarly, the ternary SNARE complex was made by mixing SNAP25, Syx_{1-262} and Synaptobrevin (Syb_{1-96}) in a 1:1:1 ratio and allowing it to incubate overnight. Anisotropy measurements indicated that Cpx interacts with the t-SNARE complex in solution (Figure 3-22B). A decrease in the EPR signal amplitude in the presence of the Syx:SNAP25 tSNARE complex suggested that Cpx interacts with the tSNARE complex at concentrations where it does not interact with either SNAP25 or Syx alone (Figure 3-22A). As expected, Cpx also interacted with the ternary SNARE complex in solution (Figure 3-22C).

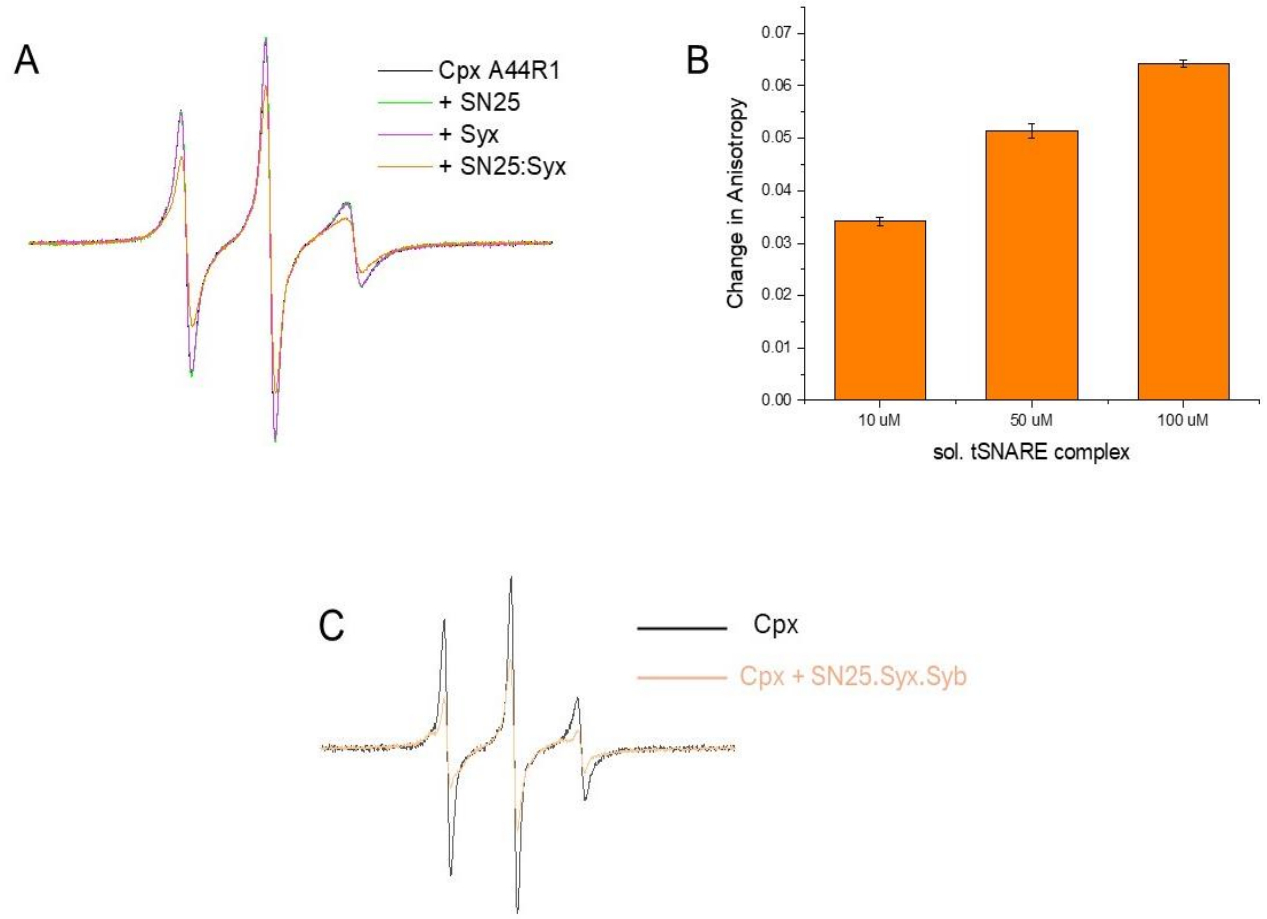

Figure 3-22 *Complexin interacts with assemble SNARE complexes in solution. (A) EPR spectra of Cpx alone or with SNAP25, Syx or SNAP25:Syx complex in solution. (B) Change in the anisotropy of CpxT119Alexa in the presence of increasing concentration of the tSNARE SNAP25:Syx complex. (C) EPR spectra of Cpx in the absence and presence of the assembled ternary SNARE complex.*

3.3.3 In the presence of vesicles and assembled SNARE complexes in solution, Cpx prefers to bind to SNARE complexes.

Previous experiments demonstrated that the assembled t-SNARE or ternary SNARE complex (tern. cmpx), when tethered to a membrane bilayer, increased Cpx-membrane interactions (Figure 3-20). To investigate the effect of SNAREs in solution rather than in the membrane bound state, we

prepared soluble SNARE complexes and added them to pre-formed lipid vesicles. For the soluble SNARE complexes, SN25 and Syx_{1-262} were mixed in a 1:1 ratio to form the t-SNARE complex while SN25, $Syx_{1-262,}$ Syb_{1-96} were mixed in a 1:1 or 1:1:1 ratio to form the ternary complex. Protein free vesicles were prepared via dialysis. The preassembled SNAREs and vesicles were then mixed post dialysis. The membrane bound SNAREs were prepared as described previously.

When SNAREs were in solution with lipid vesicles, there was a decrease in the partition coefficient compared to their membrane bound counterparts or to protein free vesicles (Figure 3-23A). This could be because Cpx prefers to bind to an assembled SNARE complex rather than to membranes when SNAREs are in solution. Lipid vesicles are larger than the SNARE complexes, and when bound to Cpx, results in increased anisotropy changes. If Cpx binds to the SNAREs rather than vesicles, the change in anisotropy is smaller, and this could explain the reduced partition coefficient.

Intensity ratios for EPR spectra showed that, in the presence of lipid vesicles and ternary SNARE complex in solution, Cpx interacts with SNAREs while showing little to no interaction with the vesicles (Figure 3-23C). Complexin binds to the SNARE complex via its accessory and central helices, which aligns with our findings that show a decrease in intensity ratio at the accessory helix (D27 and A40) and the central helix (K54 and D68) positions (Figure 3-23C). At 10 mM POPM1 lipid concentrations, where there is Cpx-membrane interaction, the presence of the soluble ternary complex abolishes this interaction (Figure 3-23B). Although membrane bound SNAREs act to increase Cpx-membrane interaction, the presence of an assembled SNARE complex in solution will displace Cpx from membranes lacking SNAREs at the concentrations used here.

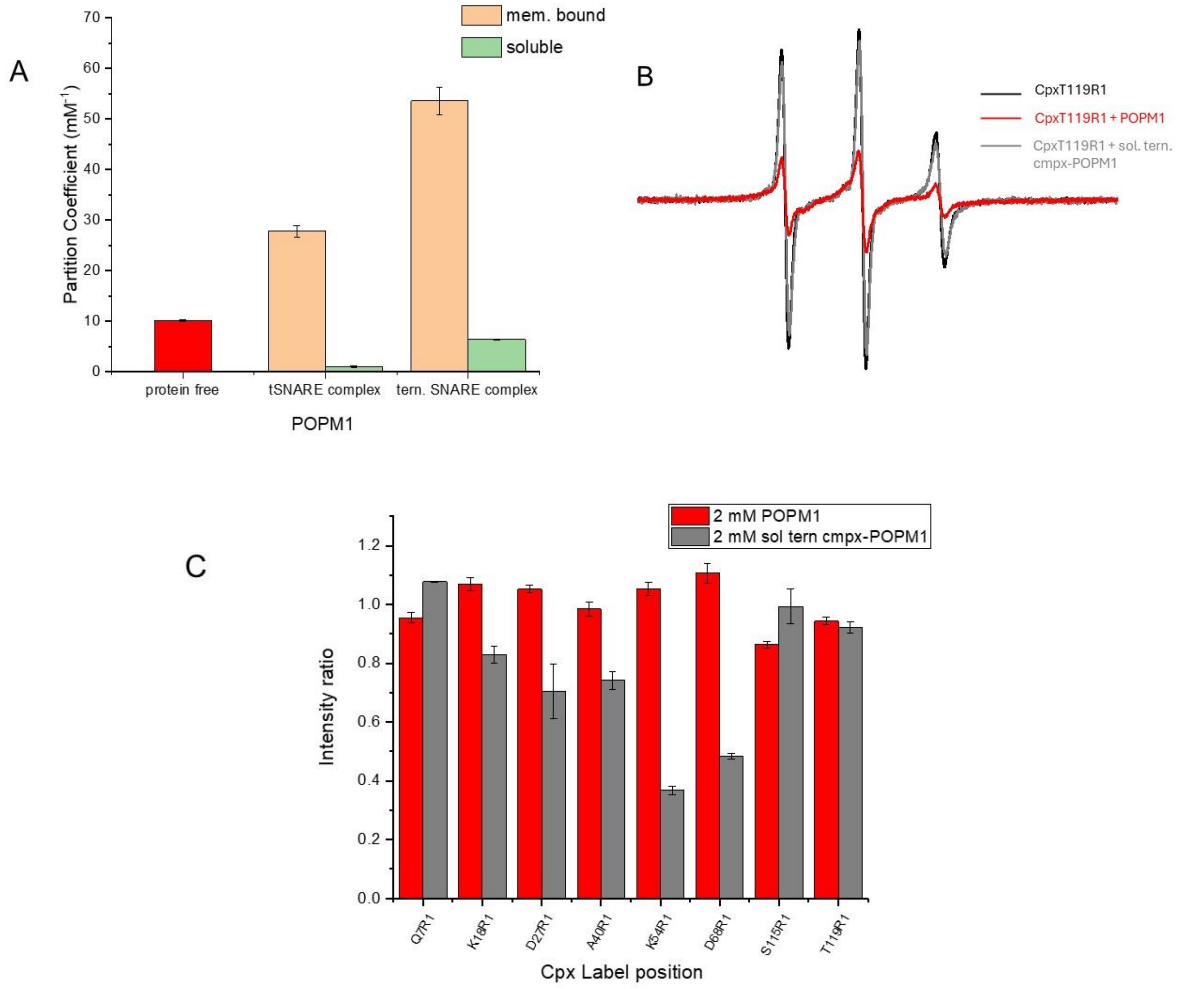

Figure 3-23 *Complexin prefers to bind to an assembled tSNARE or ternary SNARE complex. (A) Partition coefficient of Cpx binding to protein free vesicles (red), soluble (light green) or membrane bound (light brown) SNARE complexes with POPM1 vesicles. (B) EPR spectra of CpxT119 in the absence (black) or presence of 15 mM POPM1 (red) or 15 mM POPM1 with soluble ternary SNARE complex (grey). (C) Intensity ratio of Cpx mutants in the presence of POPM1 (red) or POPM1 with soluble ternary SNARE complex (grey)*

3.3.4 When SNAREs are membrane bound, Cpx only interacts with the fully assembled ternary SNARE complex

To examine conditions that more closely mimic physiological conditions, we investigated the interactions of Cpx with membrane bound SNAREs. Complexin was spin-labelled along its accessory and central helix at position D27, A40, K54 or D68, which are positions where Cpx shows SNARE interactions while exhibiting no membrane interaction (Figure 3-24). Membrane bound SNAREs were

prepared via dialysis as described previously. EPR spectra were recorded for Cpx in the absence and presence of protein-free or POPM1 vesicles with associated SNAREs. A complexin-SNARE interaction resulted in a decrease in normalized amplitude, which translates to a lower intensity ratio.

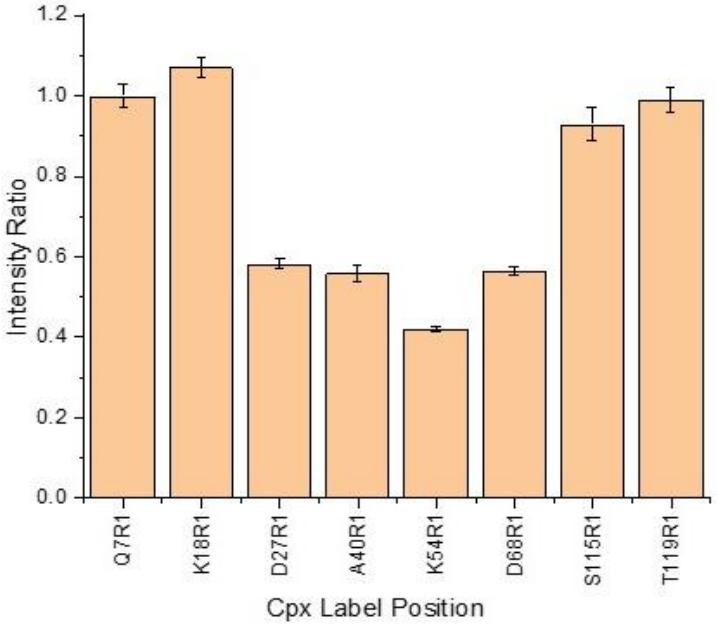

Figure 3-24 *Complexin interacts with the ternary SNARE complex at its accessory and central helix domains. Intensity ratio of Cpx mutants with assembled ternary SNARE complex. The SNARE complex was assembled with SNAP25, Syx$_{1-262}$ and Syb$_{1-96}$*

When 2 mM POPM1 with dSN25 attached was added to complexin, there was no change in the EPR spectrum compared to Cpx by itself in solution (Figure 3-25A, B). Increasing the proteoliposome concentration to 15 mM yielded no change in the EPR spectra (Figure 3-25C). These results show that Complexin does not interact with dSNAP25 when SNAP25 is membrane bound. Similarly, Cpx did not interact with Syx when Syx was membrane bound (Figure 3-26). Increasing the concentration of the Syx-POPM1 did not yield any change in the Cpx EPR spectra for sites that interact with SNAREs (Figure 3-26). This contrasts with the behavior seen in solution, where Cpx is clearly seen to interact with Syx (see Figure 3.3-1).

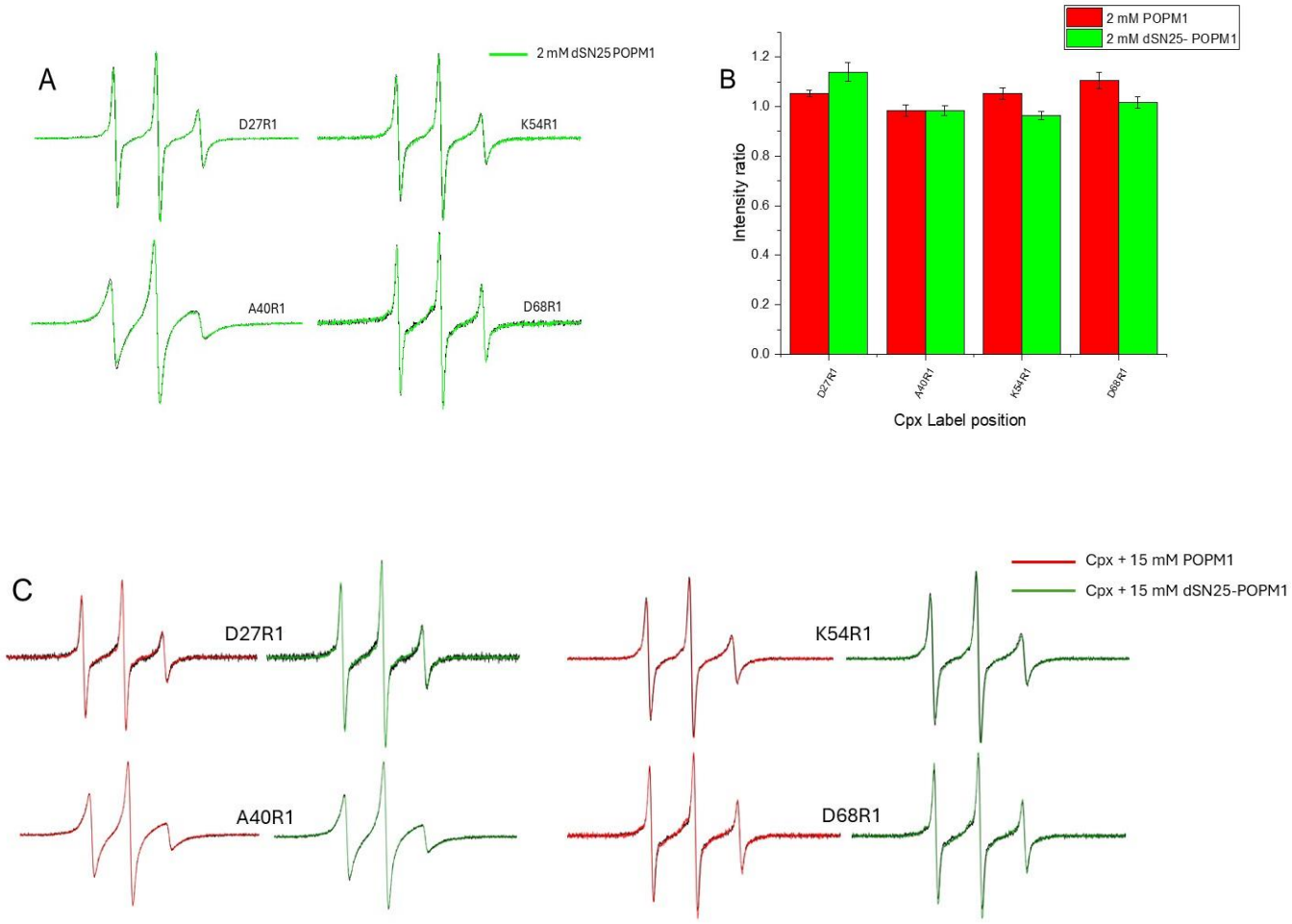

Figure 3-25 *(A) Normalized EPR spectra of Cpx mutants alone (black) or with 2 mM dSN25-POPM1 proteoliposomes (green). (B) Intensity ratio of high field resonance line of Cpx with POPM1 (red) or dSN25-POPM1 (green). (C) Normalized EPR spectra of Cpx mutants alone (black), with 15 mM POPM1 (red) or dSN25-POPM1 proteoliposomes (green).*

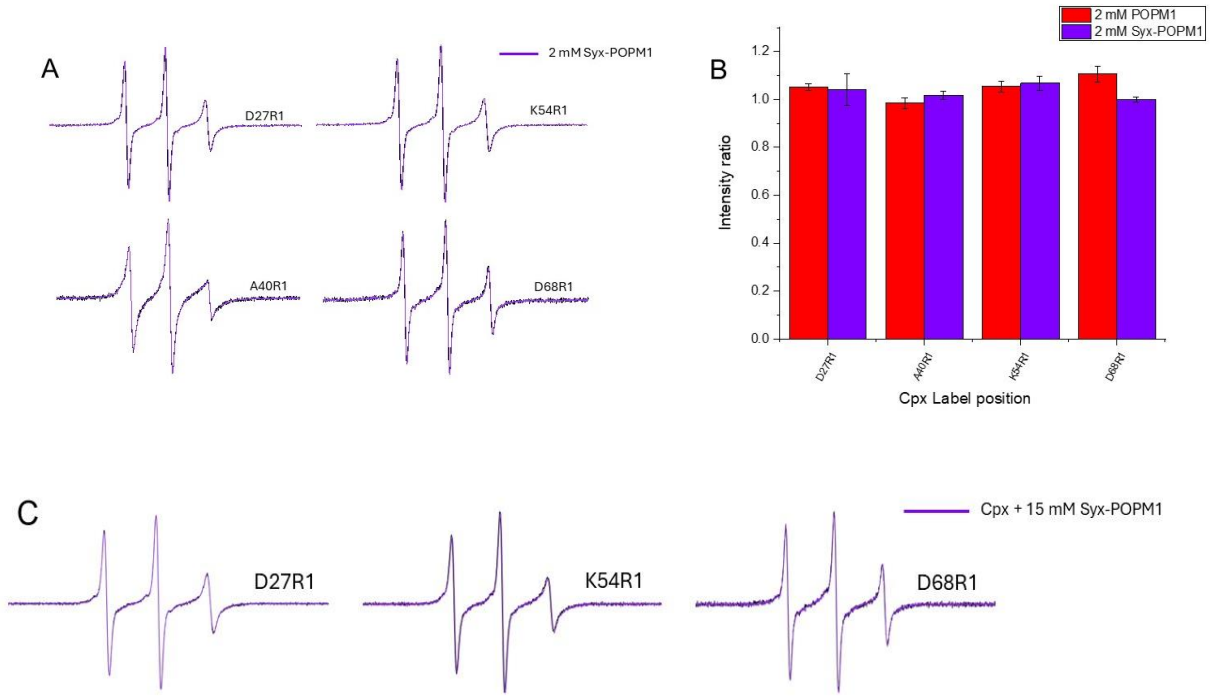

Figure 3-26 *(A) Normalized EPR spectra of Cpx mutants alone (black) or with 2 mM Syx$_{183-288}$-POPM1 proteoliposomes (violet). (B) Intensity ratio of high field resonance line of Cpx with POPM1 (red) or Syx$_{183-288}$-POPM1 (violet). (C) Normalized EPR spectra of Cpx mutants alone (black) or with 15 mM Syx$_{183-288}$-POPM1 proteoliposomes (violet).*

Syx binds to SN25 with high affinity to form a 2:1 tSNARE complex in solution.[13,122,123] This results in a stable, inactive four helix bundle where Syx replaces the Synaptobrevin (Syb) helix in the ternary SNARE complex. Complexin interacts with this complex and could potentially convert the 2:1 complex to a 1:1 Syx:SNAP25 complex.[124] This 1:1 complex is capable of binding Syb to form the ternary SNARE complex. In neuronal cells, SNAREs are localized on membranes and the lipid environment can alter the conformation of tSNAREs.[125] SNAP25 and Syx t-SNAREs colocalize into clusters and can interact on the plasma membrane.[13,125] Additionally, Cpx was shown to increase probability of vesicle fusion and Ca^{2+} sensitivity when preincubated with tSNAREs.[124]

When Syx and SNAP25 are incubated in solution, they predominantly form the 2:1 complex. Zdanowicz et al. proposed a method using 0.1% DPC where SNAP25 and Syx formed an acceptor complex that could be purified on a MonoQ column.[105,126] This acceptor complex was able to bind

Syb to achieve fast fusion and it was proposed to be 1:1 SNAP25:Syx complex.[126] In their study, Cpx was able to bind to this acceptor complex both in solution and when the acceptor complex was membrane bound.[105] In POPC:POPS vesicles, Cpx bound more strongly to tSNARE liposome compared to the post fusion SNARE complex. Cpx also reduced the affinity of the acceptor complex for Syb. They concluded that Cpx was able to inhibit fusion by blocking Syb insertion into the SNARE complex.[105]

In light of the more recent experiments highlighting the crucial role PIP2 plays in Cpx-membrane interaction,[111] we wanted to investigate these interactions in a more physiological environment using POPM1 vesicles. To make the t-SNARE complex, dSN25 and $Syx_{183-288}$ were mixed in a 1:1 molar ratio in 0.1% DPC and allowed to incubate overnight. The complex was then purified on a MonoQ column. A native gel was run to confirm the presence of the 1:1 complex. While there was a small band representing the 1:1 complex, the majority of the complex formed was the 2:1 Syx:SN25 complex. Increasing the ratio of dSN25 to favor the formation of the 1:1 complex was not very successful either. The small band of 1:1 Syx:dSN25 complex formed was contaminated by the 2:1 and other higher-order complexes. Attempts to purify the complex on a size exclusion chromatography (SEC) column were also unsuccessful. Ultimately, we decided to use the tSNARE mixture as is, mixing dSN25 and Syx in a 1:1 molar ratio and adding the complex to POPM1 lipids to form proteoliposome via dialysis.

EPR spectra were recorded for spin-labelled complexin in the presence and absence of dSN25:Syx proteoliposome, and Cpx did not show any association with tSNARE complex (Figure 3-27A, B). Increasing the concentration of the proteoliposome did not alter this result (Figure 3-27C). This contrasts with results using soluble tSNARE complex and work done by Zdanowicz et al. Although complexin was able to bind to tSNARE in solution or incorporated into POPC:POPS vesicles, no interaction was detected once the tSNARE is associated with POPM1 vesicles.

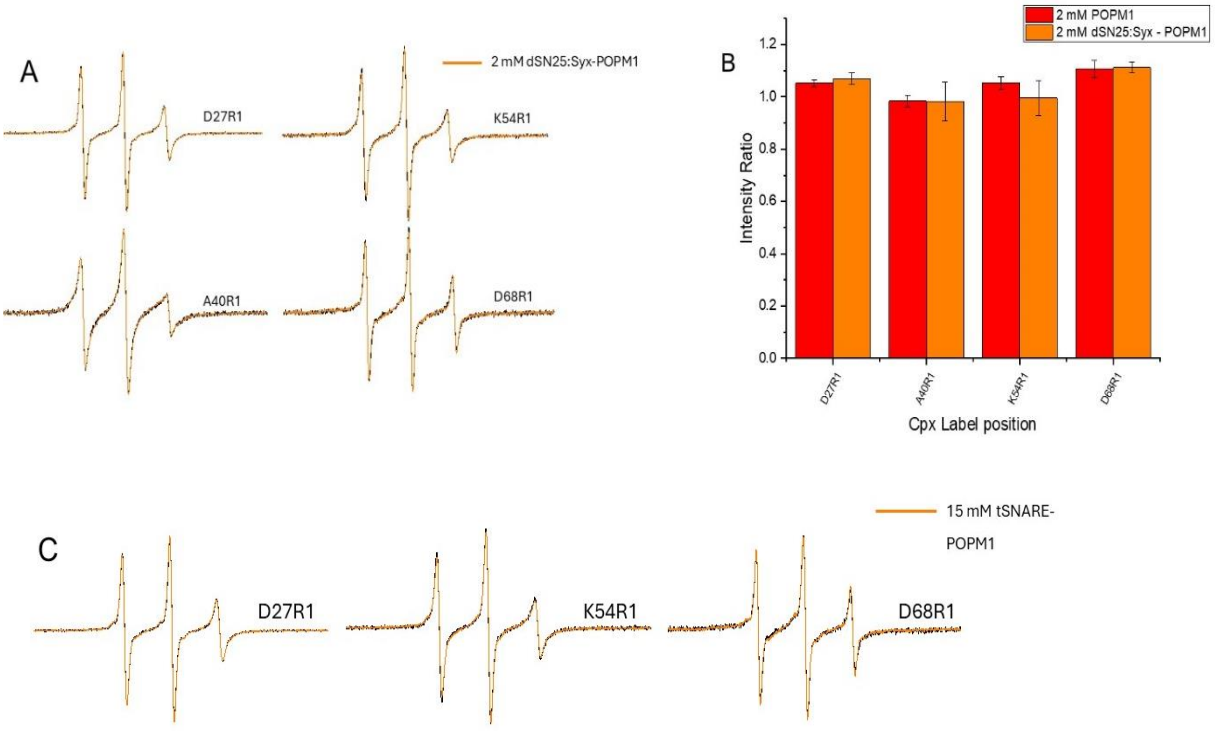

Figure 3-27 *(A) Normalized EPR spectra of Cpx mutants alone (black) or with 2 mM dSN25:Syx$_{183-288}$-POPM1 proteoliposomes (orange). (B) Intensity ratio of high field resonance line of Cpx with POPM1 (red) or dSN25:Syx$_{183-288}$-POPM1 (orange). (C) Normalized EPR spectra of Cpx mutants alone (black) or with 15 mM dSN25:Syx$_{183-288}$-POPM1 proteoliposomes (orange).*

Finally, we explored Cpx's interaction with assembled, membrane-associated SNARE complexes. The ternary SNARE complex was preassembled with dSN25, Syx$_{183-288}$ and Syb$_{1-116}$ in a 1:1:1 molar ratio. The complex was incorporated into to POPM1 lipids, where proteoliposomes were formed via detergent dialysis. The addition of these proteoliposome led to a decrease in normalized amplitude of the EPR spectra across the accessory and central helices of Cpx (Figure 3-28), confirming that Cpx can associate with the assembled SNARE complex when the SNAREs are

membrane-bound. Another ternary complex preassembled with dSN25, Fl Syx and Syb_{1-1116} was incorporated into POPM1 lipids. Similar to the ternary complex assembled with $Syx_{183-288}$, there was a decrease in normalized amplitude across the central and accessory helices of Cpx when the ternary complex was formed with FL Syx instead (Figure 3-29). However, at position 68 (D68R1), there is a smaller decrease in the intensity ratio suggesting that Cpx does not interact strongly with the SNARE complex at that position. A proposed intermediate in the SNARE complex formation[113] composed of dSN1, $Syx_{183-288}$ and Syb_{1-116} was assembled also and incorporated into POPM1 vesicles. EPR measurements indicated that Cpx did not bind to this complex when it was membrane bound (Figure 3-30). Complexin only interacts with the fully assembled ternary complex when SNAREs are membrane bound.

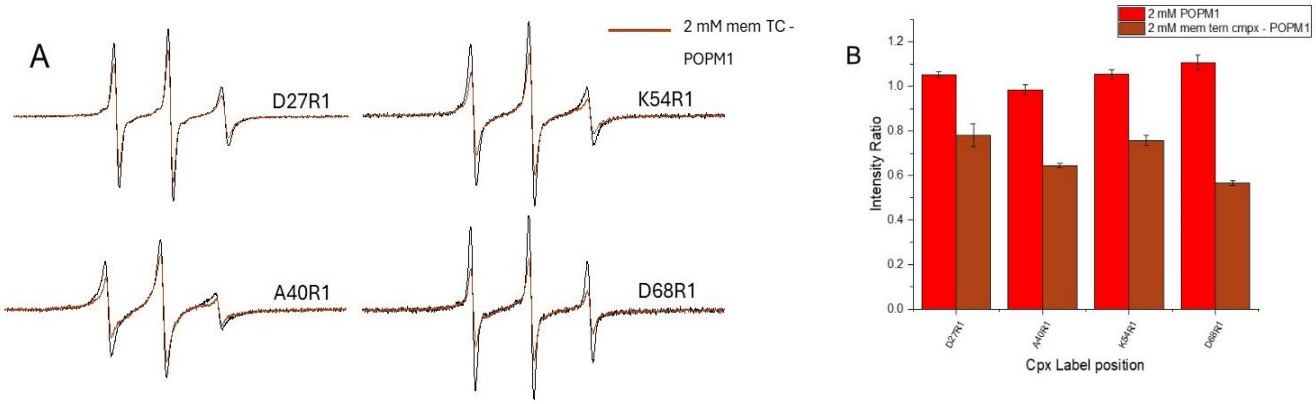

Figure 3-28 *(A) Normalized EPR spectra of Cpx mutants alone (black) or with dSN25:$Syx_{183-288}$:Syb_{1-116}-POPM1 proteoliposomes (brown). (B) Intensity ratio of high field resonance line of Cpx with POPM1 (red) or dSN25:$Syx_{183-288}$:Syb_{1-116}-POPM1 (brown).*

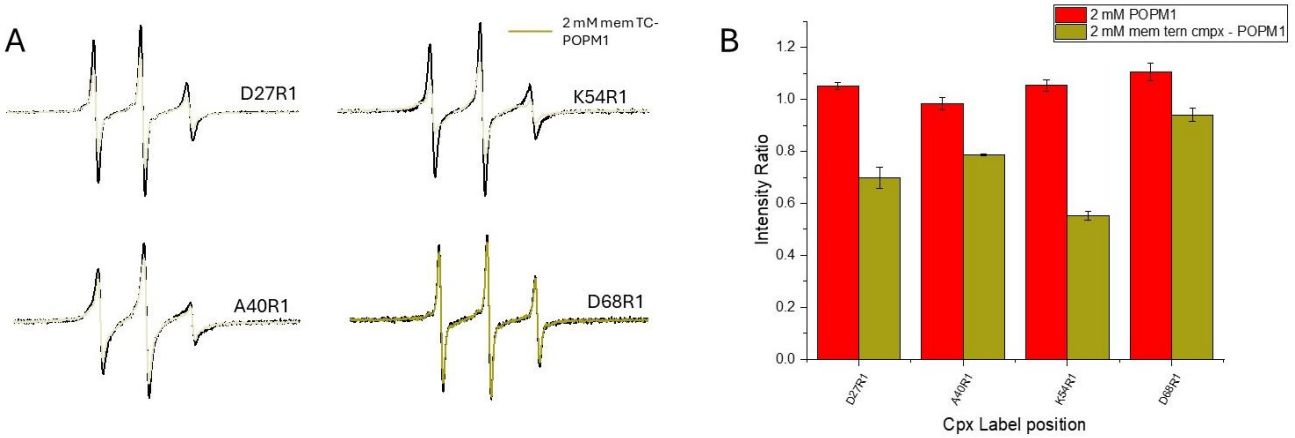

Figure 3-29 *(A) Normalized EPR spectra of Cpx mutants alone (black) or with dSN25:FL Syx:Syb$_{1-116}$-POPM1 proteoliposomes (olive green). (B) Intensity ratio of high field resonance line of Cpx with POPM1 (red) or dSN25:FL Syx:Syb$_{1-116}$-POPM1 (brown).*

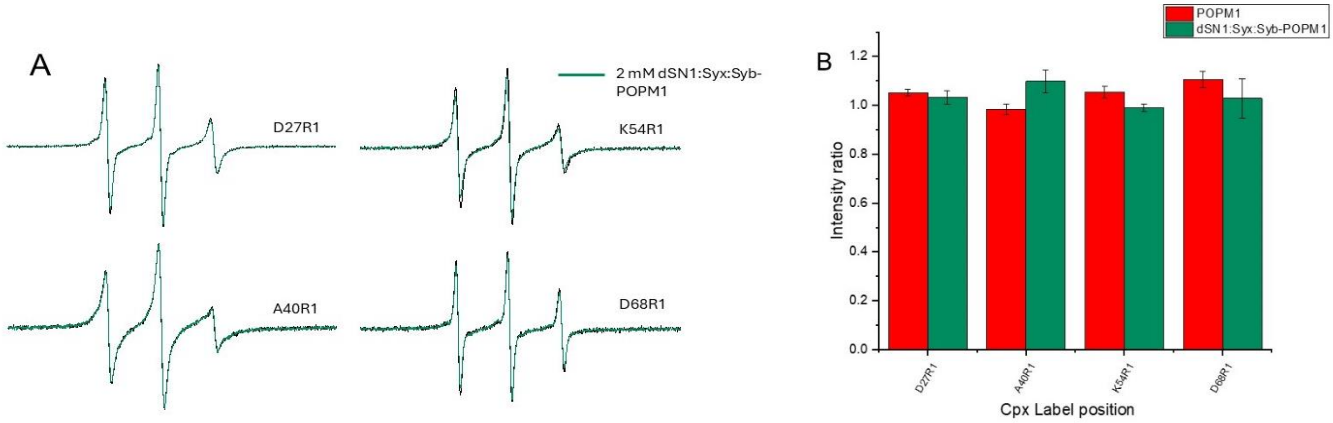

Figure 3-30 *(A) Normalized EPR spectra of Cpx mutants alone (black) or with dSN1:Syx$_{183-288}$:Syb$_{1-116}$-POPM1 proteoliposomes (cyan). (B) Intensity ratio of high field resonance line of Cpx with POPM1 (red) or dSN1:Syx$_{183-288}$:Syb$_{1-116}$-POPM1.*

To investigate the binding affinity to membrane-bound SNAREs, we recorded the EPR spectra of spin-labelled complexin in the presence and absence of proteoliposomes. These proteoliposomes were prepared with individual and assembled SNARE proteins attached to POPM1 vesicles. The intensity ratio, defined as the ratio of the normalized amplitude of the high field resonance line of Cpx bound to proteoliposomes to Cpx in solution, was used as a measure of Cpx-SNARE interaction. The results are summarized in (Figure 3-31). The intensity ratio of all proteoliposomes, with the exception of those containing the membrane-bound ternary complex, was approximately 1. This indicates that Cpx does not interact significantly with the membrane-bound individual or intermediate SNARE complexes. However, when the ternary SNARE complex was membrane-bound, there was a notable decrease in the intensity ratio, suggesting a strong Cpx-SNARE interaction. These findings indicate that Cpx only binds the fully assembled membrane-bound ternary SNARE complex. This suggests that the presence of all three SNARE proteins in an

assembled complex is necessary for significant Cpx interaction when these proteins are membrane-bound.

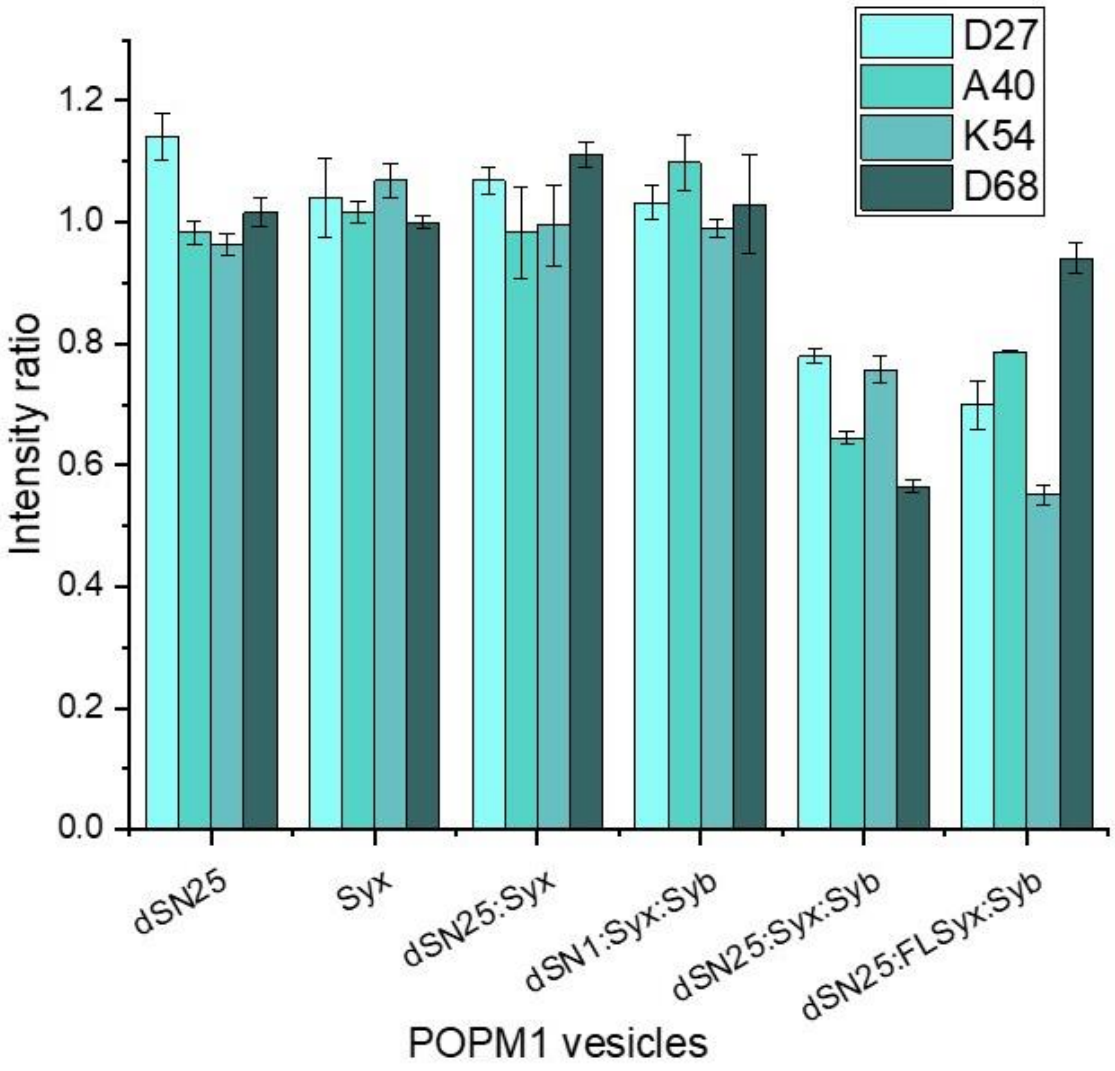

Figure 3-31 *Intensity ratio of Cpx mutants with membrane-bound SNAREs. Syx represents* $Syx_{183\text{-}288}$

3.4 Role of Munc18 in modulating Complexin's interactions with membranes and tSNAREs

Munc18 is a member of the Sec1/Munc18 (SM) family of cytosolic proteins that are critical for fusion as demonstrated by the loss of all forms of release in Munc18 knockout mice.[127] Munc18 binds tightly to and stabilizes a closed conformation of Syx and has been proposed to act as a template for SNARE assembly.[20,128,129] It also binds to the SNARE complex through its interaction with the N-terminal domain of Syx.[19] Munc18 has also been shown to bind to a tSNARE complex and convert the 2:1 Syx:SNAP25 complex to a 1:1:1 Syx:SNAP25:Munc18 complex.[130] We investigate Munc18 interaction with membrane-bound tSNAREs and how that alters Cpx binding to SNAREs or membrane lipids.

3.4.1 Munc18 does not significantly bind to POPM1 vesicles

Initial experiments were conducted to assess whether Munc18 binds to POPM1 lipid vesicles in the absence of other proteins. POPM1 vesicles prepared via extrusion were added to fluorophore labelled Munc18. The binding isotherm indicates that Munc18 alone does not exhibit significant binding to POPM1 lipids vesicles (Figure 3-32). This suggests that Munc18 does not interact directly with the lipid bilayer, and instead its role in modulating interactions between Cpx and membrane-bound SNAREs likely depends on its interactions with other SNARE proteins.

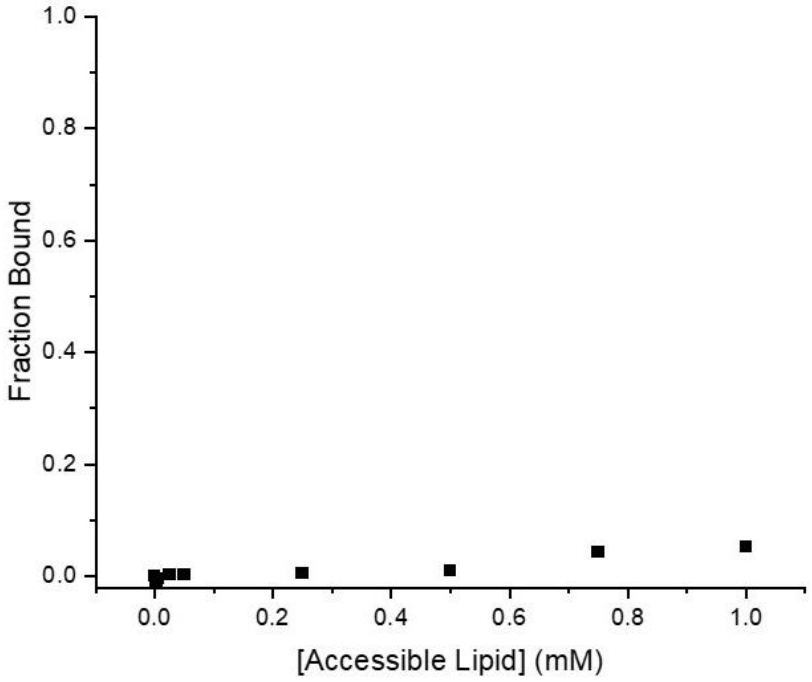

Figure 3-32 *Munc18 does not bind to POPM1 vesicles. Fraction of Munc18 bound as a function of accessible lipid concentration.*

3.4.2 Munc18 does not alter Cpx interactions with Syx-POPM1

To further investigate the role of Munc18 in SNARE interactions, we examined its effects on Syx-POPM1 vesicles. $Syx_{183\text{-}288}$-POPM1 proteoliposomes were prepared as in previous experiments and incubated with Munc18 overnight. Complexin binding was measured with fluorescence anisotropy. Ther results showed that the presence of Munc18 did not significantly alter the measured partition coefficient (Figure 3-33). Regardless of the presence of Munc18, there is an overall decrease in Cpx binding to Syx-POPM1 vesicles.

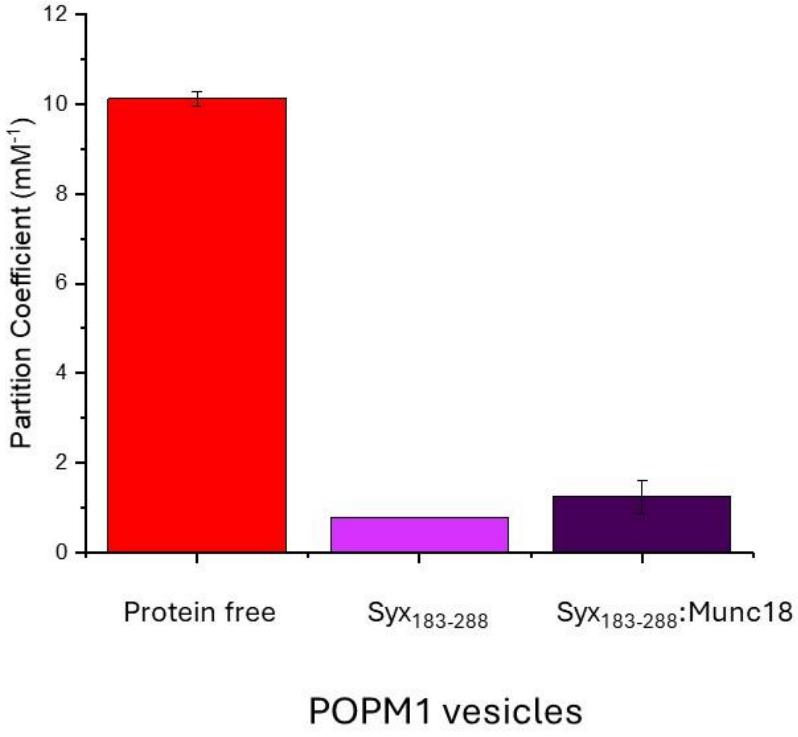

Figure 3-33. *Munc18 does not alter Cpx binding to Syx-POPM1 vesicles. Partition coefficients of Cpx binding to protein free (red), Syx (light purple) or Syx:Munc18 POPM1 vesicles.*

3.4.3 Effect of Munc18 on tSNARE proteoliposomes

Next, we explored how Munc18 influences tSNARE proteoliposomes and their interactions with Cpx. The tSNARE liposomes were prepared as previously described, using either full length Syx (FL Syx) or $Syx_{183-288}$ in combination with dSNAP25, and then incubated with Munc18 overnight. When the tSNARE was assembled with FL Syx and dSN25, Munc18 did not alter the binding of Cpx,

as evidenced by the unchanged partition coefficient

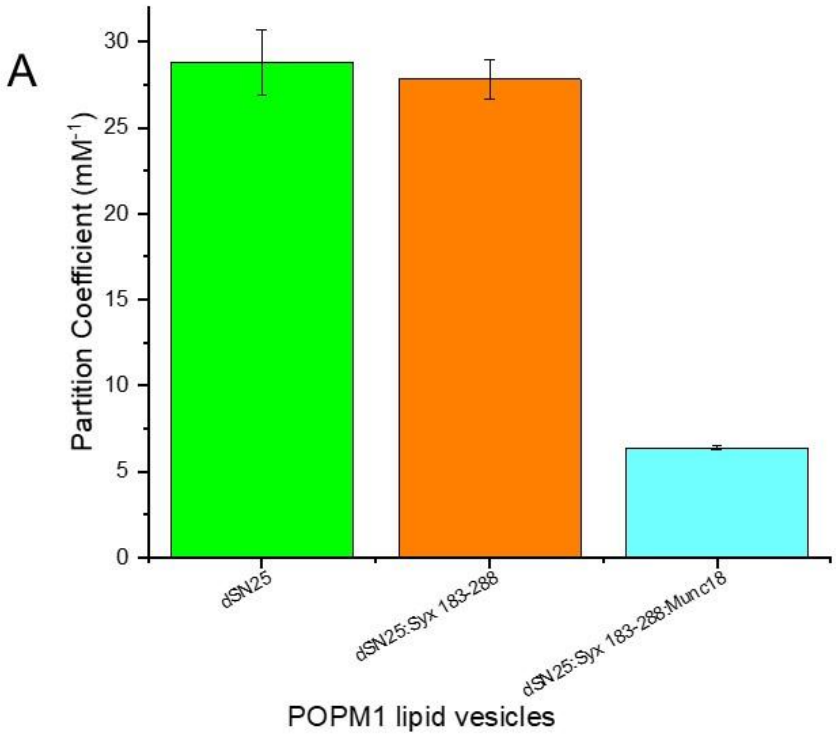

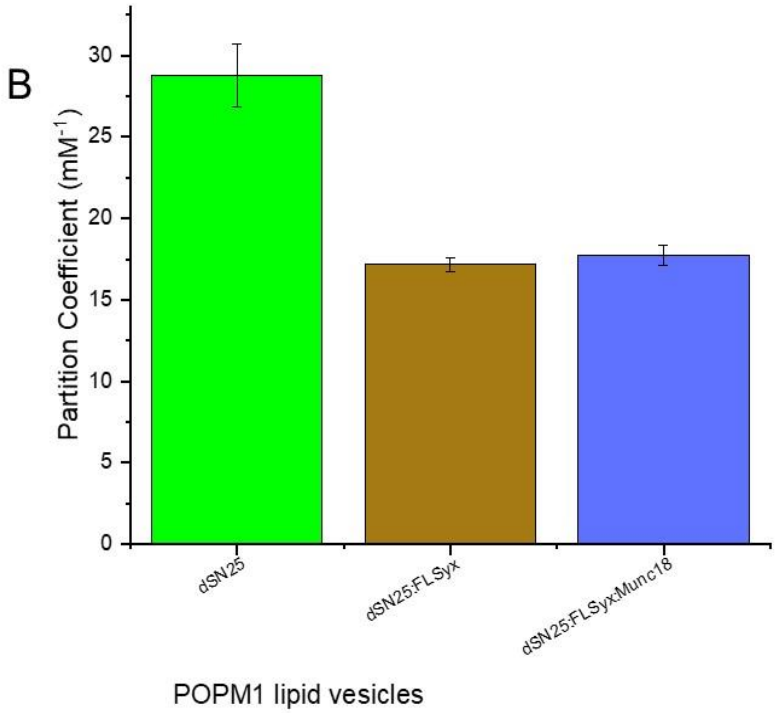

Figure 3-34B). However, when $Syx_{183-288}$ was used in the tSNARE complex, the presence of Munc18 resulted in a drastic decrease in the partition coefficient (Figure 3-36A). This decreased Cpx binding was further replicated with EPR measurements (Figure 3-35). This decrease in binding was time-dependent with longer incubations times between Munc18 and tSNARE proteoliposomes resulting in progressively lower partition coefficients (Figure 3-36).

This suggests that Munc18 dissociates Syx183-288 from the t-SNARE complex, which in turn restores Syx's inhibitory effect on Cpx membrane binding. Interestingly, the presence of SNAP25 did not reverse Syx's inhibitory action, indicating that Munc18's interaction with Syx183-288 destabilizes the t-SNARE complex. In contrast, Munc18 had no discernible effect on t-SNARE complexes formed with FL Syx, suggesting that the FL Syntaxin may form a more stable interaction with dSNAP25, which is not easily disrupted by Munc18.

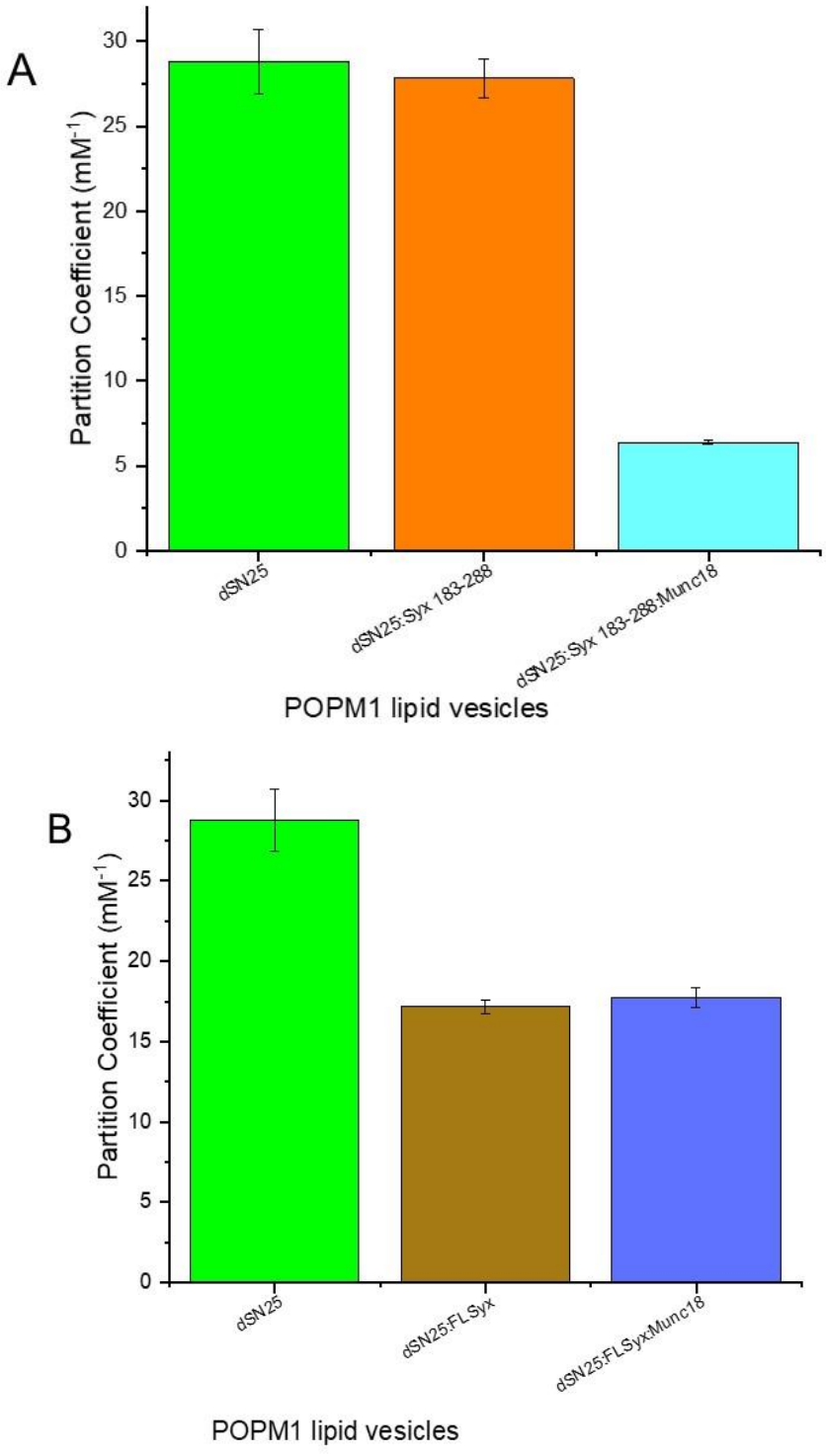

Figure 3-34 *Partition coefficient of Cpx binding to protein free or SNARE anchored POPM1 vesicles. The presence of Munc18 decreases Cpx interaction with dSN25:Syx$_{183-288}$-POPM1 vesicles (A) but does not affect binding to dSN25:FLSyx-POPM1 vesicles (B).*

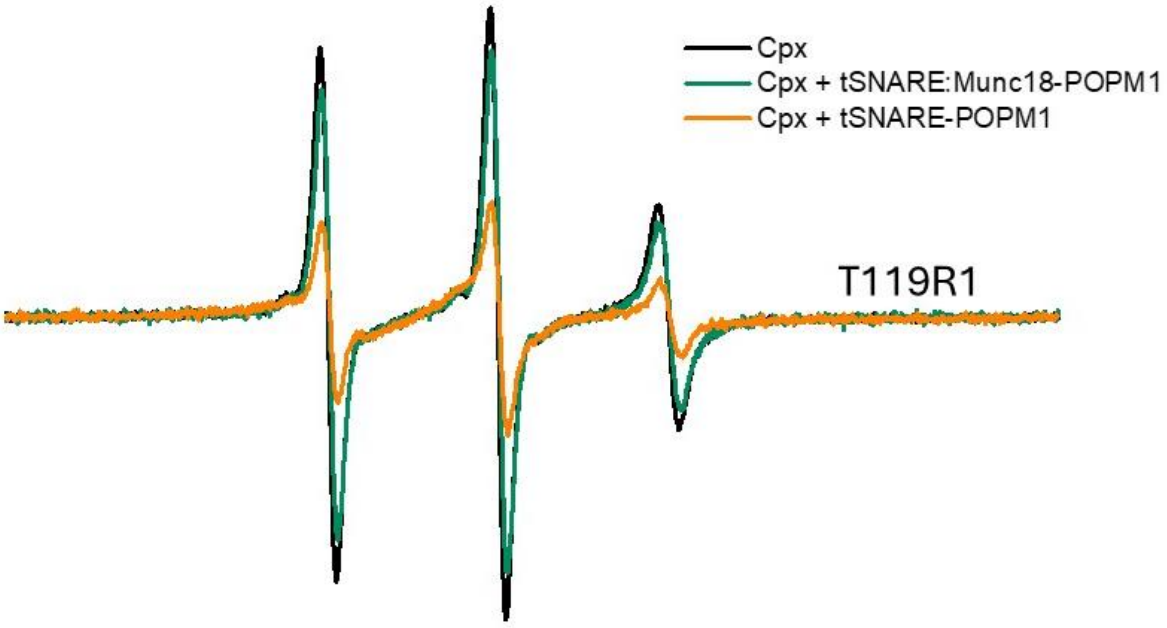

Figure 3-35 *Normalized cwEPR spectra of Cpx T119R1 alone (black) or bound to tSNARE-POPM1 (orange) or tSNARE:Munc18-POPM1.*

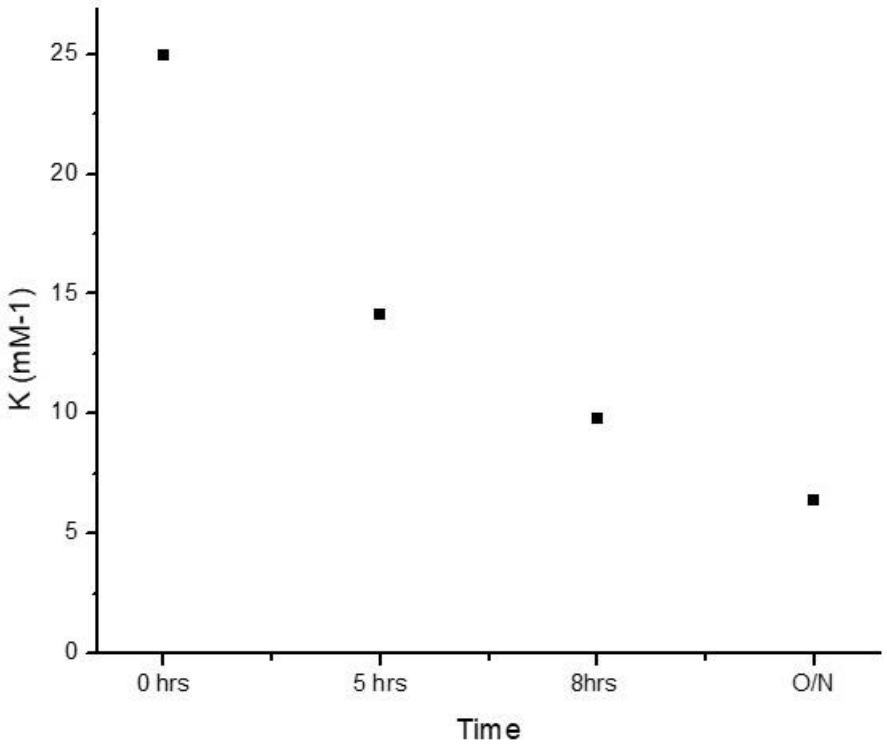

Figure 3-36 *Time dependent effect of Munc18 on Cpx affinity to tSNARE-POPM1 vesicles. Munc18 was incubated with tSNARE-POPM1 for different lengths of time. After the incubation, the proteoliposomes were titrated into solution containing fluorophore labelled Cpx. The anisotropy was measured and the derived partition coefficients (K) plotted.*

To further investigate the effects of Munc18 on Cpx interactions with SNARE proteins and membrane, spin-labelled Cpx mutants were used in EPR experiments. These measurements revealed minimal interactions between Cpx and SNARE proteins or lipid vesicles (Figure 3-37). Small but detectable membrane interactions were observed at positions K18, S115 and T119, although these interactions were weak. Increasing the concentration of the proteoliposome resulted in a small but detectable reduction in amplitude of the spectra across accessory and central helices of Cpx (Figure 3-39). This suggests that Munc18 may facilitate Cpx interactions with the some SNARE complex. This is a very weak interaction compared to Cpx's interaction with the ternary complex which occurs at much lower proteoliposome concentrations.

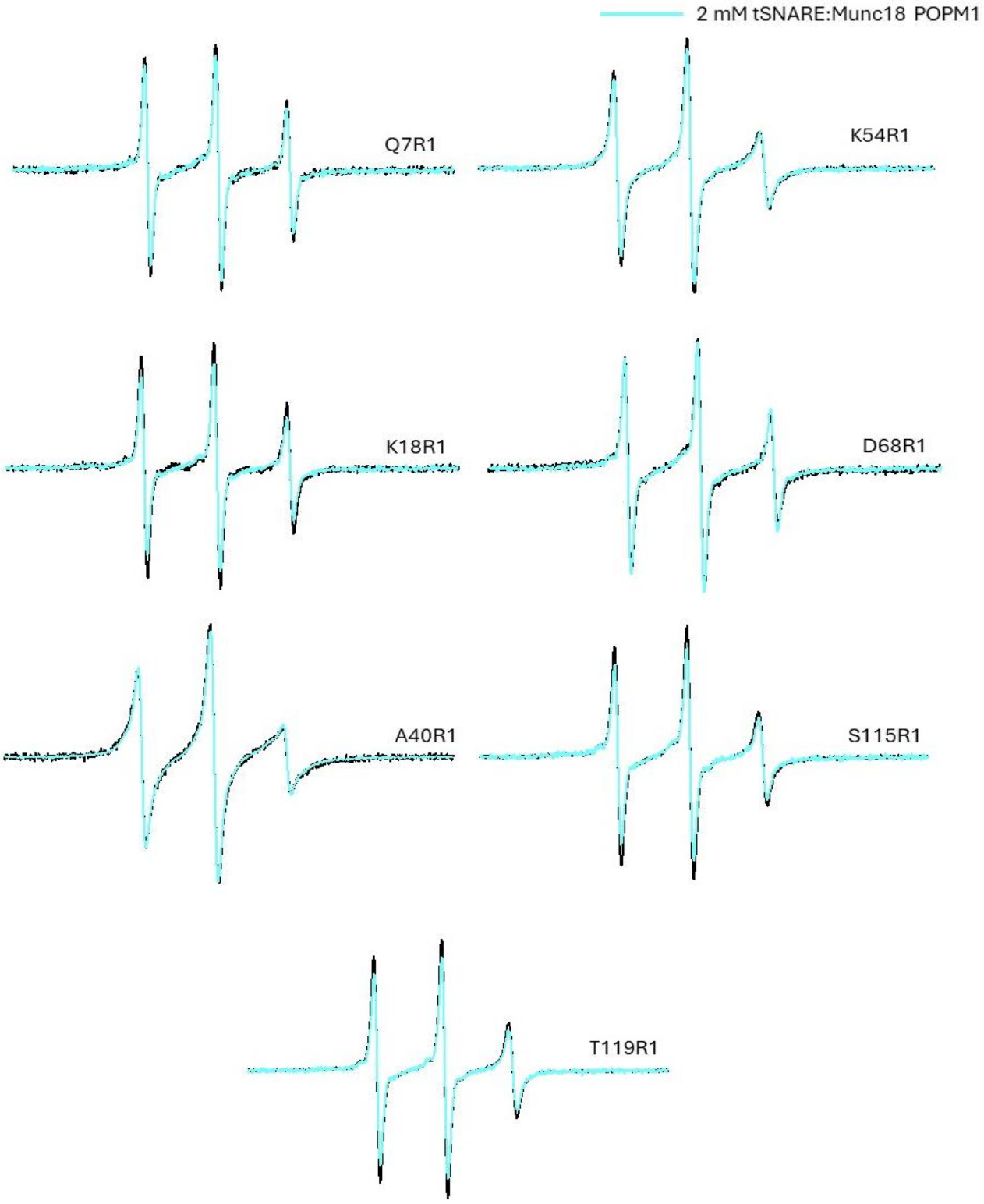

Figure 3-37 *Normalized cwEPR spectra of Cpx alone (black) or with 2 mM tSNARE:Munc18-POPM1 (cyan). Munc18 was incubated overnight with tSNARE-POPM1 vesicles*

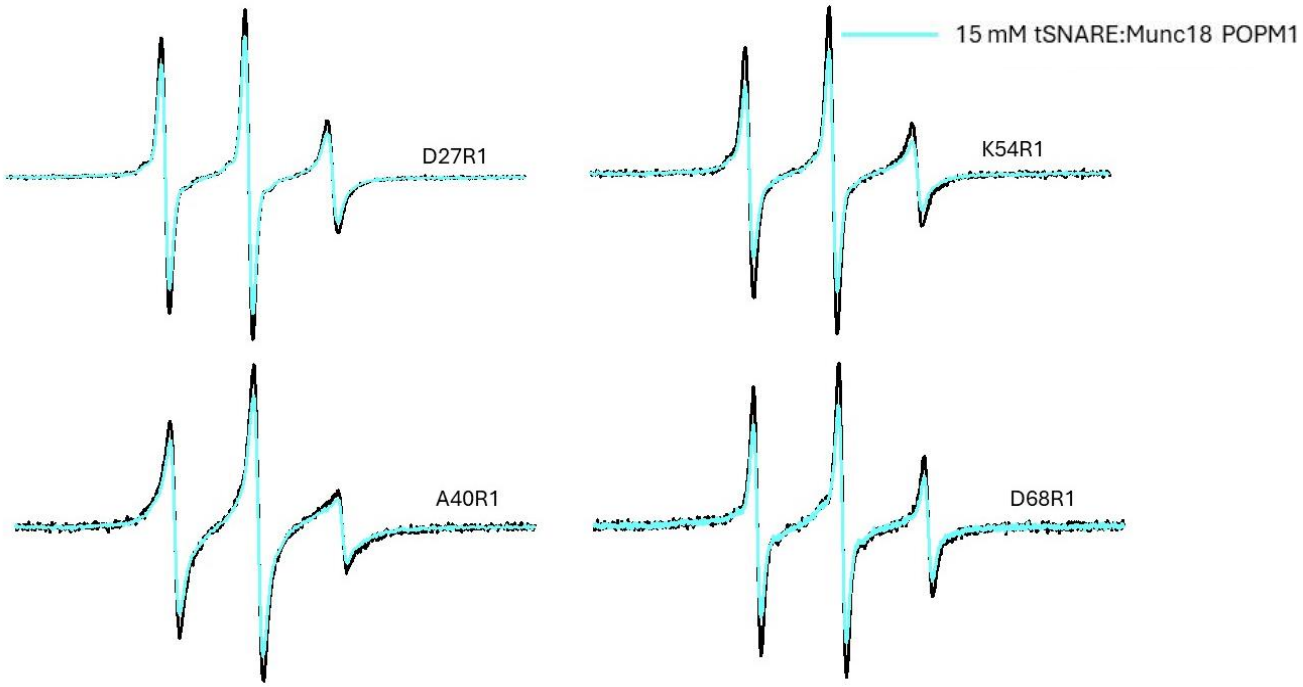

Figure 3-39 *Normalized cwEPR spectra of Cpx alone (black) or with 15 mM tSNARE:Munc18-POPM1 (cyan). Munc18 was incubated overnight with tSNARE-POPM1 vesicles*

Finally, we examined how increasing proteoliposome concentrations affected Cpx's membrane binding in the presence of Munc18 and t-SNARE complexes. At higher proteoliposome concentrations, the t-SNARE:Munc18 complexes still support Cpx membrane binding (Figure 3-40). Unlike Syx, which abolishes Cpx-membrane binding, tSNARE:Munc18 reduces Cpx's membrane interaction without fully inhibiting it. This suggests that Munc18 modulates Cpx binding in a more nuanced way, potentially by altering the stability of the tSNARE complex or the membrane environment.

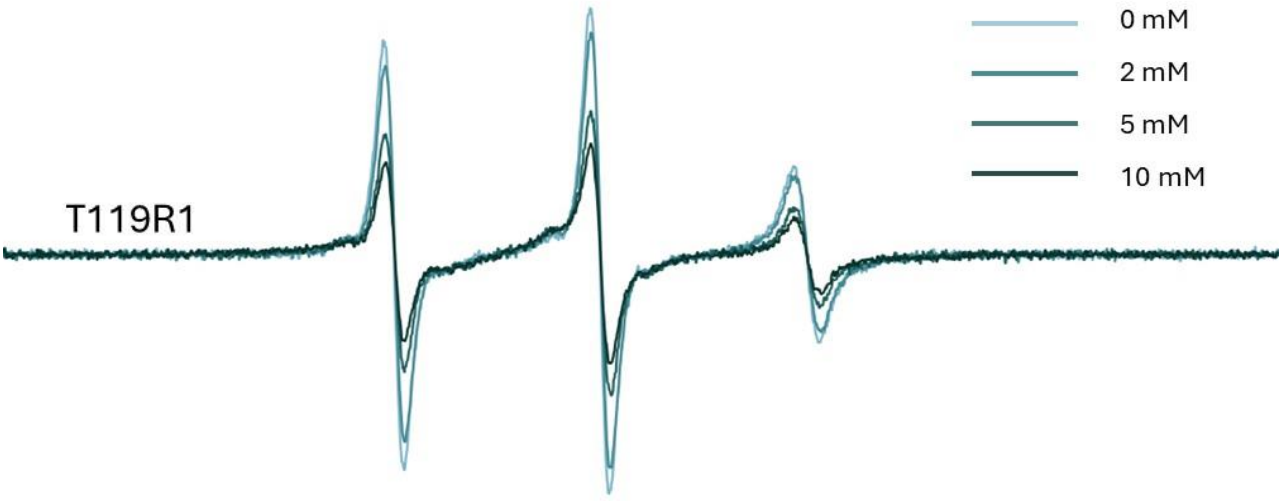

Figure 3-40 *Normalized cwEPR spectra of spin labelled CpxT119R1 with increasing concentrations of tSNARE:Munc18-POPM1*

3.5 Synaptotagmin prefers to bind to unsaturated lipid vesicles.

Synaptotagmin (Syt) binding to lipid vesicles was measured using fluorescence emission from fluorophore-labelled Syt. PM1 lipid vesicles were prepared using extrusion to produce 100 nm sucrose loaded vesicles. A sedimentation assay was used to measure Syt binding to these vesicles. In this assay, varying concentration of vesicles with different acyl chain composition were incubated with 200 nM of fluorophore labelled Syt. After ultracentrifugation, bound and unbound fractions of Syt were separated and fluorescence emission in the supernatant was measured. The partition coefficient was obtained similarly to anisotropy assays but with fluorescence emission intensities replacing anisotropy values.

Our results indicate that Syt has a strong preference for binding to lipids with unsaturated acyl chains (Figure 3-41). DPPM1, with two unsaturated chains, shows the weakest binding to Syt. The introduction of one unsaturated chain in POPM1 results in a significant 7-fold increase in binding. This binding is further enhanced with the doubly unsaturated DOPM1. This binding mirrors Cpx binding to unsaturated lipid chains and highlights the importance of disordered membranes in promoting protein binding.

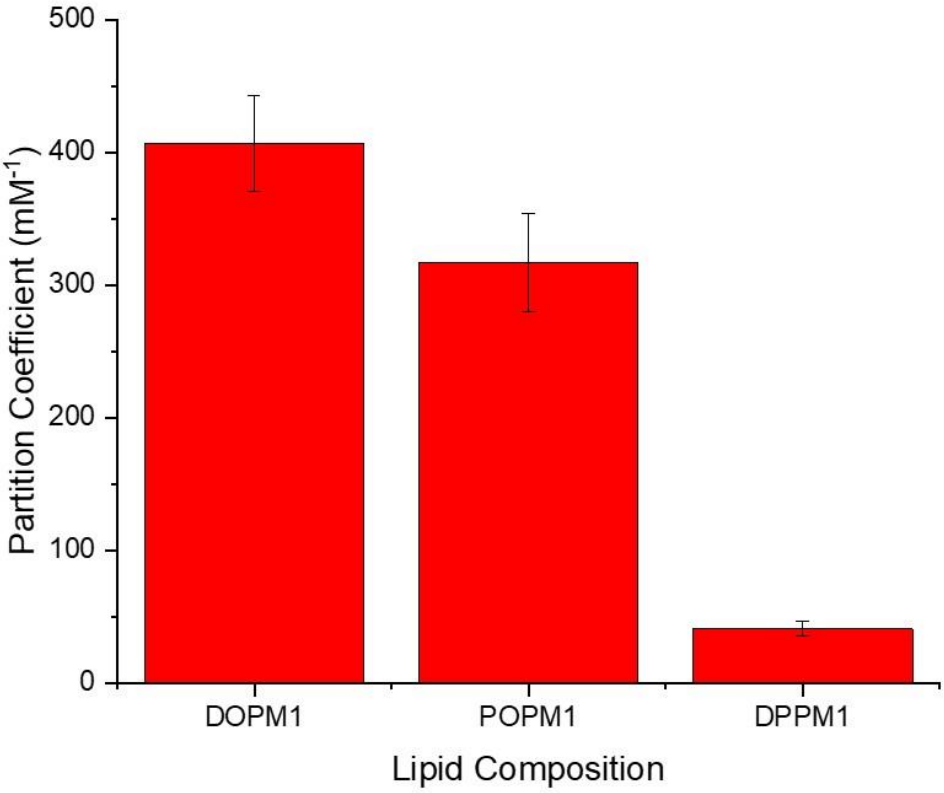

Figure 3-41 *Partition coefficient of fluorophore labelled C2AB (residues 136-241) binding to PM1 vesicles with varying acyl chain saturations.*

Chapter 4 DISCUSSION and Future Directions.

4.1 Discussion

Proposed Mechanism for Cpx's Clamping Function

While multiple studies have demonstrated that Cpx can act as a fusion clamp to prevent spontaneous fusion, the precise molecular mechanism behind this function remains elusive. One way in which complexin has been proposed to inhibit fusion is by binding the tSNARE complex and competing with Syb for tSNARE binding.[105,131,132] We tested this hypothesis with soluble and membrane bound tSNARE complex. Our result show that although Cpx binds to a tSNARE complex in solution, it fails to bind to a tSNARE complex when associated with the membrane interface. It should be noted that in some previous studies evidence for tSNARE binding to Cpx was obtained;[105,132] however, in these cases the tSNARE were embedded in membranes that did not contain PIP2. It is possible that the membrane environment alters the conformation of the SNAREs or the accessibility of the Cpx to the SNAREs, but in any case, the presence of PIP2 is needed to reconstitute fusion.[133] Our studies show that in lipid membranes that support fusion and contain PIP2, Cpx does not interact with a membrane associated tSNARE complex. As a result, Cpx is not likely to inhibit fusion by blocking the binding of Syb to a pre-fusion SNARE complex.

The fusion of biological membranes requires significant deformation of lipid bilayers, leading to the formation of highly curved intermediates. These highly curved structures introduce stress into the lipid bilayer and create packing defects, where the hydrophobic tails of the lipid experience some exposure to water.[134,135 136] Increasing the levels of acyl chain unsaturation in the membrane lipid also increases the number of packing defects. Studies have shown that increasing

membrane curvature and unsaturation lipid tails leads to an increase in packing defects, which in turns facilitated the fusion process. [137]

The C-terminal domain of Cpx has been shown to suppress spontaneous fusion [138–141] and our studies have highlighted the importance of the C-terminal domain in modulating Cpx-membrane binding. Given that the C-terminal domain has a strong affinity for highly curved membranes and disordered bilayers, it is likely that Cpx plays a role in regulating these lipid deformations. In our study, we found that assembling the SNARE complex increases the Cpx's membrane affinity at its C-terminal domain. Our results support a model in which Cpx acts as a fusion clamp by binding to membrane deformations that promote membrane fusion and stabilizing them, thereby reducing the fusogenic potential of the lipid bilayer. This may occur through Cpx's C-terminal interaction with highly curved or disordered membranes where lipid packing defects are common. By binding to these membrane regions, Cpx stabilizes membranes in a less fusogenic state and prevents the bilayer from progressing to fusion. In this model, the clamping function of Cpx is not due to its SNARE interactions but rather to the membrane interactions made by its C-terminal domain with packing defects.

Synaptotagmin, which also interacts with membranes has been shown to compete with Cpx for membrane binding.[76] Both Cpx and Syt share similar membrane preferences including an affinity for PIP2, curved bilayer surfaces and disordered lipids (Figure 3-1, Figure 3-41).[12,105,111] We propose that Syt competes with Cpx for membrane binding sites and may release Cpx from these high energy membrane surfaces. After Ca^{2+} influx, Ca^{2+}-bound Syt binds to the membrane surface and displaces Cpx from these critical membrane regions, releasing Cpx's clamping action and allowing fusion to proceed. In addition, Syt1's C2 domain insertion into membrane further increases curvature stress and disorder in the bilayer that also promote fusion.[73]

Cpx stimulates fusion by binding to the SNARE complex.

In addition to its clamping function, Cpx is also known to stimulate evoked fusion, and binding to the SNARE complexes may be important for this function. Mutations that reduce the Cpx-SNARE affinity also reduce Cpx's stimulatory function, suggesting an important role of direct Cpx-SNARE interactions on evoked fusion.[131] Cpx has been proposed to promote fusion by binding to the membrane-proximal region of the SNARE complex and stabilizing the assembled complex.[142] Our EPR data indicate that when SNAREs are membrane-bound, Cpx interacts exclusively with the fully assembled ternary SNARE complex through the accessory and central helices of Cpx. The inability of Cpx to interact with intermediate SNARE complexes (SN25:Syx or SN1:Syx:Syb) when they are membrane-bound suggests that Cpx's stimulatory function is tightly coupled with the final stages of SNARE assembly.

N-terminus of Cpx stimulates fusion by an unknown mechanism.[143,144] Cpx's N-terminal domain also interacts with membranes but its contribution to Cpx-membrane affinity is significantly weaker than that made by the C-terminal region.[105,112,145] It has been proposed that N-terminal interactions increase Cpx's stimulatory function either by relieving Cpx's accessory helix inhibition or by interactions with the C-terminal (membrane proximal) end of SNAREs, thereby stabilizing the SNARE interactions.[144–146] Our results show that when the SNAREs are fully assembled, there is a small but significant increase in the membrane interaction made by the N-terminus. The N-terminal binding was observed only when the SNAREs are fully assembled. Our data supports a model where Cpx stimulates fusion by interactions with the SNARE complex and membranes at Cpx's N-terminal domain.

Plasma membrane localization of Cpx

Previous work has shown that Cpx exhibits a preference for small, curved membranes, and as a result, it has been suggested that Cpx may associate with synaptic vesicles. However, our studies demonstrate that Cpx has a strong affinity for PIP2, which is enriched in the plasma membrane. In addition, the presence of SNAP25 on membranes significantly increases Cpx membrane association. This, coupled with the fact that the presence of Syb reduces the membrane binding of Cpx, suggests that localization of Cpx may be towards the plasma membrane rather than the synaptic vesicle. Due to the differences in experimental conditions, a quantitative comparison of contributions from membrane curvature versus the presence of PIP2 and dSNAP25 in the membrane cannot be made.

How Complexin may help order SNARE assembly

The precise order of SNARE assembly remains unclear, but our findings provide insight on a model proposed by Dr. Graham, in which Syx and the SN1 domain assemble first, followed by Syb, with the SN2 domain joining the complex last.[113] Our results suggest that Cpx has a strong preference for membranes containing dSNAP25, and this is primarily due to the presence of d SN1. In contrast, dSN2 did not contribute to Cpx's increased membrane affinity, providing additional evidence that SN1 and SN2 are structurally different and may function independently.[113]

While Syx alone inhibits Cpx's membrane binding, this inhibition is reversed when the tSNAREs (Syx and SNAP25) form a complex. This reversal in Syx's inhibitory action was again driven by the action of SNAP25's SN1 domain. Additionally, an intermediate complex composed of dSN1, Syx and Syb also increased Cpx's membrane association. Although SN2 contributes minimally to membrane binding by Cpx, it is essential for Cpx-SNARE interactions.

If SNARE assembly follows the proposed sequence, our results imply that SNAP25 and Cpx are colocalized on the plasma membrane at the beginning of assembly. As the process progresses, Syx binds to SN1 while Cpx remains associated with the membrane. Syb binding to this tSNARE (SN1:Syx) complex, would further increase Cpx's membrane affinity , enhancing its clamping function to inhibit spontaneous fusion. The incorporation of SN2 into the SNARE complex will result in Cpx binding to the complex and stabilizing SNARE interactions at its C-terminal end while also clamping fusion by binding to the membrane to prepare the system for rapid exocytosis. This proposed order of assembly supports a model where Cpx not only stabilizes SNARE interactions, but also plays an active role in modulating assembly to prevent premature fusion and set the stage for vesicle fusion triggered by Ca^{2+} influx.

Importance of considering membranes when studying fusion proteins.

This study demonstrates that SNARE proteins can influence Cpx-membrane interactions and membranes can influence Cpx-SNARE interactions. In solution, SNAP25 does not affect the membrane interaction of Cpx, but does significantly increase Cpx affinity when anchored to the membrane. In contrast, Syx when in solution, does not impact Cpx-membrane interaction, but significantly reduces Cpx-membrane affinity when it is membrane-bound. The binary tSNARE and ternary SNARE complexes, while increasing Cpx-membrane affinity when membrane-bound, actually reduces Cpx's membrane binding affinity when they are in solution. Although membrane binding is integral to Cpx's function, the presence of SNAREs in solution or membrane bound can drastically change how Cpx is able to interact with membrane bilayers.

A t-SNARE complex formed with Syx and SNAP25 binds to Cpx in solution but fails to interact when the complex is membrane-bound. This indicates that these SNARE complexes may adopt distinct conformations in solution that are not accessible when anchored to the membrane,

suggesting that membranes are more than just passive anchors for SNAREs. Membranes can induce conformational changes in SNAREs,[88] and tethering SNAREs to membranes appears to alter how SNAREs interact with Cpx. These findings highlight the critical importance of studying protein interactions in the context of membranes, as interactions observed in solution may not accurately reflect behavior when proteins are membrane-bound. Understanding these differences is crucial for accurately modeling the regulatory mechanisms of vesicle fusion.

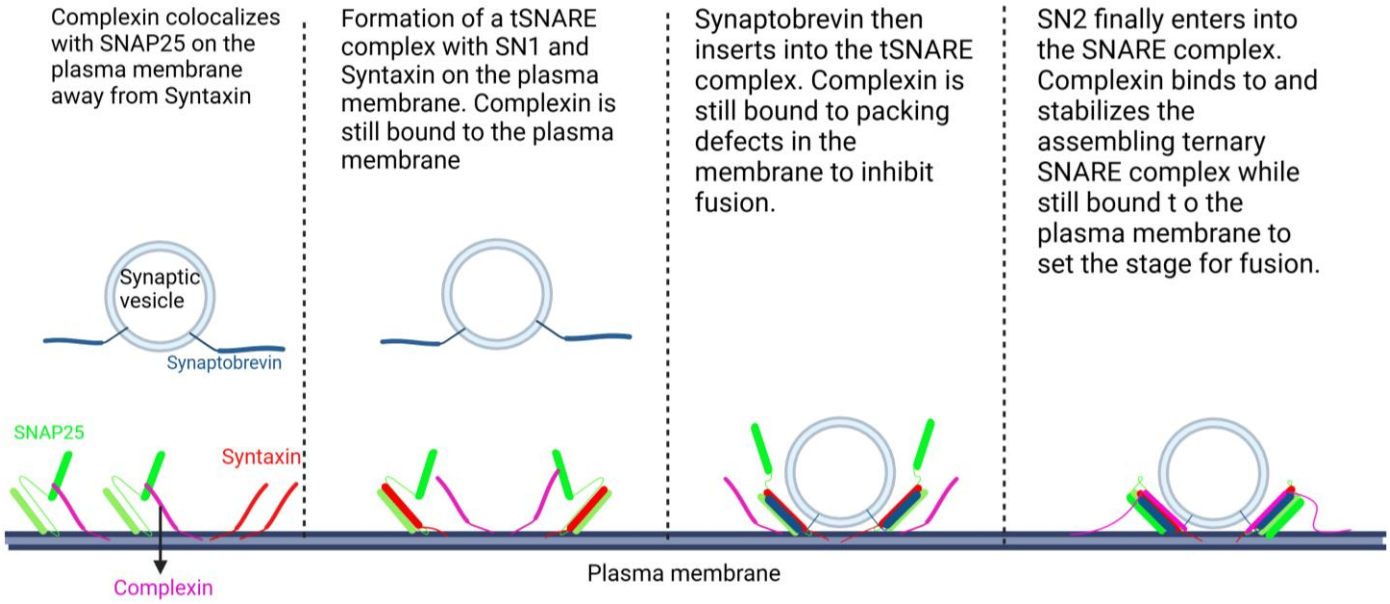

Figure 4-1 Proposed Mechanism for Complexin's function in regulating fusion.

4.2 Future directions

Although it is clear that dSNAP25 and SNARE complexes containing dSNAP25 increase Cpx's membrane affinity, the underlying mechanism remains uncertain. We propose that dSNAP25 may disorder the lipid membrane, which increases Cpx's affinity for membranes. To test this hypothesis, dSNAP25 could be reconstituted into DPPM1 and DOPM1 vesicles. If lipid disorder is driving these increased interactions, there will be minimal changes in Cpx membrane binding in DOPM1 membranes with and without dSNAP25. DPPM1 on the other hand will exhibit the largest change in Cpx binding to membranes in the presence or absence of dSNAP25.

At the low membrane concentrations used in our studies, we could not fully probe N-terminal effects of Cpx on membrane interactions. Initial experiments showed that when SNAREs are fully assembled, there is a small increase in Cpx's interactions with membrane at its N-terminal. N-terminal domain could play a role in stabilizing Cpx-membrane interactions when SNAREs are fully assembled. Increasing the concentration of lipid vesicles will increase Cpx membrane interactions, to help better explore how SNAREs alter Cpx N-terminal interactions.

Munc18 influences Cpx's interactions with the acceptor complex and membranes in a more nuanced way. While It reduces Cpx membrane binding with acceptor complex formed with $Syx_{183-288}$, it has no effect on the complex formed with FL Syx. The reduction in affinity is time dependent and occurs slowly, suggesting it may may not be physiologically relevant during rapid synaptic events. Despite reducing Cpx binding, Munc18:Syx:dSNAP25 does not block Cpx membrane access as $Syx_{183-288}$ does. This could be due to the presence of SNAP25, which as shown in this study, increases Cpx membrane binding. The opposing effect of Syx-Munc18 inhibition and dSNAP25 promotion suggests an antagonistic balance that prevents complete block of the Cpx-membrane interaction, while also limiting the enhanced binding seen with dSNAP25

alone. Moreover, while Munc18 reduces Cpx affinity to tSNARE liposomes, it supports a weak Cpx interaction with SNAREs that is not seen with tSNARE complex by itself. Given that Cpx does not interact with membrane-bound SNAP25 or Syx, it raises the question: what is Cpx interacting with at its SNARE-binding interactions? This further complicates these interactions and additional experiments are needed to understand the dynamics between Cpx, Munc18 and SNAREs.

List of References

(1) Gulati, A. Understanding Neurogenesis in the Adult Human Brain. *Indian J. Pharmacol.* **2015**, *47* (6), 583–584. https://doi.org/10.4103/0253-7613.169598.

(2) Hammond, C. Neurons. In *Cellular and Molecular Neurophysiology*; Elsevier, 2015; pp 3–23. https://doi.org/10.1016/B978-0-12-397032-9.00001-7.

(3) *Axons: the cable transmission of neurons*. https://qbi.uq.edu.au/brain/brain-anatomy/axons-cable-transmission-neurons (accessed 2024-07-01).

(4) Moyes, C. D.; Schulte, P. M. *Principles of Animal Physiology*, 2. ed., Pearson new international ed.; Pearson custom library; Pearson: Harlow, 2014.

(5) Ashley, K.; Lui, F. Physiology, Nerve. In *StatPearls*; StatPearls Publishing: Treasure Island (FL), 2024.

(6) Südhof, T. C. Neurotransmitter Release: The Last Millisecond in the Life of a Synaptic Vesicle. *Neuron* **2013**, *80* (3), 675–690. https://doi.org/10.1016/j.neuron.2013.10.022.

(7) Rizo, J. Mechanism of Neurotransmitter Release Coming into Focus. *Protein Sci.* **2018**, *27* (8), 1364–1391. https://doi.org/10.1002/pro.3445.

(8) *Difference Between Chemical and Electrical Synapse*. Compare the Difference Between Similar Terms. https://www.differencebetween.com/difference-between-chemical-and-vs-electrical-synapse/ (accessed 2024-07-01).

(9) Chapman, E. R. Synaptotagmin: A Ca2+ Sensor That Triggers Exocytosis? *Nat. Rev. Mol. Cell Biol.* **2002**, *3* (7), 498–508. https://doi.org/10.1038/nrm855.

(10) Jahn, R.; Fasshauer, D. Molecular Machines Governing Exocytosis of Synaptic Vesicles. *Nature* **2012**, *490* (7419), 201–207. https://doi.org/10.1038/nature11320.

(11) Masson, J.; Sagné, C.; Hamon, M.; Mestikawy, S. E. Neurotransmitter Transporters in the Central Nervous System. *Pharmacol. Rev.* **1999**, *51* (3), 439–464.

(12) Chapman, E. R. How Does Synaptotagmin Trigger Neurotransmitter Release? *Annu. Rev. Biochem.* **2008**, *77* (1), 615–641. https://doi.org/10.1146/annurev.biochem.77.062005.101135.

(13) Rickman, C.; Meunier, F. A.; Binz, T.; Davletov, B. High Affinity Interaction of Syntaxin and SNAP-25 on the Plasma Membrane Is Abolished by Botulinum Toxin E. *J. Biol. Chem.* **2004**, *279* (1), 644–651. https://doi.org/10.1074/jbc.M310879200.

(14) Pobbati, A. V.; Stein, A.; Fasshauer, D. N- to C-Terminal SNARE Complex Assembly Promotes Rapid Membrane Fusion. *Science* **2006**, *313* (5787), 673–676. https://doi.org/10.1126/science.1129486.

(15) Poirier, M. A.; Hao, J. C.; Malkus, P. N.; Chan, C.; Moore, M. F.; King, D. S.; Bennett, M. K. Protease Resistance of Syntaxin·SNAP-25·VAMP Complexes. *J. Biol. Chem.* **1998**, *273* (18), 11370–11377. https://doi.org/10.1074/jbc.273.18.11370.

(16) Jahn, R.; Scheller, R. H. SNAREs — Engines for Membrane Fusion. *Nat. Rev. Mol. Cell Biol.* **2006**, *7* (9), 631–643. https://doi.org/10.1038/nrm2002.

(17) Fasshauer, D.; Sutton, R. B.; Brunger, A. T.; Jahn, R. Conserved Structural Features of the Synaptic Fusion Complex: SNARE Proteins Reclassified as Q- and R-SNAREs. *Proc. Natl. Acad. Sci.* **1998**, *95* (26), 15781–15786. https://doi.org/10.1073/pnas.95.26.15781.

(18) Fernandez, I.; Ubach, J.; Dulubova, I.; Zhang, X.; Südhof, T. C.; Rizo, J. Three-Dimensional Structure of an Evolutionarily Conserved N-Terminal Domain of Syntaxin 1A. *Cell* **1998**, *94* (6), 841–849. https://doi.org/10.1016/S0092-8674(00)81742-0.

(19) Khvotchev, M.; Dulubova, I.; Sun, J.; Dai, H.; Rizo, J.; Südhof, T. C. Dual Modes of Munc18-1/SNARE Interactions Are Coupled by Functionally Critical Binding to Syntaxin-1 N Terminus. *J. Neurosci.* **2007**, *27* (45), 12147–12155. https://doi.org/10.1523/JNEUROSCI.3655-07.2007.

(20) Dulubova, I.; Sugita, S.; Hill, S.; Hosaka, M.; Fernandez, I.; Südhof, T. C.; Rizo, J. A Conformational Switch in Syntaxin during Exocytosis: Role of Munc18. *EMBO J.* **1999**, *18* (16), 4372–4382. https://doi.org/10.1093/emboj/18.16.4372.

(21) Rizo, J.; David, G.; Fealey, M. E.; Jaczynska, K. On the Difficulties of Characterizing Weak Protein Interactions That Are Critical for Neurotransmitter Release. *FEBS Open Bio n/a* (n/a). https://doi.org/10.1002/2211-5463.13473.

(22) Brose, N.; Petrenko, A.; Sudhof, T.; Jahn, R. Synaptotagmin: A Calcium Sensor on the Synaptic Vesicle Surface. *Science* **1992**, *256* (5059), 1021–1025. https://doi.org/10.1126/science.1589771.

(23) Paddock, B. E.; Striegel, A. R.; Hui, E.; Chapman, E. R.; Reist, N. E. Ca^{2+} -Dependent, Phospholipid-Binding Residues of Synaptotagmin Are Critical for Excitation–Secretion Coupling *In Vivo*. *J. Neurosci.* **2008**, *28* (30), 7458–7466. https://doi.org/10.1523/JNEUROSCI.0197-08.2008.

(24) Pang, Z. P.; Shin, O.-H.; Meyer, A. C.; Rosenmund, C.; Südhof, T. C. A Gain-of-Function Mutation in Synaptotagmin-1 Reveals a Critical Role of Ca^{2+} -Dependent Soluble *N* -Ethylmaleimide-Sensitive Factor Attachment Protein Receptor Complex Binding in Synaptic Exocytosis. *J. Neurosci.* **2006**, *26* (48), 12556–12565. https://doi.org/10.1523/JNEUROSCI.3804-06.2006.

(25) Fernández-Chacón, R.; Königstorfer, A.; Gerber, S. H.; García, J.; Matos, M. F.; Stevens, C. F.; Brose, N.; Rizo, J.; Rosenmund, C.; Südhof, T. C. Synaptotagmin I Functions as a Calcium Regulator of Release Probability. *Nature* **2001**, *410* (6824), 41–49. https://doi.org/10.1038/35065004.

(26) Perrin, M. S.; Brose, N.; Sudhof, T. C.; Jahn, R. Domain Structure of Synaptotagmin (P65). *J. Biol. Chem.* **1991**, *266*, 623–629.

(27) Perrin, M. S.; Fried, V. A.; Mignery, G. A.; Jahn, R.; Sudhof, T. C. Phospholipid Binding by a Synaptic Vesicle Protein Homologous to the Regulatory Region of Protein Kinase C. *Nature* **1990**, *345*, 260–263. https://doi.org/10.1038/345260a0.

(28) Fernandez, I.; Araç, D.; Ubach, J.; Gerber, S. H.; Shin, O.; Gao, Y.; Anderson, R. G. W.; Südhof, T. C.; Rizo, J. Three-Dimensional Structure of the Synaptotagmin 1 C2B-Domain:

Synaptotagmin 1 as a Phospholipid Binding Machine. *Neuron* **2001**, *32* (6), 1057–1069. https://doi.org/10.1016/S0896-6273(01)00548-7.

(29) Shao, X.; Fernandez, I.; Südhof, T. C.; Rizo, J. Solution Structures of the Ca^{2+} -Free and Ca^{2+} -Bound C_2 A Domain of Synaptotagmin I: Does Ca^{2+} Induce a Conformational Change? *Biochemistry* **1998**, *37* (46), 16106–16115. https://doi.org/10.1021/bi981789h.

(30) Grushin, K.; Wang, J.; Coleman, J.; Rothman, J. E.; Sindelar, C. V.; Krishnakumar, S. S. Structural Basis for the Clamping and Ca2+ Activation of SNARE-Mediated Fusion by Synaptotagmin. *Nat. Commun.* **2019**, *10* (1), 2413. https://doi.org/10.1038/s41467-019-10391-x.

(31) Chicka, M. C.; Hui, E.; Liu, H.; Chapman, E. R. Synaptotagmin Arrests the SNARE Complex before Triggering Fast, Efficient Membrane Fusion in Response to Ca2+. *Nat. Struct. Mol. Biol.* **2008**, *15* (8), 827–835. https://doi.org/10.1038/nsmb.1463.

(32) Xu, J.; Brewer, K. D.; Perez-Castillejos, R.; Rizo, J. Subtle Interplay between Synaptotagmin and Complexin Binding to the SNARE Complex. *J. Mol. Biol.* **2013**, *425* (18), 3461–3475. https://doi.org/10.1016/j.jmb.2013.07.001.

(33) Chicka, M. C.; Chapman, E. R. Concurrent Binding of Complexin and Synaptotagmin to Liposome-Embedded SNARE Complexes. *Biochemistry* **2009**, *48* (4), 657–659. https://doi.org/10.1021/bi801962d.

(34) Park, Y.; Seo, J. B.; Fraind, A.; Pérez-Lara, A.; Yavuz, H.; Han, K.; Jung, S.-R.; Kattan, I.; Walla, P. J.; Choi, M.; Cafiso, D. S.; Koh, D.-S.; Jahn, R. Synaptotagmin-1 Binds to PIP2-Containing Membrane but Not to SNAREs at Physiological Ionic Strength. *Nat. Struct. Mol. Biol.* **2015**, *22* (10), 815–823. https://doi.org/10.1038/nsmb.3097.

(35) Bai, J.; Tucker, W. C.; Chapman, E. R. PIP2 Increases the Speed of Response of Synaptotagmin and Steers Its Membrane-Penetration Activity toward the Plasma Membrane. *Nat. Struct. Mol. Biol.* **2004**, *11* (1), 36–44. https://doi.org/10.1038/nsmb709.

(36) Park, Y.; Ryu, J.-K. Models of Synaptotagmin-1 to Trigger Ca 2+ -Dependent Vesicle Fusion. *FEBS Lett.* **2018**, *592* (21), 3480–3492. https://doi.org/10.1002/1873-3468.13193.

(37) Hui, E.; Johnson, C.; Jun, Y.; Dunning, M.; Chapman, E. R. Synaptotagmin-Mediated Bending of the Target Membrane Is a Critical Step in Ca2+-Regulated Fusion. **2009**, *138*, 709–721. https://doi.org/10.1016/j.cell.2009.05.049.

(38) Lin, C.-C.; Seikowski, J.; Pérez-Lara, A.; Jahn, R.; Höbartner, C.; Walla, P. J. Control of Membrane Gaps by Synaptotagmin-Ca2+ Measured with a Novel Membrane Distance Ruler. *Nat. Commun.* **2014**, *5* (1), 5859. https://doi.org/10.1038/ncomms6859.

(39) Bowers, M. R.; Reist, N. E. Synaptotagmin: Mechanisms of an Electrostatic Switch. *Neurosci. Lett.* **2020**, *722*, 134834. https://doi.org/10.1016/j.neulet.2020.134834.

(40) Rapid and Selective Binding to the Synaptic SNARE Complex Suggests a Modulatory Role of Complexins in Neuroexocytosis. *J. Biol. Chem.* **2002**, *277* (10), 7838–7848. https://doi.org/10.1074/jbc.M109507200.

(41) Li, Y.; Augustine, G. J.; Weninger, K. Kinetics of Complexin Binding to the SNARE Complex: Correcting Single Molecule FRET Measurements for Hidden Events. *Biophys. J.* **2007**, *93* (6), 2178–2187. https://doi.org/10.1529/biophysj.106.101220.

(42) Pabst, S.; Hazzard, J. W.; Antonin, W.; Südhof, T. C.; Jahn, R.; Rizo, J.; Fasshauer, D. Selective Interaction of Complexin with the Neuronal SNARE Complex: DETERMINATION OF THE BINDING REGIONS*. *J. Biol. Chem.* **2000**, *275* (26), 19808–19818. https://doi.org/10.1074/jbc.M002571200.

(43) Chen, X.; Tomchick, D. R.; Kovrigin, E.; Araç, D.; Machius, M.; Südhof, T. C.; Rizo, J. Three-Dimensional Structure of the Complexin/SNARE Complex. *Neuron* **2002**, *33* (3), 397–409. https://doi.org/10.1016/s0896-6273(02)00583-4.

(44) Bracher, A.; Kadlec, J.; Betz, H.; Weissenhorn, W. X-Ray Structure of a Neuronal Complexin-SNARE Complex from Squid *. *J. Biol. Chem.* **2002**, *277* (29), 26517–26523. https://doi.org/10.1074/jbc.M203460200.

(45) Seiler, F.; Malsam, J.; Krause, J. M.; Söllner, T. H. A Role of Complexin-Lipid Interactions in Membrane Fusion. *FEBS Lett.* **2009**, *583* (14), 2343–2348. https://doi.org/10.1016/j.febslet.2009.06.025.

(46) Trimbuch, T. Should I Stop or Should I Go? The Role of Complexin in Neurotransmitter Release. 8.

(47) López-Murcia, F. J.; Lin, K.-H.; Berns, M. M. M.; Ranjan, M.; Lipstein, N.; Neher, E.; Brose, N.; Reim, K.; Taschenberger, H. Complexin Has a Dual Synaptic Function as Checkpoint Protein in Vesicle Priming and as a Promoter of Vesicle Fusion. *Proc. Natl. Acad. Sci.* **2024**, *121* (15), e2320505121. https://doi.org/10.1073/pnas.2320505121.

(48) Reim, K.; Wegmeyer, H.; Brandstätter, J. H.; Xue, M.; Rosenmund, C.; Dresbach, T.; Hofmann, K.; Brose, N. Structurally and Functionally Unique Complexins at Retinal Ribbon Synapses. *J. Cell Biol.* **2005**, *169* (4), 669–680. https://doi.org/10.1083/jcb.200502115.

(49) *Evolutionary conservation of complexins: from choanoflagellates to mice*. https://doi.org/10.15252/embr.201540305.

(50) Wragg, R. T.; Parisotto, D. A.; Li, Z.; Terakawa, M. S.; Snead, D.; Basu, I.; Weinstein, H.; Eliezer, D.; Dittman, J. S. Evolutionary Divergence of the C-Terminal Domain of Complexin Accounts for Functional Disparities between Vertebrate and Invertebrate Complexins. *Front. Mol. Neurosci.* **2017**, *10*, 146. https://doi.org/10.3389/fnmol.2017.00146.

(51) Snead, D.; Wragg, R. T.; Dittman, J. S.; Eliezer, D. Membrane Curvature Sensing by the C-Terminal Domain of Complexin. *Nat. Commun.* **2014**, *5* (1), 4955. https://doi.org/10.1038/ncomms5955.

(52) Bykhovskaia, M.; Jagota, A.; Gonzalez, A.; Vasin, A.; Littleton, J. T. Interaction of the Complexin Accessory Helix with the C-Terminus of the SNARE Complex: Molecular-Dynamics Model of the Fusion Clamp. *Biophys. J.* **2013**, *105* (3), 679–690. https://doi.org/10.1016/j.bpj.2013.06.018.

(53) Malsam, J.; Bärfuss, S.; Trimbuch, T.; Zarebidaki, F.; Sonnen, A. F.-P.; Wild, K.; Scheutzow, A.; Rohland, L.; Mayer, M. P.; Sinning, I.; Briggs, J. A. G.; Rosenmund, C.; Söllner, T. H. Complexin Suppresses Spontaneous Exocytosis by Capturing the Membrane-Proximal Regions of VAMP2 and SNAP25. *Cell Rep.* **2020**, *32* (3), 107926. https://doi.org/10.1016/j.celrep.2020.107926.

(54) Trimbuch, T.; Xu, J.; Flaherty, D.; Tomchick, D. R.; Rizo, J.; Rosenmund, C. Re-Examining How Complexin Inhibits Neurotransmitter Release. *eLife* **2014**, *3*, e02391. https://doi.org/10.7554/eLife.02391.

(55) Kümmel, D.; Krishnakumar, S. S.; Radoff, D. T.; Li, F.; Giraudo, C. G.; Pincet, F.; Rothman, J. E.; Reinisch, K. M. Complexin Cross-Links Prefusion SNAREs into a Zigzag Array. *Nat. Struct. Mol. Biol.* **2011**, *18* (8), 927–933. https://doi.org/10.1038/nsmb.2101.

(56) Tracey, T. J.; Steyn, F. J.; Wolvetang, E. J.; Ngo, S. T. Neuronal Lipid Metabolism: Multiple Pathways Driving Functional Outcomes in Health and Disease. *Front. Mol. Neurosci.* **2018**, *11*. https://doi.org/10.3389/fnmol.2018.00010.

(57) van Meer, G.; Voelker, D. R.; Feigenson, G. W. Membrane Lipids: Where They Are and How They Behave. *Nat. Rev. Mol. Cell Biol.* **2008**, *9* (2), 112–124. https://doi.org/10.1038/nrm2330.

(58) Ingólfsson, H. I.; Carpenter, T. S.; Bhatia, H.; Bremer, P.-T.; Marrink, S. J.; Lightstone, F. C. Computational Lipidomics of the Neuronal Plasma Membrane. *Biophys. J.* **2017**, *113* (10), 2271–2280. https://doi.org/10.1016/j.bpj.2017.10.017.

(59) Tracey, T. J.; Kirk, S. E.; Steyn, F. J.; Ngo, S. T. The Role of Lipids in the Central Nervous System and Their Pathological Implications in Amyotrophic Lateral Sclerosis. *Semin. Cell Dev. Biol.* **2021**, *112*, 69–81. https://doi.org/10.1016/j.semcdb.2020.08.012.

(60) Müller, C. P.; Reichel, M.; Mühle, C.; Rhein, C.; Gulbins, E.; Kornhuber, J. Brain Membrane Lipids in Major Depression and Anxiety Disorders. *Biochim. Biophys. Acta BBA - Mol. Cell Biol. Lipids* **2015**, *1851* (8), 1052–1065. https://doi.org/10.1016/j.bbalip.2014.12.014.

(61) Mattson, M. P.; Magnus, T. Ageing and Neuronal Vulnerability. *Nat. Rev. Neurosci.* **2006**, *7* (4), 278–294. https://doi.org/10.1038/nrn1886.

(62) Yoon, J. H.; Seo, Y.; Jo, Y. S.; Lee, S.; Cho, E.; Cazenave-Gassiot, A.; Shin, Y.-S.; Moon, M. H.; An, H. J.; Wenk, M. R.; Suh, P.-G. Brain Lipidomics: From Functional Landscape to Clinical Significance. *Sci. Adv.* **2022**, *8* (37), eadc9317. https://doi.org/10.1126/sciadv.adc9317.

(63) Yeagle, P. *The Membranes of Cells*, Third edition.; Elsevier/AP: Amsterdam ; Boston, 2016.

(64) Cermenati, G.; Mitro, N.; Audano, M.; Melcangi, R. C.; Crestani, M.; De Fabiani, E.; Caruso, D. Lipids in the Nervous System: From Biochemistry and Molecular Biology to Patho-Physiology. *Biochim. Biophys. Acta BBA - Mol. Cell Biol. Lipids* **2015**, *1851* (1), 51–60. https://doi.org/10.1016/j.bbalip.2014.08.011.

(65) Gopalakrishnan, G.; Awasthi, A.; Belkaid, W.; De Faria Jr., O.; Liazoghli, D.; Colman, D. R.; Dhaunchak, A. S. Lipidome and Proteome Map of Myelin Membranes. *J. Neurosci. Res.* **2013**, *91* (3), 321–334. https://doi.org/10.1002/jnr.23157.

(66) Alberts, B. *Molecular Biology of the Cell*, Sixth edition.; Garland Science, Taylor and Francis Group: New York, NY, 2015.

(67) Voet, D.; Voet, J. G.; Pratt, C. W. *Fundamentals of Biochemistry: Life at the Molecular Level*, Fifth edition.; Wiley: Hoboken, 2016.

(68) Yesylevskyy, S. O.; Rivel, T.; Ramseyer, C. The Influence of Curvature on the Properties of the Plasma Membrane. Insights from Atomistic Molecular Dynamics Simulations. *Sci. Rep.* **2017**, *7* (1), 16078. https://doi.org/10.1038/s41598-017-16450-x.

(69) Harayama, T.; Riezman, H. Understanding the Diversity of Membrane Lipid Composition. *Nat. Rev. Mol. Cell Biol.* **2018**, *19* (5), 281–296. https://doi.org/10.1038/nrm.2017.138.

(70) Churchward, M. A.; Rogasevskaia, T.; Brandman, D. M.; Khosravani, H.; Nava, P.; Atkinson, J. K.; Coorssen, J. R. Specific Lipids Supply Critical Negative Spontaneous Curvature—An Essential Component of Native Ca2+-Triggered Membrane Fusion. *Biophys. J.* **2008**, *94* (10), 3976–3986. https://doi.org/10.1529/biophysj.107.123984.

(71) Chernomordik, L. V.; Kozlov, M. M. Protein-Lipid Interplay in Fusion and Fission of Biological Membranes. *Annu. Rev. Biochem.* **2003**, *72* (1), 175–207. https://doi.org/10.1146/annurev.biochem.72.121801.161504.

(72) Joardar, A.; Pattnaik, G. P.; Chakraborty, H. Mechanism of Membrane Fusion: Interplay of Lipid and Peptide. *J. Membr. Biol.* **2022**, *255* (2), 211–224. https://doi.org/10.1007/s00232-022-00233-1.

(73) Martens, S.; Kozlov, M. M.; McMahon, H. T. How Synaptotagmin Promotes Membrane Fusion. *Science* **2007**, *316* (5828), 1205–1208. https://doi.org/10.1126/science.1142614.

(74) Bigay, J.; Antonny, B. Curvature, Lipid Packing, and Electrostatics of Membrane Organelles: Defining Cellular Territories in Determining Specificity. *Dev. Cell* **2012**, *23* (5), 886–895. https://doi.org/10.1016/j.devcel.2012.10.009.

(75) Gong, J.; Lai, Y.; Li, X.; Wang, M.; Leitz, J.; Hu, Y.; Zhang, Y.; Choi, U. B.; Cipriano, D.; Pfuetzner, R. A.; Südhof, T. C.; Yang, X.; Brunger, A. T.; Diao, J. C-Terminal Domain of Mammalian Complexin-1 Localizes to Highly Curved Membranes. *Proc. Natl. Acad. Sci.* **2016**, *113* (47). https://doi.org/10.1073/pnas.1609917113.

(76) Courtney, K. C.; Wu, L.; Mandal, T.; Swift, M.; Zhang, Z.; Alaghemandi, M.; Wu, Z.; Bradberry, M. M.; Deo, C.; Lavis, L. D.; Volkmann, N.; Hanein, D.; Cui, Q.; Bao, H.; Chapman, E. R. The Complexin C-Terminal Amphipathic Helix Stabilizes the Fusion Pore Open State by Sculpting Membranes. *Nat. Struct. Mol. Biol.* **2022**, *29* (2), 97–107. https://doi.org/10.1038/s41594-021-00716-0.

(77) Sharma, S.; Lindau, M. T-SNARE Transmembrane Domain Clustering Modulates Lipid Organization and Membrane Curvature. *J. Am. Chem. Soc.* **2017**, *139* (51), 18440–18443. https://doi.org/10.1021/jacs.7b10677.

(78) McMahon, H. T.; Kozlov, M. M.; Martens, S. Membrane Curvature in Synaptic Vesicle Fusion and Beyond. *Cell* **2010**, *140* (5), 601–605. https://doi.org/10.1016/j.cell.2010.02.017.

(79) Brown, M. F. Curvature Forces in Membrane Lipid-Protein Interactions. *Biochemistry* **2012**, *51* (49), 9782–9795. https://doi.org/10.1021/bi301332v.

(80) Mandal, K. Review of PIP2 in Cellular Signaling, Functions and Diseases. *Int. J. Mol. Sci.* **2020**, *21* (21), 8342. https://doi.org/10.3390/ijms21218342.

(81) McLaughlin, S.; Wang, J.; Gambhir, A.; Murray, D. PIP2 and Proteins: Interactions, Organization, and Information Flow. *Annu. Rev. Biophys. Biomol. Struct.* **2002**, *31* (1), 151–175. https://doi.org/10.1146/annurev.biophys.31.082901.134259.

(82) Berridge, M. J.; Irvine, R. F. Inositol Trisphosphate, a Novel Second Messenger in Cellular Signal Transduction. *Nature* **1984**, *312* (5992), 315–321. https://doi.org/10.1038/312315a0.

(83) Milosevic, I. Plasmalemmal Phosphatidylinositol-4,5-Bisphosphate Level Regulates the Releasable Vesicle Pool Size in Chromaffin Cells. *J. Neurosci.* **2005**, *25* (10), 2557–2565. https://doi.org/10.1523/JNEUROSCI.3761-04.2005.

(84) Brown, D. A. PIP2Clustering: From Model Membranes to Cells. *Chem. Phys. Lipids* **2015**, *192*, 33–40. https://doi.org/10.1016/j.chemphyslip.2015.07.021.

(85) Waugh, M. G. PIPs in Neurological Diseases. *Biochim. Biophys. Acta BBA - Mol. Cell Biol. Lipids* **2015**, *1851* (8), 1066–1082. https://doi.org/10.1016/j.bbalip.2015.02.002.

(86) *Brain PI(4,5)P2 | 383907-42-4 | Avanti*. Avanti Research. https://avantiresearch.com/product/840046 (accessed 2024-10-19).

(87) James, D. J.; Khodthong, C.; Kowalchyk, J. A.; Martin, T. F. J. Phosphatidylinositol 4,5-Bisphosphate Regulates SNARE-Dependent Membrane Fusion. *J. Cell Biol.* **2008**, *182* (2), 355–366. https://doi.org/10.1083/jcb.200801056.

(88) Kiessling, V.; Kreutzberger, A. J. B.; Liang, B.; Nyenhuis, S. B.; Seelheim, P.; Castle, J. D.; Cafiso, D. S.; Tamm, L. K. A Molecular Mechanism for Calcium-Mediated Synaptotagmin-Triggered Exocytosis. *Nat. Struct. Mol. Biol.* **2018**, *25* (10), 911–917. https://doi.org/10.1038/s41594-018-0130-9.

(89) Pokorny, A.; Birkbeck, T. H.; Almeida, P. F. F. Mechanism and Kinetics of δ-Lysin Interaction with Phospholipid Vesicles. *Biochemistry* **2002**, *41* (36), 11044–11056. https://doi.org/10.1021/bi020244r.

(90) Bartlett, G. R. Phosphorus Assay in Column Chromatography. *J. Biol. Chem.* **1959**, *234* (3), 466–468.

(91) Jameson, D. M.; Ross, J. A. Fluorescence Polarization/Anisotropy in Diagnostics and Imaging. *Chem. Rev.* **2010**, *110* (5), 2685. https://doi.org/10.1021/cr900267p.

(92) Lakowicz, J. R.; Masters, B. R. Principles of Fluorescence Spectroscopy, Third Edition. *J. Biomed. Opt.* **2008**, *13* (2), 029901. https://doi.org/10.1117/1.2904580.

(93) *Fluorescence Polarization Detection | BMG LABTECH*. https://www.bmglabtech.com/en/fluorescence-polarization/ (accessed 2024-08-20).

(94) Stone, T. J.; Buckman, T.; Nordio, P. L.; McConnell, H. M. Spin-Labeled Biomolecules. *Proc. Natl. Acad. Sci.* **1965**, *54* (4), 1010–1017. https://doi.org/10.1073/pnas.54.4.1010.

(95) Cornish, V. W.; Benson, D. R.; Altenbach, C. A.; Hideg, K.; Hubbell, W. L.; Schultz, P. G. Site-Specific Incorporation of Biophysical Probes into Proteins. *Proc. Natl. Acad. Sci.* **1994**, *91* (8), 2910–2914. https://doi.org/10.1073/pnas.91.8.2910.

(96) Klug, C. S.; Feix, J. B. Methods and Applications of Site-Directed Spin Labeling EPR Spectroscopy. In *Methods in Cell Biology*; Elsevier, 2008; Vol. 84, pp 617–658. https://doi.org/10.1016/S0091-679X(07)84020-9.

(97) Sahu, I. D.; McCarrick, R. M.; Lorigan, G. A. Use of Electron Paramagnetic Resonance To Solve Biochemical Problems. *Biochemistry* **2013**, *52* (35), 5967–5984. https://doi.org/10.1021/bi400834a.

(98) Perozo, E.; Cortes, D. M.; Cuello, L. G. Three-Dimensional Architecture and Gating Mechanism of a K+ Channel Studied by EPR Spectroscopy. *Nat. Struct. Biol.* **1998**, *5* (6), 459–469. https://doi.org/10.1038/nsb0698-459.

(99) Xu, Y.; Zhang, F.; Su, Z.; McNew, J. A.; Shin, Y.-K. Hemifusion in SNARE-Mediated Membrane Fusion. *Nat. Struct. Mol. Biol.* **2005**, *12* (5), 417–422. https://doi.org/10.1038/nsmb921.

(100) Yang, K.; Farrens, D. L.; Altenbach, C.; Farahbakhsh, Z. T.; Hubbell, W. L.; Khorana, H. G. Structure and Function in Rhodopsin. Cysteines 65 and 316 Are in Proximity in a Rhodopsin Mutant As Indicated by Disulfide Formation and Interactions between Attached Spin Labels. *Biochemistry* **1996**, *35* (45), 14040–14046. https://doi.org/10.1021/bi962113u.

(101) Hubbell, W. L.; Mchaourab, H. S.; Altenbach, C.; Lietzow, M. A. Watching Proteins Move Using Site-Directed Spin Labeling. *Structure* **1996**, *4* (7), 779–783. https://doi.org/10.1016/S0969-2126(96)00085-8.

(102) 1_theory.Pdf. https://webhome.auburn.edu/~duinedu/epr/1_theory.pdf (accessed 2024-09-10).

(103) Gaffney, B. J. Electron Spin Resonance of Biomolecules. In *Encyclopedia of Molecular Cell Biology and Molecular Medicine*; Meyers, R. A., Ed.; Wiley-VCH Verlag GmbH & Co. KGaA: Weinheim, Germany, 2006; p mcb.200300104. https://doi.org/10.1002/3527600906.mcb.200300104.

(104) Sahu, I. D.; Lorigan, G. A. Site-Directed Spin Labeling EPR for Studying Membrane Proteins. *BioMed Res. Int.* **2018**, *2018*, e3248289. https://doi.org/10.1155/2018/3248289.

(105) Zdanowicz, R.; Kreutzberger, A.; Liang, B.; Kiessling, V.; Tamm, L. K.; Cafiso, D. S. Complexin Binding to Membranes and Acceptor T-SNAREs Explains Its Clamping Effect on Fusion. *Biophys. J.* **2017**, *113* (6), 1235–1250. https://doi.org/10.1016/j.bpj.2017.04.002.

(106) Liu, J.; Bu, B.; Crowe, M.; Li, D.; Diao, J.; Ji, B. Membrane Packing Defects in Synaptic Vesicles Recruit Complexin and Synuclein. *Phys. Chem. Chem. Phys.* **2021**, *23* (3), 2117–2125. https://doi.org/10.1039/D0CP03546G.

(107) Martin, T. F. J. Role of PI(4,5)P2 in Vesicle Exocytosis and Membrane Fusion. In *Phosphoinositides II: The Diverse Biological Functions*; Balla, T., Wymann, M., York, J. D., Eds.; Subcellular Biochemistry; Springer Netherlands: Dordrecht, 2012; Vol. 59, pp 111–130. https://doi.org/10.1007/978-94-007-3015-1_4.

(108) Grishanin, R. N.; Kowalchyk, J. A.; Klenchin, V. A.; Ann, K.; Earles, C. A.; Chapman, E. R.; Gerona, R. R. L.; Martin, T. F. J. CAPS Acts at a Prefusion Step in Dense-Core Vesicle Exocytosis as a PIP2 Binding Protein. *Neuron* **2004**, *43* (4), 551–562. https://doi.org/10.1016/j.neuron.2004.07.028.

(109) Kabachinski, G.; Yamaga, M.; Kielar-Grevstad, D. M.; Bruinsma, S.; Martin, T. F. J. CAPS and Munc13 Utilize Distinct PIP2-Linked Mechanisms to Promote Vesicle Exocytosis. *Mol. Biol. Cell* **2014**, *25* (4), 508–521. https://doi.org/10.1091/mbc.E12-11-0829.

(110) Grishanin, R. N.; Klenchin, V. A.; Loyet, K. M.; Kowalchyk, J. A.; Ann, K.; Martin, T. F. J. Membrane Association Domains in Ca2+-Dependent Activator Protein for Secretion Mediate Plasma Membrane and Dense-Core Vesicle Binding Required for Ca2+-Dependent Exocytosis. *J. Biol. Chem.* **2002**, *277* (24), 22025–22034. https://doi.org/10.1074/jbc.M201614200.

(111) Liang, Q.; Ofosuhene, A. P.; Kiessling, V.; Liang, B.; Kreutzberger, A. J. B.; Tamm, L. K.; Cafiso, D. S. Complexin-1 and Synaptotagmin-1 Compete for Binding Sites on Membranes Containing PtdInsP2. *Biophys. J.* **2022**. https://doi.org/10.1016/j.bpj.2022.08.023.

(112) Liang, Q. Characterization of the Complexin Membrane Interactions, University of Virginia, Charlottesville, VA, 2021.

(113) Graham, A. C. Determining the Mechanism of SNARE Complex Assembly through Site-Directed Spin Labeling, 2023.

(114) *Action of Complexin on SNARE Complex* | Elsevier Enhanced Reader*. https://doi.org/10.1074/jbc.M205044200.

(115) McMahon, H. T.; Missler, M.; Li, C.; Südhof, T. C. Complexins: Cytosolic Proteins That Regulate SNAP Receptor Function. *Cell* **1995**, *83* (1), 111–119. https://doi.org/10.1016/0092-8674(95)90239-2.

(116) Hao, T.; Feng, N.; Gong, F.; Yu, Y.; Liu, J.; Ren, Y.-X. Complexin-1 Regulated Assembly of Single Neuronal SNARE Complex Revealed by Single-Molecule Optical Tweezers. *Commun. Biol.* **2023**, *6* (1), 1–12. https://doi.org/10.1038/s42003-023-04506-w.

(117) Martin, T. F. J. PI(4,5)P2-Binding Effector Proteins for Vesicle Exocytosis. *Biochim. Biophys. Acta BBA - Mol. Cell Biol. Lipids* **2015**, *1851* (6), 785–793. https://doi.org/10.1016/j.bbalip.2014.09.017.

(118) Hayashi, T.; McMahon, H.; Yamasaki, S.; Binz, T.; Hata, Y.; Südhof, T. C.; Niemann, H. Synaptic Vesicle Membrane Fusion Complex: Action of Clostridial Neurotoxins on Assembly. *EMBO J.* **1994**, *13* (21), 5051–5061. https://doi.org/10.1002/j.1460-2075.1994.tb06834.x.

(119) Stein, A.; Weber, G.; Wahl, M. C.; Jahn, R. Helical Extension of the Neuronal SNARE Complex into the Membrane. *Nature* **2009**, *460* (7254), 525–528. https://doi.org/10.1038/nature08156.

(120) Margittai, M.; Fasshauer, D.; Pabst, S.; Jahn, R.; Langen, R. Homo- and Heterooligomeric SNARE Complexes Studied by Site-Directed Spin Labeling. *J. Biol. Chem.* **2001**, *276* (16), 13169–13177. https://doi.org/10.1074/jbc.M010653200.

(121) Misura, K. M. S.; Scheller, R. H.; Weis, W. I. Self-Association of the H3 Region of Syntaxin 1A. *J. Biol. Chem.* **2001**, *276* (16), 13273–13282. https://doi.org/10.1074/jbc.M009636200.

(122) Fasshauer, D.; Otto, H.; Eliason, W. K.; Jahn, R.; Brünger, A. T. Structural Changes Are Associated with Soluble N-Ethylmaleimide-Sensitive Fusion Protein Attachment Protein Receptor Complex Formation. *J. Biol. Chem.* **1997**, *272* (44), 28036–28041. https://doi.org/10.1074/jbc.272.44.28036.

(123) Xiao, W.; Poirier, M. A.; Bennett, M. K.; Shin, Y.-K. Complex Is a Parallel Four-Helix Bundle. *Nat. Struct. Biol.* **2001**, *8* (4).

(124) Kim, J.; Zhu, Y.; Shin, Y.-K. Preincubation of T-SNAREs with Complexin I Increases Content-Mixing Efficiency. *Biochemistry* **2016**, *55* (26), 3667–3673. https://doi.org/10.1021/acs.biochem.6b00114.

(125) Rickman, C.; Medine, C. N.; Dun, A. R.; Moulton, D. J.; Mandula, O.; Halemani, N. D.; Rizzoli, S. O.; Chamberlain, L. H.; Duncan, R. R. T-SNARE Protein Conformations Patterned by the Lipid Microenvironment. *J. Biol. Chem.* **2010**, *285* (18), 13535–13541. https://doi.org/10.1074/jbc.M109.091058.

(126) Kreutzberger, A. J. B.; Liang, B.; Kiessling, V.; Tamm, L. K. Assembly and Comparison of Plasma Membrane SNARE Acceptor Complexes. *Biophys. J.* **2016**, *110* (10), 2147–2150. https://doi.org/10.1016/j.bpj.2016.04.011.

(127) Verhage, M.; Maia, A. S.; Plomp, J. J.; Brussaard, A. B.; Heeroma, J. H.; Vermeer, H.; Toonen, R. F.; Hammer, R. E.; van den Berg, T. K.; Missler, M.; Geuze, H. J.; Südhof, T. C. Synaptic Assembly of the Brain in the Absence of Neurotransmitter Secretion. *Science* **2000**, *287* (5454), 864–869. https://doi.org/10.1126/science.287.5454.864.

(128) Misura, K. M.; Scheller, R. H.; Weis, W. I. Three-Dimensional Structure of the Neuronal-Sec1-Syntaxin 1a Complex. *Nature* **2000**, *404* (6776), 355–362. https://doi.org/10.1038/35006120.

(129) Jiao, J.; He, M.; Port, S. A.; Baker, R. W.; Xu, Y.; Qu, H.; Xiong, Y.; Wang, Y.; Jin, H.; Eisemann, T. J.; Hughson, F. M.; Zhang, Y. Munc18-1 Catalyzes Neuronal SNARE Assembly by Templating SNARE Association. *eLife* **2018**, *7*, e41771. https://doi.org/10.7554/eLife.41771.

(130) Dawidowski, D.; Cafiso, D. S. Munc18-1 and the Syntaxin-1 N Terminus Regulate Open-Closed States in a t-SNARE Complex. *Structure* **2016**, *24* (3), 392–400. https://doi.org/10.1016/j.str.2016.01.005.

(131) Yoon, T.-Y.; Lu, X.; Diao, J.; Lee, S.-M.; Ha, T.; Shin, Y.-K. Complexin and Ca2+ Stimulate SNARE-Mediated Membrane Fusion. *Mol. Biol.* **2008**, *15* (7), 7.

(132) Weninger, K.; Bowen, M. E.; Choi, U. B.; Chu, S.; Brunger, A. T. Accessory Proteins Stabilize the Acceptor Complex for Synaptobrevin, the 1:1 Syntaxin/SNAP-25 Complex. *Structure* **2008**, *16* (2), 308–320. https://doi.org/10.1016/j.str.2007.12.010.

(133) Kreutzberger, A. J. B.; Kiessling, V.; Liang, B.; Seelheim, P.; Jakhanwal, S.; Jahn, R.; Castle, J. D.; Tamm, L. K. Reconstitution of Calcium-Mediated Exocytosis of Dense-Core Vesicles. *Sci. Adv.* **2017**, *3* (7), e1603208. https://doi.org/10.1126/sciadv.1603208.

(134) Tahir, M. A.; Van Lehn, R. C.; Choi, S. H.; Alexander-Katz, A. Solvent-Exposed Lipid Tail Protrusions Depend on Lipid Membrane Composition and Curvature. *Biochim. Biophys. Acta BBA - Biomembr.* **2016**, *1858* (6), 1207–1215. https://doi.org/10.1016/j.bbamem.2016.01.026.

(135) Cui, H.; Lyman, E.; Voth, G. A. Mechanism of Membrane Curvature Sensing by Amphipathic Helix Containing Proteins. *Biophys. J.* **2011**, *100* (5), 1271–1279. https://doi.org/10.1016/j.bpj.2011.01.036.

(136) Vanni, S.; Hirose, H.; Barelli, H.; Antonny, B.; Gautier, R. A Sub-Nanometre View of How Membrane Curvature and Composition Modulate Lipid Packing and Protein Recruitment. *Nat. Commun.* **2014**, *5* (1), 4916. https://doi.org/10.1038/ncomms5916.

(137) Malinin, V. S.; Lentz, B. R. Energetics of Vesicle Fusion Intermediates: Comparison of Calculations with Observed Effects of Osmotic and Curvature Stresses. *Biophys. J.* **2004**, *86* (5), 2951–2964. https://doi.org/10.1016/S0006-3495(04)74346-5.

(138) Wragg, R. T.; Snead, D.; Dong, Y.; Ramlall, T. F.; Menon, I.; Bai, J.; Eliezer, D.; Dittman, J. S. Synaptic Vesicles Position Complexin to Block Spontaneous Fusion. *Neuron* **2013**, *77* (2), 323–334. https://doi.org/10.1016/j.neuron.2012.11.005.

(139) Lai, Y.; Diao, J.; Cipriano, D. J.; Zhang, Y.; Pfuetzner, R. A.; Padolina, M. S.; Brunger, A. T. Complexin Inhibits Spontaneous Release and Synchronizes Ca2+-Triggered Synaptic Vesicle Fusion by Distinct Mechanisms. *eLife* **2014**, *3*, e03756. https://doi.org/10.7554/eLife.03756.

(140) Kaeser-Woo, Y. J.; Yang, X.; Sudhof, T. C. C-Terminal Complexin Sequence Is Selectively Required for Clamping and Priming But Not for Ca2+ Triggering of Synaptic Exocytosis. *J. Neurosci.* **2012**, *32* (8), 2877–2885. https://doi.org/10.1523/JNEUROSCI.3360-11.2012.

(141) Bera, M.; Ramakrishnan, S.; Coleman, J.; Krishnakumar, S. S.; Rothman, J. E. Molecular Determinants of Complexin Clamping and Activation Function. *eLife 11*, e71938. https://doi.org/10.7554/eLife.71938.

(142) Pierson, J.; Shin, Y.-K. Stabilization of the SNARE Core by Complexin-1 Facilitates Fusion Pore Expansion. *Front. Mol. Biosci.* **2021**, *8*, 805000. https://doi.org/10.3389/fmolb.2021.805000.

(143) Xue, M.; Reim, K.; Chen, X.; Chao, H.-T.; Deng, H.; Rizo, J.; Brose, N.; Rosenmund, C. Distinct Domains of Complexin I Differentially Regulate Neurotransmitter Release. *Nat. Struct. Mol. Biol.* **2007**, *14* (10), 949–958. https://doi.org/10.1038/nsmb1292.

(144) Xue, M.; Craig, T. K.; Xu, J.; Chao, H.-T.; Rizo, J.; Rosenmund, C. Binding of the Complexin N Terminus to the SNARE Complex Potentiates Synaptic-Vesicle Fusogenicity. *Nat. Struct. Mol. Biol.* **2010**, *17* (5), 568–575. https://doi.org/10.1038/nsmb.1791.

(145) Lai, Y.; Choi, U. B.; Zhang, Y.; Zhao, M.; Pfuetzner, R. A.; Wang, A. L.; Diao, J.; Brunger, A. T. N-Terminal Domain of Complexin Independently Activates Calcium-Triggered Fusion. *Proc. Natl. Acad. Sci.* **2016**, *113* (32). https://doi.org/10.1073/pnas.1604348113.

(146) Choi, U. B.; Zhao, M.; Zhang, Y.; Lai, Y.; Brunger, A. T. Complexin Induces a Conformational Change at the Membrane-Proximal C-Terminal End of the SNARE Complex. *eLife* **2016**, *5*, e16886. https://doi.org/10.7554/eLife.16886.